The Strongman trait: Clinical and molecular characterization of a dominant Herculean myalgic disorder

By

Talita Cristiane Conte

Department of Human Genetics
McGill University, Montreal
May, 2019

A thesis submitted to McGill in partial fulfillment of the requirements of the degree of Doctor of Philosophy

ABSTRACT

Herculean strength has always fascinated humans. Several studies have suggested that muscular strength is a trait proposing that genetic factors contribute to the development of an increased strength phenotype. Most male French-Canadian settlers that came to Quebec during the French Regime (1608-1760) were soldiers chosen by merchants for their strength. This may have influenced the relative increase in carrier frequencies of certain alleles related to muscle strength that have been passed down through generations in Quebec. We recruited several French-Canadian families with individuals presenting a muscle disorder that we have called the Strongman trait (ST). Affected individuals present with a familial and personal history of superior strength, which is accompanied by myalgia, prolonged contractions and weakness after repetitive contractions as negative symptoms, and superior muscle strength and mass as positive findings. We identified an autosomal dominant mutation segregating in two families in an uncharacterized gene called DC-STAMP Domain Containing 2 (*DCST2)*. By further exploring the function of DCST2, we found that it is localized to the sarcoplasmic reticulum (SR) and forms puncta that lie juxtaposed to the transverse-tubules (TT) in the I-band. We observed that DCST2 formed larger puncta in the muscle of a ST patient and it often colocalized with stromal interaction molecule 1 (STIM1) and ATPase sarcoplasmic/endoplasmic reticulum Ca^{2+} transporting 1 (SERCA1), a finding that was rarely observed in control muscles. We performed an unbiased approach through a proximity biotinylation (BioID) assay to identify some DCST2's proximity interactors. Several proteins of the endoplasmic reticulum (ER) were identified as well as important proteins involved with cellular calcium handling. Two of the proteins involved with calcium handling with the highest scores in the BioID were STIM1 and coiled-coil domain containing 47 (CCDC47 or calumin). Considering that these two proteins have been described to have important roles as calcium sensors influencing ER calcium replenishing through the store-operated calcium entry (SOCE), we then performed cellular calcium assays to identify if the mutation in *DCST2* could have an effect on cellular calcium transients. We observed that ST differentiating myoblasts elicited lower SR calcium release and we confirmed that this effect is probably due to a defective SERCA activity that is unable to properly reuptake calcium ions from the cytosol back to the SR. We also detected lower extracellular calcium entry by

measuring calcium-release calcium activated (CRAC) channels activity. This result indicated that STIM1 is partially dysfunctional to allow proper extracellular calcium entry through the CRAC channels. We also detected that ST myoblasts presented a greater number of larger DCST2 puncta and that this number tended to increase when cells were exposed to calcium deficit stress. These larger DCST2 puncta also contained STIM1 and SERCA1 suggesting that DCST2 is probably involved in the dynamics of STIM1-SERCA1 multi-protein complex formation. DCST2-L759P found in the ST cells appears to lead to an improper complex formation impacting cellular calcium transients. We showed that ST patients that do not carry *DCST2* mutations presented overlapping clinical and pathological (larger DCST2 puncta) features as ST patients carrying a *DCST2* mutation, underlining that they could be used to support the ST diagnosis in a clinical setting. This thesis presents the original description of the ST phenotype and the identification of its first causal gene while concluding that calcium handling dysfunctions are responsible for this new Herculean myopathy.

RÉSUMÉ

La force herculéenne a toujours fasciné les êtres humains. Plusieurs études suggèrent que la force musculaire est un trait et que des facteurs génétiques contribuent au développement d'un phénotype de force accrue. Durant le Régime français (1608-1760), la majorité des colons Canadien français qui arrivèrent au Québec furent des soldats choisis par les marchands intéressés par leur force physique. Ceci pourrait avoir eu une incidence sur l'augmentation relative de la fréquence de porteurs de certains allèles liés à la force musculaire et transmis à travers les générations au Québec. Nous avons recruté plusieurs familles canadiennes-françaises avec des individus qui présentent un trouble musculaire que nous appelons le trait de l'homme fort (THF). Les individus atteints présentent une histoire personnelle et familiale de force accrue. Celle-ci s'accompagne de symptômes négatifs tels que la myalgie, des contractions prolongées et une faiblesse aux contractions répétées, et de symptômes positifs, tels qu'une force et masse musculaire supérieure. Nous avons identifié des mutations autosomiques dominantes ségrégant dans deux familles dans un gène de fonction inconnue appelé DC-STAMP domain containing 2 (*DCST2*). En explorant la fonction de DCST2, nous avons découvert qu'il se localise dans le réticulum sarcoplasmique (RS) et qu'il forme des puncta juxtaposés aux tubules transverses dans la bande-I du sarcomère. Nous avons observé que DCST2 forme des puncta plus larges dans le muscle d'un patient HF et qu'il est fréquemment colocalisé avec la molécule d'interaction stromale 1 (STIM1) et l'ATPase sarcoplasmic/endoplasmic reticulum Ca^{2+} transporting 1 (SERCA1) ; trouvaille rarement observée chez les contrôles. Nous avons complété un essai non-biaisé de BioID pour identifier des interacteurs à proximité de DCST2. Plusieurs protéines du réticulum endoplasmique (RE) ont été identifiées ainsi que des protéines importantes liées au contrôle de l'homéostasie calcique cellulaire. Deux de ces protéines avec le score le plus élevé étaient STIM1 et coiled-coil domain containing 47 (CCDC47 ou calumin). Étant donné que ces deux protéines sont connues d'avoir des rôles clés qu'influencent le remplissage de calcium du RE à travers de l'entrée du calcium dépendant de la libération des réserves (ECDLR), nous avons décidé de procéder à des essaies de calcium afin de savoir si la mutation dans *DCST2* pourrait influencer l'homéostasie calcique cellulaire. Nous avons observé que les myoblastes en différentiation d'un patient avec le THF évoquèrent moins la libération du calcium du RS et nous

avons confirmé que cet effet est probablement dû à une dysfonction partielle au niveau de l'activité SERCA qui n'est pas en mesure de pomper le calcium du cytosol vers le RS. De plus, nous avons détecté une entrée diminuée de calcium extracellulaire en mesurant l'activité de canaux de calcium activés par le calcium (ACCAC). Ce résultat nous a indiqué que STIM1 a aussi une dysfonction partielle diminuant l'entrée du calcium extracellulaire. Nous avons de plus observé que ces mêmes myoblastes ont présenté une quantité plus élevée de puncta plus larges et que ce nombre a tendance à augmenter lorsque les cellules sont exposées au stress d'un déficit en calcium. Ces puncta plus larges de DCST2 contenaient également STIM1 et SERCA1, ce qui suggère que DCST2 est probablement impliqué dans la dynamique de la formation du complexe multi-protéique de STIM1-SERCA1. La protéine DCST2-L759P trouvée chez les patients avec le THF semble être liée à la formation erronée d'un complexe protéique qui cause un impact dans l'homéostasie calcique cellulaire. Nous avons démontré également que les patients avec le THF qui ne présentent pas de mutations dans *DCST2* présentent un chevauchement des caractéristiques cliniques et pathologiques (puncta plus larges de DCST2) tout comme les patients ayant la mutation dans *DCST2*, soulignant le fait que ces données pourront être utilisées pour appuyer le diagnostic des patients avec le THF dans un milieu clinique. Cette thèse présente la description originale du phénotype du THF et l'identification du gène responsable de la maladie et conclue que la dysfonction au niveau de l'homéostasie du calcium est responsable de ce nouveau phénotype qui cause une myopathie herculéenne.

Table of contents

LIST OF ABREVIATIONS

2D-PAGE: two-dimensional polyacrylamide gel electrophoresis

4EBPs: eIF4E-binding proteins

ACh: acetylcholine

ACVR2A: activing type II receptor A

ACVR2B: activing type II receptor B

ADP: adenosine diphosphate

AKT: serine-threonine protein kinase AKT

ALK: type I receptor for activin

AMFR: autocrine motility factor receptor

ANO1: anoctamine 1

ANO2: anoctamine 2

ANO5: anoctamine 5

ANO6: anoctamine 6

ANOVA: analysis of variance

APC/C: anaphase-promoting complex/cyclosome

ATP: adenosine triphosphate

ATP2A1: sarcoplasmic/endoplasmic reticulum Ca^{2+}-ATPase 1

ATP2A2: sarcoplasmic/endoplasmic reticulum Ca^{2+}-ATPase 2

BARD1: BRCA1 associated RING domain 1

BCL2: BCL2 apoptosis regulator

BioID: proximity-dependent biotinylation assay

BNIP3: adenovirus E1B interacting protein 3

bp: base pair

BRCA1: BRCA1 DNA repair associated

BSA: bovine serum albumin

CACNA1S: calcium voltage-gated channel subunit alpha1 S

CADD: combined annotation dependent depletion

Cas9: CRISPR associated protein 9

CAV3: caveolin 3

CCDC47: coiled-coil domain containing 47

CCTG: citosine-citosine-timine-guanine

CEUs: calcium entry units

CK: creatine kinase

CLCN1: chloride voltage-gated channel 1

CnA: calcineurin

CNBP: cellular nucleic-acid- binding protein

CNS: central nervous system

CRAC: calcium-release calcium activated

CRISPR: clustered regularly interspaced short palindromic repeats

CRUs: calcium release units

CSA: cross-sectional area

CTG: cytosine, thymine, guanine

CUGBP1: CUG-binding protein 1

DCST1: DC-STAMP domain containing 1

DCST2: DC-STAMP domain containing 2

DCSTAMP: dendrocyte expressed seven transmembrane protein

DHPR: dihydropyridine receptor

DM1: myotonic dystrophy type 1

DM2: myotonic dystrophy type 2

DMEM: Dulbecco's modified Eagle's medium

DMPK: dystrophia myotonica protein kinase

DNA: deoxyribonucleic acid

E2: ubiquitin-conjugating enzyme

E3: ubiquitin ligase

EC: excitation-contraction

eIF2B: eukaryotic translation initiation factor 2B

eIF4E: eukaryotic translation initiation factor 4E

EMG: electromyography

ER: endoplasmic reticulum

ERAD: ER associated degradation

ERK: extracellular signal regulated kinase

FBS: fetal calf serum

FDR: false discovery rate

FoxO: forkhead box O

FZD7: frizzled class receptor 7

GAP: GTPase activating protein

GATA: guanine-adenosine-thymine-adenosine

GDF8: growth and differentiation factor 8

gnomAD: genome aggregation database

GO: gene ontology

GPR37: G protein-coupled receptor 37

GSK3b: glycogen synthase kinase 3b

GTEx: genotype-tissue expression

H&E: hematoxylin and eosin

HEK293: human embryonic kidney

hnRNP H: heterogeneous nuclear bibonucleoprotein H

HRD1: HMG-CoA reductase degradation 1 homolog

HS: horse serum

IGF1: insulin-like growth factor 1

IGF1R: insulin-like growth factor 1 receptor

IgG: Immunoglobulin G

IR: insulin receptor

IRS: insulin receptor substrate

ITPR3: onositol 1,4,5-trisphosphate receptor type 3

KD: knockdown

kDa: kilodalton

KDEL: Lys-Asp-Glu-Leu ER signal peptide

KO: knockout

LAMP2: lysosomal associated membrane protein 2

LB: lysogeny broth

LC3: microtubule-associated protein 1 light chain 3

LGMD2L: limb-girdle muscle dystrophy type 2L

LMAN1: lectin mannose binding 1

LMNA: lamin A/C

LOD: logarithm of odds

MAFbx: muscle atrophy F-box

MAPK: mitogen-activated protein kinase

MBNLs: muscle blind-like proteins

MEF2: myocyte enhancer factor

mg: milligram

MHC: myosin heavy chain

mL: milliliter

mM: millimolar

MMD3: Miyoshi muscular dystrophy 3

MRI: magnetic resonance imaging

mTOR: mammalian target of rapamycin

mTORC: rapamycin-sensitive mTOR complex

MTSN: myostatin

MuRF1: muscle ring finger 1

N: Newtons

NADH: nicotinamide adenine dinucleotide

NDS: normal donkey serum

NFAT: nuclear factor of activated T-cells

NFATc1: nuclear factor of activated T cells 1

NFATc2: nuclear factor of activated T cells 2

ng: nanogram

NMJ: neuromuscular junction

nNOS: neuronal nitric oxide synthase

OCSTAMP: osteoclast stimulatory transmembrane protein

OMIM: online Mendelian inheritance in man

OPA1: optic atrophy protein 1

ORAI1: ORAI calcium release-activated calcium modulator 1

p62: SH2 domain of 62 kDa

PAX7: paired box 7

PDK1: phosphoinositide-dependent kinase 1

PFA: paraformaldehyde

PGC1α4: PPARG coactivator 1 alpha 4

PHYRE2: protein fold recognition server

Pi: inorganic phosphate

PI3K: phosphoinositide-3-kinase

PIP2: phosphoinositide-4,5-biphosphate

PIP3: phosphoinositide-3,4,5-triphosphate

PIRIC: percussion-induced rapid contraction

PLIN1: perilipin 1

PROMM: proximal myotonic myopathy

PYGM: glycogen phosphorylase, muscle associated

Rheb: small G protein Ras homolog enriched in brain

RING: really interesting new gene

RMD: rippling muscle disease

RNA: ribonucleic acid

RNF25: ring finger protein 25

RT: room temperature

RYR: ryanodine receptors

S6K: S6 kinase

SCN4A: voltage-gated channel alpha subunit 4

SD: standard deviation

SEM: standard error of the mean

SERCA1: ATPase sarcoplasmic/endoplasmic reticulum Ca^{2+} transporting 1

SERCA2: ATPase sarcoplasmic/endoplasmic reticulum Ca^{2+} transporting 2

SIFT: sorting intolerant from tolerant

SKP1: S-phase kinase-associated protein 1

SMAD2: SMAD Family Member 2

SMAD3: SMAD Family Member 3

SMAD4: SMAD Family Member 4

SNP: single nucleotide polymorphism

SOCE: store operated calcium entry

SPE-42: spaetzle-processing enzyme 42

SR: sarcoplasmic reticulum

ST: strongman trait

STAT2: signal transducer and activator of transcription 2

STAU1: Staufen Double-Stranded RNA Binding Protein 1

STIM1: stromal interaction molecule 1

SYVN1: synoviolin

TG: thapsigargin

TGFb: transforming growth factor beta

TMA: tubular aggregate myopathy

TMEM16E: transmembrane protein 16 E

TNNT3: cardiac troponin T 3

TRAF6: TNF receptor associated factor 6

TRPV1: transient receptor potential cation channel subfamily V member 1

TSC: tuberous sclerosis complex

TT: transverse tubules

μm: micrometers

μM: micromolar

U/L: units per liter

UPS: ubiquitin-proteasome system

WES: whole exome sequencing

WNT7A: Wnt family member 7A

ZNF9: zinc finger protein 9

LIST OF FIGURES

Chapter 1

Chapter 2

Chapter 3

Chapter 4

Appendix

LIST OF TABLES

ACKNOWLEDGEMENTS

This thesis was supported by the scholarships from the Association Française contre les Myopathies (AFM) and the Fondation du Grand Défi Pierre Lavoie.

First, I would like to express my gratitude to Dr. Bernard Brais for having accepted supervising me and for giving me the opportunity to work in this project. Being able to share his knowledge and his passion for research were crucial to my professional development. Thanks for all your support and patience, and for trusting in my abilities.

It has also been a great pleasure to have worked with such amazing people. I would like to say a special thank you to Marie-Josée for all technical, professional and personal guidance during all those years. Thanks Véronique for training me and for all the support you gave me at the beginning of my PhD. Thanks Martine and Karine for giving me invaluable advice for the advance of my project. Thanks Roxanne and Rebecca R. for all your support and for taking the time to discuss with me all those crazy theories about DCST2. Thank you Xavier, Roberta, Catherine, Nicolas and Rebecca G. for all your help and for the great memories that we have shared together. I also would like to thank Benjamin and Sharon, undergraduate students that I had the opportunity to supervise. Thank you all the members of the Rare Neurological Diseases Group for sharing wonderful moments and for giving me the opportunity to expand my knowledge.

I am grateful for having the opportunity to have collaborated with Erin, Ariel, Philippe, Russell and Tanja. Thank you for your technical support and for sharing your knowledge with me.

I would also like to say thank you to the members of my supervisory committee, Eric Shoubridge and Frederic Charron. Their guidance and support were key for the accomplishment of this thesis. Thank you for always being available and understanding during challenging times of my PhD.

And a very special thanks to my family and friends for their constant support, without them none of this work would have been done. Thanks to my parents and sister for their

unconditional love and support. Special thanks to my husband who has been closely accompanying and supporting me during all those years. Thanks for being so patient and for giving me the best gift of my life, my forever baby Liam. Thanks to my friends Andrea, Camilla, Isadora and Monique for always being supportive and for your frequent encouragements. Thanks to my friends Patricia and Rejiane for keeping our long-time friendship and for every valuable piece of advice.

I would like to dedicate this thesis to my maternal uncle, Antonio Ambrosio Pereira, who has inspired me to go after my dreams and for having been a great influence in my pursuit of education.

PREFACE

This thesis is written according to the guidelines of the McGill University Graduate and Postdoctoral Studies Office. It is presented in the manuscript-based format for a Doctoral thesis. The studies described herein were performed under the supervision of Dr. Bernard Brais. This thesis provides important advances on two main subjects related to the new Herculean myalgic disorder called the Strongman trait: *i)* the identification and characterization of a new mutation in a gene of unknown function, and *ii)* the clinical and pathological characterization of the Strongman trait.

This thesis is composed by five chapters. **Chapter 1** contains a general introduction reviewing important literature information relevant to this thesis. **Chapter 2** presents one manuscript describing the characterization of a new Herculean myalgic trait and the impact of its casual mutation. This first manuscript was submitted to *Brain.* **Chapter 3** is a manuscript in preparation, to be submitted once a few remaining results are obtained. It describes the clinical and molecular overlaps in patients carrying or not the mutation found on chapter 2. **Chapter 4** presents a broad discussion of the previous chapter, and finally **Chapter 5** provides the general conclusion and future directions.

Contribution of Authors

Chapter 2: This study was performed with following colleagues and collaborators: *Martine Tétreault, Marie-Josée Dicaire, Ariel R. Ase, Sylvie Provost, Marie-Pier Roussel, Hana Antonicka, Rebecca Robertson, Benjamin Beland, Véronique Bolduc, Najwa Al-Bustani, Myriam Srour, Erin K. O'Ferrall, Alexandre Janer, Tanja Taivassalo, Anne-Claude Gingras, Russell Hepple, Elise Duchesne, Marie-Pierre Dubé, Eric A. Shoubridge, Philippe Séguéla, Jean Mathieu, Bernard Brais*. I helped with the fine mapping of the gene, performed immunofluorescent labeling, imaging and quantification, western blotting, transfections, produced cell lines for BioID assay, established the patient's myoblasts cell line, designed experiments, interpreted data and wrote the paper. M.T. contributed to the linkage analyses, whole-exome sequencing analyses, validation of variants, variant screening of ST cohort and wrote the paper. M.J.D. produced all DCST2 plasmids, did the fine mapping of the linkage, the validation of variants and screening of ST cohort. A.R.A. and P.S. performed the calcium assays experiments and analyses. S.P. and M.P.D. did the linkage analysis. M.P.R. and E.D. performed the muscle biopsy in the ST patient. H.A., A.J., E.A.S. and A.C.G. analyzed the BioID data. H.A., A.J. and E.A.S also reviewed the manuscript for intellectual content. R.R. helped establishing the patient's myoblast cell line and screening of ST cohort. B.Be. helped with the validation of variants and screening of ST cohort. V.B. did the linkage analysis. M.S., N.A.B. and E.K.O evaluated clinically the ST patients. T.T. and R.H. provided age-match control muscle biopsies and contributed to the analyses of the biopsy results. J.M. recruited and evaluated clinically ST patients. B.Br. recruited and evaluated clinically ST patients, designed the experiments, interpreted data, coordinated the study and wrote the paper.

Chapter 3: This study was performed with following colleagues and collaborators: *Xavier Allard, Rebecca Robertson, Tanja Taivassalo, Russell Hepple, Jason Karamchandani, Erin K. O'Ferrall, Bernard Brais*. I designed experiments, performed immunofluorescent labeling, imaging and quantification, interpreted data and wrote the paper. X.A. and R.R. screened the variant in the ST patients and performed some of the immunofluorescent labeling. T.T. and R.H. provided age-match control muscle biopsies and contributed to the analyses of the biopsy results. J.K. provided skeletal muscle sections stained with H&E, Gomori Thricome and NADH. E.K.O

evaluated clinically the ST patients and performed the muscle biopsies. B.B. recruited and evaluated clinically ST patients, designed the experiments, interpreted data, coordinated the study and wrote the paper.

Original Contribution to Knowledge

The work described in this thesis provides meaningful contributions to a better understanding of the clinical and molecular basis of a new Herculean myalgic muscle disorder: the Strongman Trait (ST).

Chapter 2 shows original data about a new dominant mutation in two French-Canadian families presenting a new Strongman trait in *DCST2*, a gene of uncharacterized function. We demonstrate for the first time the localization of DCST2 in skeletal muscle and myoblasts, and the effect of the mutation in the dynamics of DCST2 puncta formation. All the localization data and western blot data for DCST2 was generated with a new proprietary polyclonal DCST2 antibody that was validated and showed to have specific activity. In addition, we provide information about some of DCST2's binding partners. Moreover, we show that this novel *DCST2* mutation can influence important cellular calcium handling mechanisms explaining in part the signs and symptoms present ST patients. Together our original results demonstrate that the Strongman trait is a new myopathy and that it should be considered as a diagnosis in individuals with negative workups presenting with myalgia, prolonged contractions and reduced endurance, prominent muscles and personal and familial history of supra normal strength.

Chapter 3 describes common clinical and pathological features in Strongman trait patients between patients whether or not they carry or not a *DCST2* mutation. We show that in the muscle of these *DCST2* negative patients, the size, number and content of the DCST2 puncta can serve as a shared confirmatory finding for all ST cases despite the underlining mutation.

CHAPTER 1: General Introduction

Herculean strength has been a subject of fascination in the history of mankind. French-Canadian celebrities like Victor Delamarre or Louis Cyr are just some examples of individuals that became very popular due to their power performances, which went far beyond normal strength [1,2]. Moreover, Louis Cyr had a daughter who was also known to be very strong, supporting the hypothesis that muscular strength is a hereditary dominant trait [1]. The French-Canadian population has frequently been the source of studies for genetic diseases due to its founder effect [3,4]. One can speculate that, since a large fraction of male immigrants during the French Regime (1608-1760) were soldiers or men chosen by merchants to transport heavy goods, that many may have had above average muscle mass and strength [5]. This historical emigration bias may have favoured the introduction of certain alleles related to muscle strength and make them, centuries later, more frequent in the French-Canadian population. In this thesis, we took advantage of having access to a very large French-Canadian family and a large cohort of patients presenting familial symptoms of muscle pain accompanied by superior muscle strength to identify a first gene for a Strongman trait.

In Chapter 2, I focus on the identification and characterization of an original mutation in the *DCST2* gene found in two French-Canadian families presenting with what we describe as the new Strongman trait. I start this chapter with an introduction on the description of the clinical spectrum of the patients that were selected for this study, following by the identification and validation of a mutation in the *DCST2* gene. We report that this gene codes for a protein of unknown function that localizes to the I-band of skeletal muscles in enlarged puncta with proteins that play important roles in calcium handling. We show that the DCST2 mutation leads to a perturbation of calcium levels that may explain the clinical phenotype

In Chapter 3, I present evidence that quantification of DCST2 and SERCA1 positive puncta in muscle can be used to support the diagnosis of the Strongman trait in cases that do not carry a DCST2 mutation.

1.1 Skeletal muscle properties

1.1.1 Skeletal muscle structure and composition

Skeletal muscle is a highly organized tissue responsible for generating voluntary movements, present since early in evolution from invertebrates to vertebrates. Moreover, it is involved in posture, breathing, various metabolic pathways and immunological response in higher vertebrates. In humans, the skeletal muscle represents approximately half of the total body weight and thus considered the most abundant tissue of the human body [6,7].

Skeletal muscle tissue is mainly composed of polygonal elongated multinucleated cells that are called myofibers (or muscle fibers) which can reach up to 100 μm^2 in diameter and 30 cm in length. During development, embryonic myoblasts fuse to several other myoblasts to form multinucleated myofibers. These multiple nuclei ensure the production of large amounts of proteins and enzymes necessary for muscle contraction. Within the cytosol of each myofiber, there are numerous thin cylindrical striated structures called myofibrils that contain the contractile unit of the skeletal muscle: the sarcomere (figure 1.1). Within each sarcomere present in the myofibrils, we can find the main myofibrillar proteins myosin and actin. Myosin constitutes the thick filaments and actin constitutes the thin filaments, and the interaction between these two proteins will generate muscle contraction, which will be discussed later in this section [6,7].

Every skeletal muscle is enclosed by three layers of connective tissue that provide structure to the muscle, as well as compartmentalize muscle fibers within the muscle. Each muscle is wrapped by a dense connective tissue sheath called the epimysium. Bundles of myofibers, called fascicles, are surrounded by fibrous sheaths that are called the perimysium that also contain blood vessels, lymph vessels and nerves. Furthermore, each muscle fiber is enclosed by a thin connective layer of collagen and reticular fibers called the endomysium that also contain capillaries and nerve fibers (figure 1.1). All the nutrients needed to support the muscle fibers come from these capillaries. This highly organized connective tissue has a key role in ensuring the integrity of the muscle's structure by contributing to its tensile strength and resistance to stretching [6,8].

Muscles are historically classified according to their color (red or white) and type of contraction (fast or slow) due to the different biochemical properties. Myofibers present distinct metabolic and structural phenotypes that are the basis of their classification into three major types: Type 1 are slow twitch fibers that generate low mechanical power output, are fatigue resistant and rely on aerobic metabolism; Type 2X are fast twitch fibers that generate high mechanical power output, are quickly fatigable and rely on glycolytic metabolism; while Type 2A are intermediate twitch fibers that generate high power output and are fatigue resistant [9,10].

Today various techniques are used to differentiate fiber types: histochemical staining for myosin ATPase, myosin heavy chain isoform identification, and biochemical identification of metabolic enzymes [11]. These techniques assess different myosin isoforms associated with different physiological properties. Moreover, these techniques allowed the observation that myofibers might co-express different myosin isoforms at the same time (i.e. MHC1 and MHC2A or MHC2A and MHC2X) [10,12].

The phenotype of these different fiber types is defined according to the type of motor neuron innervation. A motor unit is comprised of an α-motor neuron that lies in the anterior horn of the spinal cord and all the muscle fibers it innervates. Every muscle fibers of a motor unit have similar metabolic and structural characteristics. Motor units can be divided into groups based on the contractile and fatigue characteristics of the myofiber. Based on contractile speed, motor units are classified as slow-twitch or fast-twitch. The fast-twich motor units are further subdivided into fast-twitch fatigue-resistant, fast-twitch fatigue-intermediate, and fast-twitch fatigable [9,10].

Despite the fact that the types of myofiber and motor neurons are well-established, these units are plastic indicating that they can change in response to different stimuli (i.e., hormonal, level of activity, injury) [9].

1.1.2 Skeletal muscle contraction

Skeletal muscle contraction is a complex phenomenon that is only possible due to exceptional orchestrated machinery composed by the neuromuscular junction (NMJ), the sarcotubular system, and the cross bridges (figure 1.2 and 1.3) [6,7].

The NMJ is composed of three types of cells: the nerve ending of the α-motor neuron, the muscle fibers, and the perisynaptic Schwann cells. The presynaptic nerve terminal at the distal end of the α-motor neuron harbours synaptic vesicles containing acetylcholine, synaptic vesicle associated apparatus and mitochondria. The postsynaptic terminal of the NMJ is composed of a large cluster of nicotinic acetylcholine receptors on the muscle fiber surface that form the motor endplate. In order to increase the surface area of the endplate several invaginations named postsynaptic folds are formed and nicotinic acetylcholine receptors are localized all over these folds. The clusters of receptors perfectly mirror the shape of the presynaptic terminal for efficient transmission of acetylcholine at the synaptic cleft. Around every synapse, there are perisynaptic Schwann cells providing trophic support to the NMJ [13,14].

Once acetylcholine is released from the presynaptic nerve terminal, it binds to the acetylcholine receptors at the NMJ causing an endplate potential. Nicotinic acetylcholine receptors are ligand-gated inward-rectifier channels meaning that once they are activated they allow sodium ions to pass the plasma membrane leading to sarcolemma depolarization. This depolarization triggers an action potential that travels along a very organized network of membranes composed of the transverse tubules (or T-tubules) that are invaginations of the sarcolemma that runs transversally to the long axis of the muscle fiber, and the sarcoplasmic reticulum (SR) membrane that form the sarcotubular system (figure 1.2). This action potential activates dihydropyridine receptors (DHPR) localized to the T-tubules which in turn bind to ryanodine receptors (RYR) localized to the terminal cisternae of the SR [15,16]. DHPR and RYR mechanical coupling forms the triad or calcium release units (CRUs) that are composed of T-tubules flanked by two terminal cisternae of the sarcoplasmic reticulum (SR) [17]. The name CRU describes exactly what happens once these units are formed: RYR opens and releases calcium from the sarcoplasmic reticulum raising the level of cytosolic free calcium [15,17]. This rise in cytosolic calcium together with adenosine triphosphate (ATP) availability will lead to muscle contraction [15,16].

Once calcium is released from the SR to the cytosol, it binds to troponin, which through its interaction with tropomyosin exposes a myosin binding site on actin filaments. In the presence of ATP, the myosin head attaches to actin and pulls the thin filament along the thick filament, allowing the sarcomere to shorten [13,18]. While calcium and ATP are present, the myosin heads will bind to actin molecules, pull, release, and reattach; this process is known as cross-bridge cycling (figure 1.3) [18]. This whole process, starting with the action potential leading to muscle contraction, is known as excitation-contraction (EC)-coupling [14,18].

While the rise of free calcium in the cytosol leads to muscle contraction, its removal leads to muscle relaxation. A key protein responsible for the removal of cytosolic calcium back to the SR is the ATPase Sarcoplasmic/Endoplasmic Reticulum Ca^{2+} Transporting (SERCA) [19,20].

1.1.3 Skeletal muscle strength and determinants

Muscular strength is defined as "the maximal force capabilities of a muscle or muscle group that can be exerted against a resistance in a particular movement pattern and at a defined velocity of movement" [21]. It is important to understand that muscular strength must be distinguished from muscular power and endurance [21]. Power can be expressed by work divided by time while endurance is the ability to maintain a muscle contraction or repetitive contractions for a prolonged period to a defined endpoint [21,22].

The force generated by a muscle fiber depends on the amount of cross-bridge activity. Some of the main factors influencing modifications of the kinetics of actomyosin interactions are: ATP, calcium and availability of binding sites on the thin filament [21,23]. Mitochondria are the powerhouse of the cell, being responsible for producing the ATP needed for contraction [21]. Any dysfunction leading to decreased ATP production will cause reduced attachment of the myosin head to actin and will impact muscle contraction [24,25]. The same is true for calcium, once there is any dysregulation in SR calcium release there will be an impact in muscle contraction[16,19]. The availability of binding sites on the thin filament can be influenced by the amount of muscle mass or myofibers of a specific muscle [18,26]. Atrophied muscles presenting with decreased myofiber cross-sectional area are weaker, in part because they have less binding sites on the thin filament [24,26]. The contrary is also true; hypertrophied muscles with increased myofiber cross-section area

have more binding sites on the thin filament and consequently, they are stronger [26]. Recent studies have also proposed that post-translational modifications of myosin or actin could influence cross-bridge activity as well [23,27].

Muscle mass is the result of a dynamic balance between protein synthesis and degradation [28]. Some strategies have been proposed to positively influence this balance, and one of them is resistance training. Resistance training is defined as a type of exercise that requires the body's musculature to move against an opposing force [23]. Resistance training is described to induce muscle hypertrophy that in turn leads to increased muscle strength [22,29].

Multiple metabolic and physiologic changes are induced by exercise [30]. During the past decade, muscle cells have been identified as cells with a high secretory capacity [31]. Earlier studies suggested that cytokines or other peptides that are produced, expressed, and released by muscle fibers exert endocrine effects [32]. It was proposed that these cytokines and peptides should be classified as myokines [32]. These myokines can exert their effects on signalling pathways within the muscle itself [33]. The main signalling pathways known to be activated during muscle hypertrophy will be reviewed in more details in the following section.

1.2 Regulation of muscle mass

1.2.1 Myostatin

Myostatin (MTSN) is one of the major regulators of muscle mass. Loss of function mutations in *MTSN* have been reported to cause increased muscle mass in several species including dog [34], sheep [35], cattle [36] and pig [37]. MTSN has drawn attention of myologists from all over the world after the publication of a case report about a hypermuscular infant carrying a homozygous recessive frameshift mutation in exon 1 of *MTSN* [38]. All animal models presenting a lack of MTSN expression present muscle hypertrophy due to increased cross-sectional area of myofibers and/or hyperplasia, and decreased fat content [34-37]. However, the impact of MSTN on muscle strength is a subject of broad discussion. Some studies have reported some animal models presenting increased strength [39,40], while others have even reported that some of these models are weaker [41-43]. Despite the variation found in different models, several studies continue

to focus on pharmacological approaches to inhibit MTSN in an effort to rescue muscle mass to treat muscle diseases [44-46].

MTSN, also known as growth and differentiation factor 8 (GDF8), is a member of the transforming growth factor beta (TGFβ) superfamily [47,48]. It codes for a 375 amino-acid inactive protein that is submitted to post-translational modifications to become active [49]. Once translated, it is cleaved forming a N-terminal propeptide and a C-terminal mature fragment. MTSN is produced and secreted by myofibers, conferring an endocrine, paracrine and autocrine activity [49]. The mature fragment of MSTN homodimerizes, binds and activates activin type II receptor (ACVR2B and to a lesser extent ACVR2A) at the plasma membrane [48]. These receptors are subjected to subsequent autophosphorylation leading to the recruitment and activation of the low affinity type I receptor for Activin ALK-4 or ALK-5 [48]. Once activated, these receptors phosphorylate the transcription factors SMAD family member 2 and 3 (SMAD2 and SMAD3) [48]. These in turn interact with SMAD4 and translocate to the nucleus targeting the transcription of specific genes which are implicated in the loss of muscle mass [48]. Conversely SMAD7 acts as a negative regulator of MSTN by downregulating its expression and by interfering in the formation of SMAD2-3/SMAD4 complex [50].

The process described above is known as the canonical MSTN pathway, and in addition to that there is also a non-canonical MSTN pathway [50]. MSTN can also inhibit serine-threonine protein kinase AKT and activate forkhead box O (FoxO) signaling pathway that will be reviewed with more details in the following section [50]

1.2.2 IGF1/AKT/mTOR

The insulin-like growth factor 1 – phosphoinositide-3-kinase – AKT / protein kinase B – mammalian target of rapamycin (IGF1–PI3K–AKT/ PKB–mTOR) pathway is a major positive regulator of muscle growth [51]. Several gain and loss-of-function genetic models have supported the crucial role of IGF1 pathway in skeletal muscle mass regulation [51]. A rodent model presenting a muscle-specific inactivation of IGF1 receptor presents with reduced muscle growth due to decreased myofiber number and size [52]. On the other hand, overexpression of a muscle-specific IGF1 leads to muscle hypertrophy and increased muscle strength [53].

IGF1 is known to activate two distinct molecular pathways, the mitogen-activated protein kinase/ extracellular signal regulated kinase (MAPK/ERK) and the PI3K–AKT pathway [14,54]. Activation of the MAPK/ERK pathway has been described to cause no change in hypertrophy whereas specific activation of PI3K–AKT pathway induces increased muscle mass. IGF1 is produced and secreted by the liver and skeletal muscles [54,55]. Additionally, it also has an endocrine, paracrine and autocrine activity in several tissues [54].

Once IGF1 binds to insulin-like growth factor 1 receptor (IGF1R) at the plasma membrane, it activates its intrinsic tyrosine kinase leading to autophosphorylation and creating docking sites for insulin receptor substrate (IRS), which is also phosphorylated by IGF1R [51]. Phosphorylated IRS then acts as docking site to recruit and activate PI3K which phosphorylates membrane phospholipids generating phosphoinositide-3,4,5-triphosphate (PIP3) from phosphoinositide-4,5-biphosphate (PIP2) [54]. PIP3 recruits two kinases, phosphoinositide-dependent kinase 1 (PDK1) and AKT, and the subsequent phosphorylation of AKT by PDK1 leads to AKT activation [54,56]. AKT acts as an inhibitor of protein degradation by phosphorylating and repressing transcription factors of the FoxO family, and stimulates protein synthesis via mTOR and glycogen synthase kinase 3b (GSK3b) [56]. FoxO factors regulate the transcription of the ubiquitin ligases atrogin-1, also called muscle atrophy F-box (MAFbx) and muscle ring finger 1 (MuRF1) [57]. These proteins are known to ubiquitylate myosin and other muscle proteins that consequently, are degraded via the ubiquitin-proteasome system (UPS) [57]. FoxO factors are also required for the transcriptional regulation of the microtubule-associated protein 1 light chain 3 (LC3), which together with BCL2 apoptosis regulator (BCL2)/ adenovirus E1B interacting protein 3 (BNIP3) are necessary for triggering the autophagy-lysosome pathway [57].

AKT does not activate mTOR directly, instead it inhibits the tuberous sclerosis complex (TSC) proteins 1 and 2, which act as a GTPase activating protein (GAP) to inhibit the small G protein Ras homolog enriched in brain (Rheb) which activates mTOR signaling [58]. mTOR can form two different protein complexes, the rapamycin-sensitive mTOR complex 1 (mTORC1) when bound to Raptor, and the rapamycin-insensitive mTOR complex 2 (mTORC2) when bound to Rictor [58]. mTORC2 is required for AKT phosphorylation and activation. mTORC1 phosphorylates S6 kinase (S6K), which in turn phosphorylates the ribosomal protein S6 and other factors involved in translation initiation and elongation, thus stimulating protein synthesis

[58]. mTORC1 also activates eukaryotic translation initiation factor 4E (eIF4E) by phosphorylating the inhibitory eIF4E-binding proteins (4EBPs) [58].

AKT also promotes protein synthesis by phosphorylating and inactivating GSK3b, thus releasing the GSK3b-dependent inhibition of the eukaryotic translation initiation factor 2B (eIF2B) [51,56]

In summary, the IGF1–PI3K–AKT/ PKB–mTOR pathway has a profound effect on both protein synthesis and degradation in ways that, once activated, it has a positive effect on muscle mass while its inhibition leads to loss of muscle mass.

1.2.3 Calcineurin

Calcineurin (CnA), also known as protein phosphatase 3, is a serine/threonine phosphatase that is activated by sustained increased levels of intracellular calcium [59]. CnA is a heterodimeric complex composed of a catalytic A subunit and smaller calcium-binding regulatory B subunit [60]. The three 59–62 kDa isoforms of the catalytic CnA subunit have been identified that arise from separate genes: CnAα, CnAβ, and CnAγ [60]. CnAα and CnAβ are abundant in a wide variety of tissues including skeletal muscle. In contrast, CnAγ is predominately located in the testis and brain as a result of differential gene expression [60]. Although the downstream effectors of CnA have not been fully elucidated, CnA signaling is known to be important for proper function of both cardiac and skeletal muscle [61].

In skeletal muscle, CnA participates in a variety of processes including myoblast recruitment and myotube differentiation [62], fiber type specification [63,64], recovery from muscle injury [65] and dystrophic muscle damage [66].

Some studies show that overexpressing CnA is sufficient to induce hypertrophy of muscle fibers [67,68]. Additionally, transgenic mice with decreased levels of CnA exhibit reduced fiber size demonstrating a role for CnA in hypertrophy [69]. In contrast, mice with either global or muscle-specific CnA depletion subjected to muscle hypertrophic growth by mechanical overload or IGF-1 stimulation do not show defects in muscle growth [70]. However, these mice did show impairment in overload-mediated fiber-type switching. These studies suggest that CnA is

important for muscle growth and remodeling, however different animal models may lead to different levels of perturbation of CnA action and diverse compensatory mechanisms associated with the experimental approach [67].

1.2.4 Cross-talks affecting myostatin/IGF1/calcineurin pathways

The pathways reviewed above are the main known pathways directly involved with muscle mass regulation. However, specific players of these pathways can have their activities influenced by other pathways' cross-talks [28,51].

β2-adrenergic agents have well-known anabolic effects on skeletal muscles [71]. Androgens potently stimulate muscle growth: testosterone loss in male mice decreases muscle Igf1 mRNA, AKT phosphorylation and the rate of myofibrillar protein synthesis [72]. Muscle hypertrophy induced by β2-adrenergic agents, such as clenbuterol or formoterol, is accompanied by a significant increase in AKT phosphorylation and is completely blocked by rapamycin (mTORC1 inhibitor) [71]. A pathway linked to mTOR activation involves neuronal nitric oxide synthase (nNOS) [73]. When activated in myofibers by functional overload, nNOS generates nitric oxide (NO) and causes peroxynitrite dependent activation of the transient receptor potential cation channel subfamily V member 1 (TRPV1), located in the sarcoplasmic reticulum [73]. The resulting increase in intracellular calcium induced by TRPV1 triggers activation of mTOR [73]. Wnt family member 7A (WNT7A), an extracellular protein involved in muscle growth, acts on myofibers by activating the PI3K–AKT pathway via its frizzled class receptor 7 (FZD7) [74]. Furthermore, mTOR is also activated by mechanical stimulation via an AKT-independent pathway involving phosphatidic acid and activated phospholipase D [75,76].

PPARG coactivator 1 alpha 4 (PGC1α4) is involved in muscle growth as shown by the finding that mice with skeletal muscle specific transgenic expression of PGC1α4 show increased muscle mass and strength [77]. In cultured muscle cells, PGC1α4 was found to induce IGF1 and repress MSTN, thus promoting myotube hypertrophy, which was blocked by an IGF1 receptor inhibitor [78]. Myotube growth induced by treatment with clenbuterol was also blunted by PGC1α4 knockdown [79].

Insulin and IGF-1 also have an effect on CnA since they induce calcium dynamics through both calcium influx and release from IP3R and RYR-operated stores [80]. Moreover, another hormone-like signaling molecule, prostaglandin F2, increases intracellular calcium concentration, activating nuclear factor of activated T cells 2 (NFATc2) and inducing muscle cell growth and nuclear accretion [81]. These studies suggest that molecularly diverse stimuli may converge at recruiting calcium signaling to implement muscle growth [82].

1.2.5. Satellite Cells

Satellite cells were first described by Mauro (1961) as cells positioned at the outside boundary of the myofiber sarcolemma [83]. Satellite cells are a distinct cell population underneath the basal lamina in charge of proper postnatal muscle development and repair [84,85]. Satellite cells are quiescent in resting adult muscle, but once there is tissue damage or a growth stimulus, these cells become activated (also known as myoblasts) and proliferate massively producing the myogenic progenitors needed for muscle growth and regeneration [84,85]. At these times, myoblasts exit cell cycle, differentiate and fuse to existing myofibers or form newly regenerating myofibers [84,85].

The issue of whether satellite cell proliferation and fusion contributes to muscle growth caused by exercise has been the subject of debate [86]. Myoblast fusion is essential for muscle growth during early stages of muscle differentiation [84]. For example, myotube growth in culture is impaired when myoblast fusion is inhibited, either during formation of the nascent myotube or during the transition from nascent to mature myotube [86]. Muscle growth during early postnatal development is also accompanied by a continuous increase in the number of myonuclei resulting from satellite cell fusion [85]. On the other hand, muscle hypertrophy at late postnatal stages takes place without a significant contribution of satellite cell fusion [86]. Similarly, myonuclear number is not increased during muscle growth upon reloading of previously atrophied muscles [87]. Satellite cell proliferation and fusion were not detected during muscle hypertrophy induced by a muscle-specific, inducible and constitutively active AKT1 transgene [88].

A recent detailed study concluded that satellite cells play little or no role in MSTN/ activin A signaling in vivo, based on the finding that satellite cell and myonuclear number were

unchanged in hypertrophic muscles after injection of soluble ACVR2B [89]. Muscle hypertrophy induced by overexpressing follistatin also occurs in mice lacking syndecan 4 or paired box 7 (PAX7), which have compromised satellite cell function or number, respectively [90]. Another recent study reported that recruitment of satellite cells is not required for muscle hypertrophy, because hypertrophy was unchanged in mice in which more than 90% of satellite cells were ablated by diphtheria toxin A using an inducible PAX7–diphtheria toxin A transgene [91].

It is likely that satellite cells are activated and contribute to hypertrophy when an acute stimulus is involved leading to muscle damage. In contrast, more gradual exercise, or reloading of immobilized muscles, does not trigger satellite cell activation and fusion.

1.3 Inherited muscular disorders causing prominent muscles

Many genetic muscle disorders lead to muscle weakness and wasting, but only a subset also show some degree of muscle hypertrophy and muscle pain. In the following section, I will cover several aspects related to known muscle disorders that can lead to positive effects on muscle strength and mass by reviewing inherited muscular disorders causing prominent muscles.

1.3.1 McArdle disease

McArdle disease is characterized by a glycogen storage deficiency caused by autosomal recessive mutations in the glycogen phosphorylase, muscle associated (*PYGM*) gene [92]. PYGM catalyzes and regulates the breakdown of glycogen to glucose-1-phosphate during glycogenolysis and its activity is absent in patients with McArdle disease [93]. Patients present accumulations of subsarcolemmal glycogen, which they are unable to degrade [93]. PYGM metabolic pathway is necessary for the generation of ATP during physical activity [94]. The absence of myophosphorylase activity causes exercise intolerance, mainly in the form of acute crises of early fatigue and contractures [93]. Symptoms can start early in childhood, but in most cases the disease is not correctly diagnosed until late 30s [95].

Patients with McArdle disease can present with such variable phenotype. For this reason, clinical severity is classified into four categories according to the Martinuzzi scale [96]: "0 = asymptomatic or virtually asymptomatic (mild exercise intolerance, but no functional limitation in any daily life activity); 1 = exercise intolerance, contractures, myalgia, and limitation of acute strenuous exercise, and occasionally in daily life activities; no record of myoglobinuria, no muscle wasting or weakness; 2 = same as 1, plus recurrent exertional myoglobinuria, moderate restriction in exercise, and limitation in daily life activities; 3 = same as 2, plus fixed muscle weakness, with or without wasting and severe limitations on exercise and most daily life activities". In a study describing the clinical phenotype of 45 genetically confirmed McArdle patients, muscle hypertrophy is observed in 24% of patients [95]. Mild muscle wasting and weakness is seen only in patients over 40 years of age. Moreover, 99% of the patients have high creatine kinase (CK) levels [95]. Typical findings in morphological analysis of muscle biopsies include subsarcolemmal glycogen blebs and absent phosphorylase staining [95].

Most patients present a clinical feature known as "second wind" which is the marked improvement in tolerance to aerobic dynamic exercise (e.g., brisk walking), with disappearance of the tachycardia and undue fatigue that were triggered by the start of exertion [97]. This phenomenon is attributed to the improved delivery of extra-muscular glucose and fatty acids to the working muscle that occurs due to a switch to alternative fuel substrates required for aerobic metabolism. After the second wind, most patients can almost double their work effort [95].

1.3.2 Non-dystrophic myotonias

Myotonia is a term used to describe a skeletal muscle disorder caused by disturbances in the membrane potential of the myofiber. Patients with myotonia will present a delayed response to muscle relaxation upon voluntary or mechanically or electrically stimulated contraction [98]. Myotonia itself is not considered as a disease, but rather a symptom of several different neuromuscular disorders [99].

In non-dystrophic patients, myotonia happens as a painless prolonged contraction right after use of a muscle [100]. Mutations in the skeletal muscle sodium (*SCN4A*) and chloride (*CLCN1*) channels were described to cause non-dystrophic myotonia, which are also called as

channelopathies [101]. Non-dystrophic myotonias can be classified in three different but sometimes overlapping categories: myotonia congenita, paramyotonia congenita, and sodium-channel myotonia [101]. These entities present some differences in clinical features, electromyography (EMG) and gene defects [100]. They are referred to as non-dystrophic myotonias because they present no progressive weakness, wasting or dystrophic histopathology [101]. Another class of myotonic disorders are the dystrophic myotonias which consist of myotonic dystrophy type 1 (DM-1) or the classical Steinert's form of myotonic dystrophy, proximal myotonic myopathy/myotonic dystrophy type 2 (PROMM/DM-2), and proximal myotonic dystrophy (a more severe variant of DM-2) [102]. These disorders will be reviewed in more detail later in this section.

Patients with myotonia congenita carry mutations in the *CLCN1* gene. They have a muscular appearance, and action and percussion myotonia that decrease with repeated contractions [103,104]. Inheritance can be dominant or recessive, the latter being more severe [104]. Patients carrying mutations in the *SCN4A* gene have more diverse dominant inherited disorders, ranging from mild myotonia that does not affect daily activities, to severe muscle stiffness or episodes of paralysis [101]. Patients with paramyotonia congenita experience cold temperature sensitivity, worsening of myotonia upon repetitive contractions, and episodic weakness [101]. On the other hand, patients with sodium-channel myotonia have variable cold sensitivity and no episodic weakness [101]. Patients with hyperkalemic periodic paralysis can present myotonia, but episodic weakness is the main dominant feature [101].

Mutations found in *SCN4A* gene in non-dystrophic myotonias are believed to cause a gain-of-function in the channel activity [100]. Once action potential is triggered by an influx of cations through acetylcholine receptors that depolarizes the end-plate region above the threshold, sodium channels open to initiate inward sodium flux, triggering further depolarization and opening of more sodium channels [100]. These currents propagate the action potential along the surface sarcolemma and T-tubule system [100]. Although sodium channels open in response to depolarization, they quickly close again (fast inactivation) and can only re-open after repolarization (recovery from inactivation) [100]. Previous studies showed that *SCN4A* mutations lead to a poor inactivation of the channel resulting in repetitive discharges upon mild depolarization, or weakness upon severe depolarization [100].

CLCN1 is a type of chloride channel (ClC1) in skeletal muscle that plays an important role in membrane repolarization following muscular contraction [100]. Mutations found in *CLCN1* gene in non-dystrophic myotonias are believed to cause a loss-of-function in the channel activity [100]. Cells carrying these mutations lose the ability of preventing the after-depolarization caused by T-tubule potassium accumulation [100].

In general, non-dystrophic myotonias are not life-threatening, however patients can present significant lifetime morbidity because of the stiffness and pain caused by the myotonia, and in some rare cases, an infantile form can cause respiratory distress.

1.3.3 RYR1 related myopathies

Ryanodine receptor 1 (RYR1) related myopathies are a very broad class of disorders ranging from extremely mild and non-progressive to very severe and lethal conditions [105]. Some of these disorders include central core disease, multiminicore disease, core–rod myopathy, centronuclear myopathy, and congenital fiber-type disproportion. New clinical phenotypes have emerged and include malignant hyperthermia, RYR1 rhabdomyolysis-myalgia syndrome, atypical periodic paralysis, congenital neuromuscular disease with uniform type 1 fibers, and late-onset axial myopathy [105]. From all of those listed above, muscle hypertrophy has been reported in malignant hyperthermia, RYR1 rhabdomyolysis-myalgia syndrome and late-onset axial myopathy [105]; and will be briefly reviewed below.

Malignant hyperthermia is a dominant pharmacogenetic trait caused by a hypermetabolic response leading to increased heat generation due to volatile anesthetic agents administration, and in some rare cases, to stressors like vigorous exercise and heat [106]. Not only have mutations in *RYR1* have been associated with malignant hyperthermia, but recent studies also identified mutations in the calcium voltage-gated channel subunit alpha1 S (*CACNA1S)* leading to the same phenotype [106]. Most of the individuals with malignant hyperthermia present no clear phenotypic changes without anesthesia meaning that it is impossible to diagnose such a disorder without exposure to the specific trigger [106]. Some key clinical features to diagnose the susceptibility to this condition include an unexplained raise of expired carbon dioxide, muscle rigidity, rhabdomyolysis, hyperthermia, tachycardia, acidosis and hyperkalemia [106].

Rhabdomyolysis-myalgia syndrome with dominant heterozygous *RYR1* mutations without the malignant hyperthermia trait was first described in 2002 [107]. They identified 14 of 39 families with unresolved exercise-induced rhabdomyolysis/myalgia carrying mutations in *RYR1* [107]. In 2018, another study described a cohort with 22 patients from 20 families with similar symptoms and *RYR1* mutations [108]. These studies suggest that *RYR1* aberrations can be a frequent cause of exercise-induced rhabdomyolysis and/or myalgia. Some patients with this disorder have muscle hypertrophy and muscle strength can vary from normal to increased [108]. Patients basal CK levels also vary from normal to elevated [108]. Patients also complain of progressive painful muscle cramps, but without compromising weakness. In general, symptoms are triggered by physical activity [108].

Late-onset axial myopathy with dominant heterozygous mutations in *RYR1* were first described in 2013 [109]. Patients described in this study presented predominant axial muscle involvement, variable degrees of lumbar hyperlordosis, scapular winging and/or camptocormia [109]. They also had myalgia and CK levels were normal or moderately elevated [109]. Muscle imaging showed involvement of the lower paravertebral muscles and the posterior thigh [109]. Some patients of this study reported that before the onset of this disorder, they had a better physical performance than their peers or had even been involved with intense physical labor, resulting in muscle hypertrophy [109].

Histopathological findings of muscle biopsies of patients with these disorders revealed similar mild features: increased variability in type 1 fiber size, increased internal nuclei and mild unevenness on oxidative enzyme staining. A few cases presented central cores and multi-minicores, but no correlation between these features and one of these disorders has been observed [43,106,109].

RYR1 is a major calcium ion channel of the skeletal muscle [110]. It is a six transmembrane-homotetrameric protein located to the SR [110]. It has 106 exons and codes for a 565 kDa amino acid protein [110]. Upon neuromuscular action potential, DHPR activates RYR1 which undergoes a conformational change resulting in RYR1 interdomain interaction followed by calcium release from the SR that leads to EC-coupling [14]. RYR1 is regulated by several different processes including protein-protein interactions, protein-ligand interactions, and post-translational modifications [110]. Mutations found in *RYR1* gene are believed to result in constant

calcium leak at rest leading to defective EC- coupling and increased mitochondrial oxidative stress [110].

1.3.4 Brody disease and syndrome

Brody disease is an inherited muscle disorder characterized by an increasing impairment of muscle relaxation during exercise due to markedly reduced calcium uptake in the sarcoplasmic reticulum (SR) [111,112]. The main clinical feature of progressive stiffness of the exercised muscles leads to painless or only mildly painful cramping that predominantly involves the legs, arms and eyelids [111-114]. Myalgia and cramps have been described, and recurrent attacks of exertional rhabdomyolysis may also occur [113,115,116]. Symptoms usually resolve after a few minutes of rest, and they may worsen in the cold [115-117]. Serum CK is normal or slightly increased, and no myotonic discharges are recorded by electromyography [111,117-119].

Muscle biopsies may show fiber size variation with atrophy of type 2 fibers and increased central nuclei, whereas no morphologic changes are observed in the triads and in the tubular elements of SR by electron microscopy [112,113,116]. Biochemical studies have demonstrated a marked reduction of calcium ATPase activity in the muscle [112,113,115,117]. In 1996, mutations in the sarcoplasmic/endoplasmic reticulum Ca^{2+}-ATPase 1 (ATP2A1 or SERCA1) gene were found to cause Brody disease [120].

SERCA1 is a membrane-bound protein that pumps calcium from the cytosol to the SR and is coupled to utilization of ATP. The catalytic and transport cycle begins with the activation of the enzyme by high-affinity binding of 2 calcium ions, followed by ATP utilization to form a phosphorylated enzyme intermediate. The dissociation of ADP and the isomerization of the phosphoenzyme then promote displacement of calcium and, finally, the hydrolytic cleavage of Pi. The protein contains 994 aa arranged in 10 helical segments (M1-M10) within the transmembrane region; 3 headpiece domains (N, P, and A domain) project from the cytosolic surface of the membrane. SERCA1 is only present in fast-twitch muscle fibers (type 2), so it is suggested that the impaired relaxation specifically occurs after phasic exercise (alternate contraction and relaxation) [112,117].

Some have proposed to distinguish patients with reduced SERCA1 activity and ATP2A1 mutations (Brody disease) from patients with reduced SERCA1 activity without ATP2A1 mutations (Brody syndrome) [55]. Brody syndrome patients generally suffer from (exercise-induced) muscle stiffness and delayed muscle relaxation; however, only a few muscle groups are involved, and onset is in adolescence or adulthood [55].

The differences between Brody disease and Brody syndrome raise the question whether Brody syndrome is a separate entity or an epiphenomenon of other underlying diseases with a final common pathway of altered calcium transport. Of all previously described conditions, Brody Syndrome is the one that has the most clinical overlap with Strongman trait, the subject of this thesis.

1.3.5 Rippling muscle disease

Rippling muscle disease (RMD) is a rare, generally benign myopathy with signs and symptoms of muscular hyperexcitability. The clinical symptoms are muscle stiffness, muscle hypertrophy, slowness of movements after rest, exercise-induced muscle pain, and cramp-like sensations. Muscle taps and passive stretching induce involuntary contractions of muscle fibers that roll over the muscle surface, which gives rise to the name of the disease [121,122].

Taps on the muscles also evoke percussion-induced rapid contraction (PIRCs) or, if performed with a reflex hammer, a localized myoedema, also termed muscle mounding. These three key features are the classical features of RMD: rippling muscles, PIRCs and myoedema [123].

Genetic studies have revealed that many cases of RMD are caused by mutations in the gene encoding caveolin-3 (*CAV3*) that lead to its reduced expression in the sarcolemma. In addition to RMD, CAV3 defects can lead to other skeletal muscle disease phenotypes—namely, limb girdle muscular dystrophy, distal myopathy, and hyperCKemia (a disorder involving elevated serum levels of CK), and familial hypertrophic cardiomyopathy [121,122]. In addition, the same CAV3 mutation can be linked to different clinical phenotypes, often within the same family. RMD has an autosomal dominant mode of inheritance, although evidence suggests that an autosomal recessive and more severe variant of RMD exists [121,122].

On EMG, rippling muscles are electrically silent, and the mechanism underlying this phenomenon is not fully understood [121,122]. Local contraction in one portion of a fiber stretches and thereby activates neighboring sarcomeres, which in turn stretches and activates sarcomeres further along the fiber [121,122]. Alternatively, action potentials generated and propagated in an aberrant tubular system, which would be silent on EMG, could play a part in the pathophysiological mechanism of rippling [121,122].

Caveolin is a 150 aa-long protein which acts as a structural determinant of plasma membrane caveolae [124]. It is thought to operate as a multifunctional scaffold through associations with several partners. In skeletal muscle, CAV3, the striated muscle isoform [124], has been shown to interact with a number of proteins including beta-dystroglycan [125], dysferlin [126], nNOS [127], PI3K [128], Src-kinase [129] and phosphofructokinase [130] and is thought to play a role in developmental processes [131,132].

A pool of CAV3 is localized to T-tubules of adult skeletal muscle [124]. Recently, the consequences of expressing the P104L dominant negative mutant form of caveolin-3 (Cav-3P104L), responsible for human type 1C limb-girdle muscular dystrophy, was evaluated in primary cultured myotubes and skeletal muscle fiber [133,134]. They observed an almost complete depletion of endogenous CAV3 and a strong reduction of the density of the voltage-dependent L-type calcium current [133,134]. They postulated that CAV3 may interact directly or indirectly with DHPR and that the observed reduction of calcium current in CAV3 deficient muscle cells could result from a loss of this interaction [133,134].

Cardiac CAV3 has been shown to be part of a macromolecular complex comprising the β2-adrenergic receptor, G-proteins, protein kinase A and the Cav1.2 pore-forming subunit of the cardiac L-type Ca^{2+} channel [135]. Caveolin-3 was also shown to co-immunoprecipitate with skeletal muscle RYR1 [136].

1.3.6 Other muscular dystrophies with skeletal muscle hypertrophy

ANO5 anoctaminopathies are a group of autosomal recessive skeletal muscle disorders with variable clinical features caused by mutations in anoctamine 5 (*ANO5* or *TMEM16E*)

[137,138]. These disorders can be divided in three main categories: limb-girdle muscle dystrophy type 2L (LGMD2L), Miyoshi muscular dystrophy 3 (MMD3) and asymptomatic hyper-CK-emia [10,138,139]. Some patients with LGMD2L and asymptomatic hyper-CK-emia can present muscle hypertrophy that can be asymmetric or not, more frequently of the calves [139] LGMD2L is the most frequent of the ANO5 presentation characterized by late adult onset, slowly progressing asymmetric weakness and atrophy of proximal muscles, high CK levels, and myopathic features on muscle histology and EMG [137,140]. Little is known about ANO5 function. It is part of the transmembrane protein family 16 (TMEM16) in which ANO1 (or TMEM16A) and ANO2 (or TMEM16B) have been described to have a calcium-activated chloride channel activity while ANO6 acts as a calcium-dependent phospholid scramblase [141]. As for the other members of the family, no such consensus on their functional roles has been shown yet. A recent study showed that overexpressed ANO5 presents a phospholipid scrambling activity as well as a non-selective ion transport activity [142]. A previous study showed an Ano5-deficient mouse model presented reduced capacity to repair the sarcolemma, delayed regeneration after injury and defective myoblast fusion, features that recapitulate what is observed in patients with LGMD2L and MMD3 [143]. How the phospholipid scramblase activity and/or non-selective ion transport activity could be linked to the features observed in patients with anoctaminopathies or in the Ano5-deficient mice is still a subject for further investigation.

Myotonic dystrophy is the most common adult onset muscular dystrophy characterized by an autosomal dominant progressive myopathy with multisystemic features. It is primarily characterized by myotonia and progressive muscle weakness as well as cardiac conduction defects, posterior iridescent cataracts, and endocrine disorders [102,144]. Myotonic dystrophy exists in two defined forms: DM1, also known as Steinert's disease; and DM2, also known as proximal myotonic myopathy. Both are inherited in an autosomal dominant fashion [102,144].. DM1 is caused by a CTG expansion in the 3' untranslated region of the dystrophia myotonica protein kinase (DMPK) gene, while DM2 is caused by a CCTG expansion located within intron 1 of the cellular nucleic-acid- binding protein (CNBP, formerly zinc finger protein 9, ZNF9) gene ([102,144]. Although DM1 and DM2 have similar symptoms, they also present different features making them clearly separate diseases. One of these differences is that in DM2 patients exhibit hypertrophy of calf and thigh muscles, which on histologic examination is true hypertrophy with

enlargement of muscle fibers [145]. Moreover, DM2 presents milder clinical features when compared to DM1 [102,144].

The DM1 and DM2 gene discoveries were perplexing because DMPK and ZNF9 have no functional connections yet the clinical features are similar [102,144]. Experimental evidence supports an RNA gain-of-function mechanism in which expanded CUG/CCUG-containing transcripts accumulate in the cell nuclei as foci, also called ribonuclear inclusions, and are responsible for the pathologic features common to both disorders [102,144]. The mutant RNAs form imperfect double-stranded structures which lead to the deregulation of several RNA binding factors, including the muscle blind-like proteins (MBNLs), CUG-binding protein 1 (CUGBP1), heterogeneous nuclear ribonucleoprotein H (hnRNP H) and Staufen Double-Stranded RNA Binding Protein 1 (STAU1) proteins [144]. Thus, the misregulation of alternative splicing caused by the deregulation of several splicing regulators clearly plays a central role in the development of important DM symptoms[144]. Among the symptoms of DM, myotonia, insulin resistance and cardiac problems are correlated with the disruption of the alternative splicing of the muscle CLCN1, of the insulin receptor (IR) and of the cardiac troponin T (TNNT3), respectively. However, there is no direct evidence of a cause–effect relationship between symptoms and missplicing [102,144].

Despite all the efforts made so far to identify the pathology of individuals that have mild inherited adult onset muscle disorders associated with prominent muscles, there is still a great number of patients that end up without a clear diagnostic. In the following chapters, I will provide significant data on a new Herculean myalgic muscle disorder, which impairs important regulators of calcium handling of the skeletal muscle.

Figures

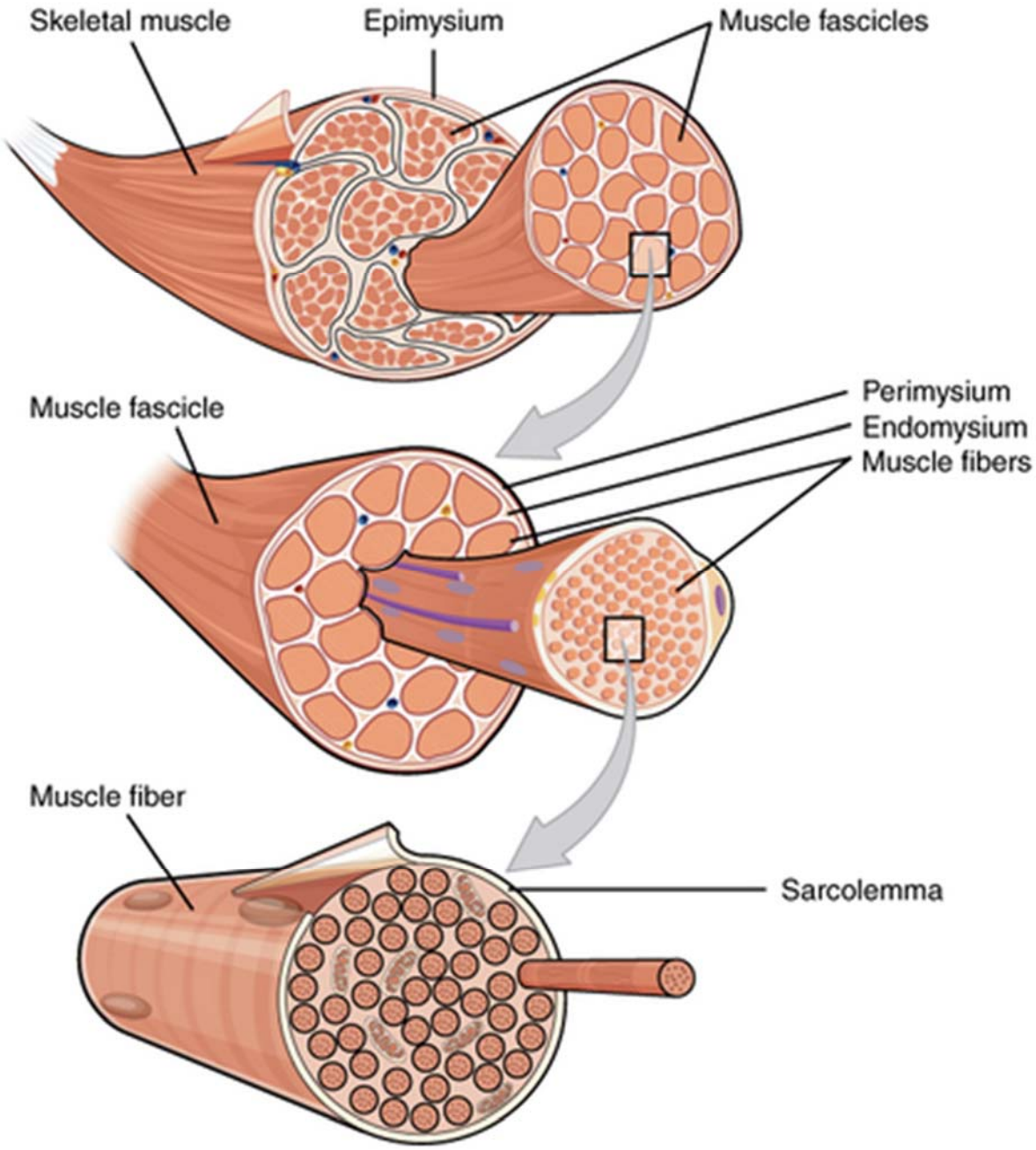

Figure 1.1 Schematic of skeletal muscle structure. Each skeletal muscle is involved by the epimysium. Every muscle contain bundles of myofibers are called fascicles and those are covered by the perimysium. Each myofiber are covered by the endomysium. Reproduced from OpenStax CNX (https://cnx.org/contents/FPtK1zmh@15.1:bfiqsxdB@6/10-2-Skeletal-Muscle).

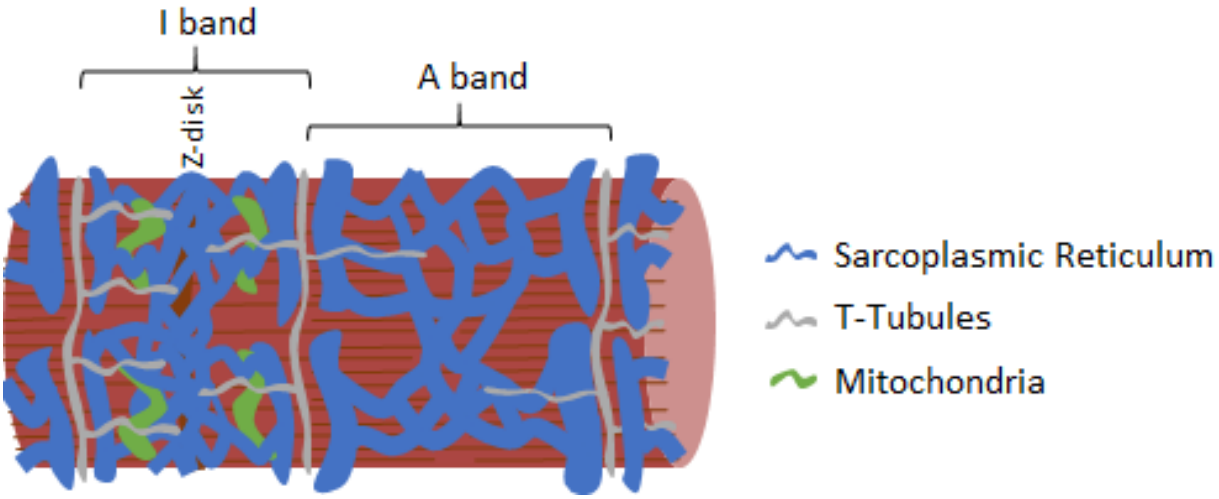

Figure 1.2 The Sarcotubular System. Each myofibril is involved by an organized network of membranes: the t-tubules (in gray) that are localized to both extremities of the I-band; the sarcoplasmic reticulum (in blue) that spreads all over the I and A-band juxtaposing the t-tubules; the mitochondria (in green) that is localized in pairs just next to the Z-disk.

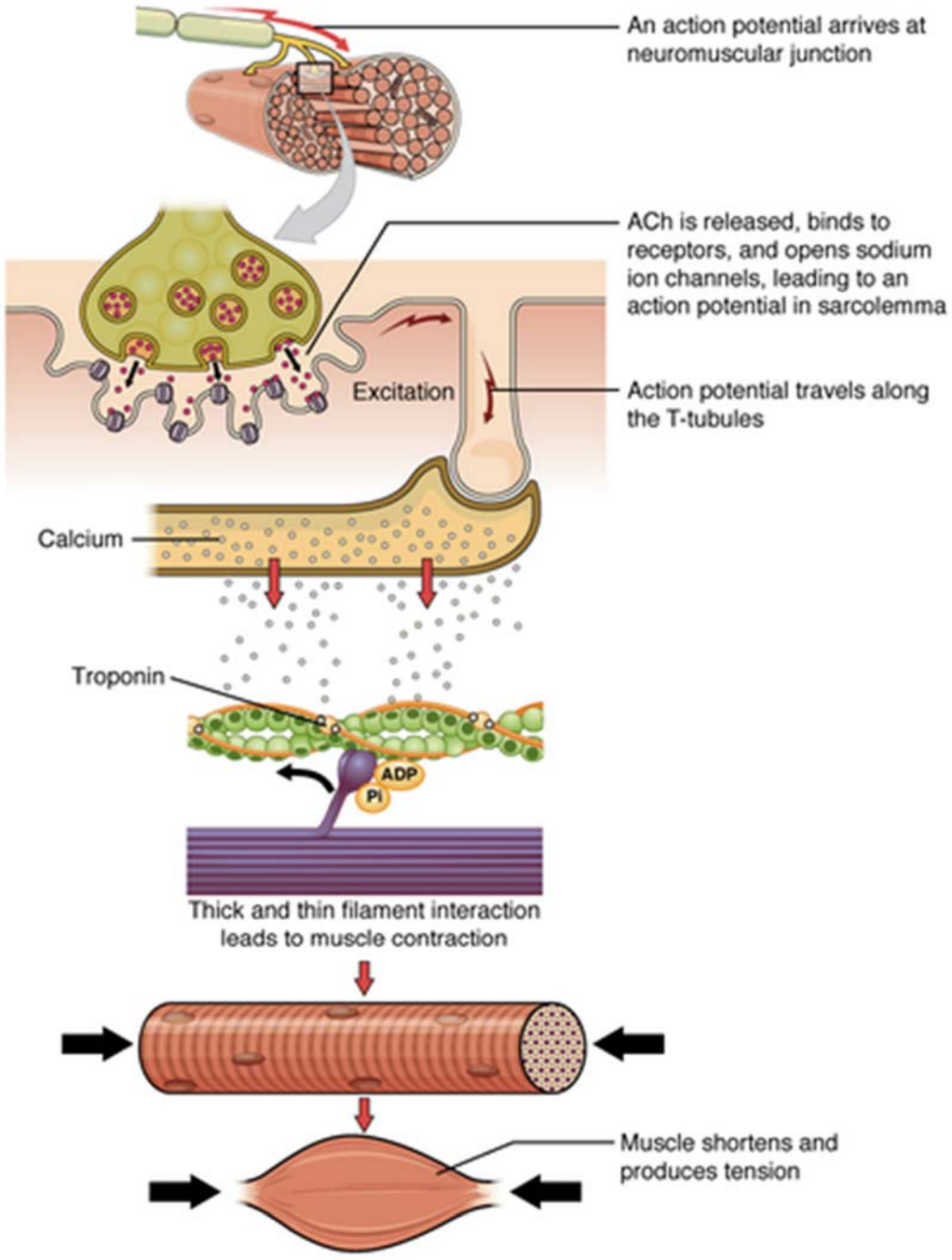

Figure 1.3 Contraction of a Muscle Fiber. Once there is an action potential, the t-tubules are depolarized and the sarcoplasmic reticulum releases calcium to the sarcoplasm. Actin and myosin form the cross-bridges triggering contraction. The calcium ions that remain in the sarcoplasm will continue to bind to troponin, and if there is ATP available, the muscle fiber will continue to contract. Reproduced from OpenStax CNX (https://cnx.org/contents/FPtK1zmh@15.1:EtWWcJM-@10/10-3-Muscle-Fiber-Contraction-and-Relaxation)

RATIONALE, HYPOTHESIS AND OBJECTIVES

There is a vast literature describing the regulation of muscular strength and mass in physiological conditions, however, very few studies have addressed this subject in the context of inherited muscular disorders. In fact, very few of these disorders are associated with generalized hypertrophy or are accompanied by true Herculean strength. A better characterization of individuals with large muscle mass, above average strength and myalgia is a fertile field of investigation where disease and trait intersect or could be seen to form a spectrum. The association of myalgia, muscle hypertrophy and known myopathies was one of the elements that convinced us that we could uncover new genetic conditions if we focused our recruitment on individuals who met the following minimum selection criteria: observed muscle hypertrophy, a personal and familial history of superior strength and myalgia. In other words, once we formed a cohort of myalgic patients that appear to suffer from inherited myopathic conditions, ***we first hypothesized that new causal genes are responsible for the ST***. Therefore, the **first objective** of this thesis was to characterize **clinically and pathologically ST and identify a first causal gene by studying a large French-Canadian family.**

Despite being able to identify and validate a variant in the *DCST2* gene and to show that the mutation was having an effect in the dynamics of DCST2 puncta formation, we were still unable to predict how this mutation would impact ST muscle since DCST2 is a gene with unknown function. We then ***hypothesized that the DCST2 ST mutation leads to a perturbation in a pathway involved in force generation causing prolonged powerful contraction leading to fatigue and weakness after repeated contractions.*** The **second objective** of this thesis was to **start to establish the localization and physiological role of DCST2 in muscle.**

DCST2 mutation was found in only two French-Canadian families indicating that the causative genes in the remaining families could be involved in the same pathological mechanism as DCST2. ***We hypothesized that ST patients that do not carry DCST2 mutations would share similar pathological findings as ST patients that carry DCST2 mutations***. The **third objective** was to **explore common pathological findings shared by ST patients carrying or not a *DCST2* mutation that could serve to support a ST diagnosis.**

PREFACE TO CHAPTER 2

The Brais laboratory specializes in identifying new mutations that cause neuromuscular diseases. Dr. Brais recruited a cohort of patients who presented at the neuromuscular clinics presenting symptoms that had never been characterized before. Patients suffered from muscle pain, cramps and reduced endurance as well as increased muscle strength and mass. These patients were recruited for further genetic studies. Chapter 2 describes the genetic, molecular and pathological characterization of this new form Herculean myalgic muscle disorder.

CHAPTER 2: A mutation in *DCST2* causes a Strongman trait by dysregulating skeletal muscle calcium handling

Short running title:

Mutated *DCST2* causes a Strongman trait

Talita C. Conte[1,2*], Martine Tétreault[3*], Marie-Josée Dicaire[1], Ariel R. Ase[4], Sylvie Provost[5], Marie-Pier Roussel[6,7], Hana Antonicka[2], Rebecca Robertson[1,2], Benjamin Beland[1], Véronique Bolduc[8], Najwa Al-Bustani[9], Myriam Srour[10], Erin K. O'Ferrall[11], Alexandre Janer[2], Tanja Taivassalo[12], Anne-Claude Gingras[13], Russell Hepple[14], Elise Duchesne[6,7], Marie-Pierre Dubé[5], Eric A. Shoubridge[2], Philippe Séguéla[4], Jean Mathieu[7], Bernard Brais[1,2]

Affiliations:

1) Neurogenetics of Motion Laboratory, Department of Neurology and Neurosurgery, Montreal Neurological Institute, McGill University, Montreal, Quebec, Canada.
2) Department of Human Genetics, McGill University, Montreal, Quebec, Canada.
3) Department of Neurosciences, Centre de Recherche du Centre Hospitalier de l'Université de Montréal (CRCHUM), Montreal, Quebec, Canada.
4) Department of Neurology & Neurosurgery, Montreal Neurological Institute, Alan Edwards Centre for Research on Pain, McGill University, Montreal, Quebec, Canada.
5) Montreal Heart Institute Research Center, Beaulieu-Saucier, Université de Montréal, Pharmacogenomics Centre, Montreal, Quebec, Canada
6) Health Sciences Department, Université du Québec à Chicoutimi, Saguenay, Quebec, Canada.
7) Groupe de Recherche Interdisciplinaire sur les Maladies Neuromusculaires, Centre Intégré Universitaire de Santé et de Services Sociaux du Saguenay-Lac-St-Jean, Saguenay, Quebec, Canada.
8) Neuromuscular and Neurogenetic Disorders of Childhood Section, Neurogenetics Branch, National Institute of Neurological Disorders and Stroke/National Institutes of Health, Bethesda, Maryland, USA.
9) Department of Neurology, Neurological Institute, Cleveland Clinic Abu Dhabi, Abu Dhabi, United Arab Emirates.
10) Division of Pediatric Neurology, Department of Pediatrics, Montreal Children's Hospital, McGill University Health Centre (MUHC), Montreal, Quebec, Canada.
11) Departments of Neurology and Neurosurgery and of Pathology, McGill University Health Centre, Montreal Neurological Institute Hospital, Montreal, Quebec, Canada.
12) Department of Physiology and Functional Genomics, University of Florida, Gainesville, Florida, USA.

13) Lunenfeld-Tanenbaum Research Institute, Sinai Health System, Toronto, Ontario, Canada; and Department of Molecular Genetics, University of Toronto, Toronto, Ontario, Canada.
14) Department of Physical Therapy and Muscle Biology, University of Florida, Gainesville, Florida, USA.

Abstract

Herculean strength has always fascinated humankind. Through history, muscle force has often been considered a familial trait. The relatively small French-Canadian founder population of Quebec has been a hot bed for strong men of international reputation. To search for genes that could influence strength, we recruited a set of 12 families whose probands consulted for muscle pain and fatigue despite having above average muscle mass and a personal and family history of superior strength. In particular we investigated a large French-Canadian family of 20 affected individuals presenting a dominant Strongman trait. Affected individuals displayed above average strength, muscle hypertrophy, prolonged contractions and a variable degree of myalgia. We mapped the strongman trait locus to chromosome 1q21.3-q23.3 and uncovered a c.2276T>C (p.Leu759Pro) dominant missense mutation that segregated in two strongman trait families in the DC-STAMP Domain Containing 2 (*DCST2*) gene. Using a proximity-dependent biotinylation (BioID), we identified potential DCST2 interactors that localize to the endoplasmic reticulum including four proteins involved in calcium handling: STIM1, CCDC47, LMAN1 and ITPR3. DCST2 forms large puncta in strongman trait skeletal muscle localized to the I-band in proximity to the T-Tubules that contain the calcium sensor stromal interaction molecule 1 (STIM1) and the calcium transporter sarco/endoplasmic reticulum Ca2+-ATPases (SERCAs). In differentiating strongman trait myoblasts, the depletion of sarcoplasmic reticulum calcium stores led to an increase in the number and size of large DCST2 puncta over time and a decrease in calcium transients. We show that DCST2 is implicated in calcium handling in differentiating myoblasts and that larger and more abundant strongman trait DCST2-L759P puncta are associated with a partial loss of function of store-operated calcium entry and SERCA dependent sarcoplasmic reticulum calcium reuptake. The significant increase in size and number of DCST2-L759P puncta containing STIM1 and SERCAs in strongman trait muscle suggest that it is related to a compensatory response to dysregulated calcium handling that is likely responsible for the increased strength and associated weakness after repeated contractions. The relatively high minor allele frequency of 0.06487% (1:1542) for the *DCST2* mutation suggests that it may be a frequent cause of muscle hypertrophy, superior strength and myalgia in humans.

Key words: Strongman trait; DCST2; calcium; SOCE

Abbreviations: DCST2 = DC-STAMP Domain Containing 2; STIM1 = sensor stromal interaction molecule 1; SERCAs = calcium transporter sarco/endoplasmic reticulum Ca^{2+}-ATPases; CCDC47 = Coiled-Coil Domain Containing 47; LMAN1 = Lectin Mannose Binding 1; ITPR3 = Inositol 1,4,5-Trisphosphate Receptor Type 3.

Introduction

The number of genes associated with neuromuscular disorders is expanding at a fast pace largely due to progress in next generation sequencing. However, contemporary neurogenetics is still facing considerable challenges in identifying new entities with milder and more variable intra-familial muscle symptoms that are often not associated with recognized electrophysiological or pathological findings [55,111,122,137,146]. Familial muscle hypertrophy associated with superior strength poses such a diagnostic challenge. True muscle hypertrophy defined as increased muscle mass has been documented in several myopathies, but is also observed in patients consulting for myalgia, cramps, prolonged contractions (myotonia) and muscle fatigue with a negative laboratory investigation [55,111,122,137,146]. In some myopathies, the increased size of certain muscles corresponds to fatty replacement referred to as pseudohypertrophy, which is usually associated with muscle weakness as seen in Duchenne muscular dystrophy (DMD) [147]. The list of hereditary myopathies associated with muscle hypertrophy and increased strength has been expanding, and includes: McArdle disease caused by recessive mutations in myophosphorylase (*PYGM*) [148], non-dystrophic myotonias caused by mutations in the chloride voltage-gated channel 1 (*CLCN1*) or the sodium voltage-gated channel alpha subunit 4 (*SCN4A*) genes [149], mutations in ryanodine receptor 1 (*RYR1*) associated with malignant hyperthermia susceptibility and other RYR1 related myopathies [108,150,151], Brody disease caused by mutations in ATPase sarcoplasmic/endoplasmic reticulum Ca^{2+} transporting 1 (*SERCA1*) [55] and rippling muscle disease caused by mutations in caveolin 3 (*CAV3*) [122]. The most widely publicized human mutation associated with muscle hypertrophy occurs in myostatin (*MSTN*), but only a single pediatric case has been reported to date [38]. Although Mstn knockout animal models show overall hypertrophied muscles, they present with a variable increase in muscle strength [41,152]. We have used a personal and familial history of supra-normal strength as means to cluster a group of patients with hypertrophied muscles who consulted for myalgia, cramps and fatigue, but with negative work-ups, to search for new genes causing a dominant Strongman Trait (ST), and identified a first mutation in the *DCST2* gene involved in calcium handling in skeletal muscle.

Materials and methods

Family recruitment

All participants underwent detailed examination by experienced neurologists. Sample collection was performed with written informed consent approved by the ethics board of the Montreal Neurological Institute according to the Declaration of Helsinki. DNA was isolated from peripheral blood lymphocytes using Gentra Puregene blood kit (Qiagen) according to the manufacturer's protocol. Specific consent was provided to print modified self-portraits that ensure confidentiality of individual I:III.

Genotyping and linkage analysis

Genotyping was first performed on 15 family members (family I) using the Illumina OmniExpress v1.2 SNPs chip containing 700K markers (Illumina, CA, USA). The SNPs chip was run at the McGill University and Genome Quebec Innovation Centre (Montreal, QC, Canada). Fine mapping of candidate regions on all 42 samples was performed using the microsatellite markers: D1S442, D1S498, D1S2343, D1S2345, D1S2715, D1S2777, D1S2624, D1S2771, D1S2707, D1S484 and D1S2844. Two-point and multipoint parametric linkage using a dominant mode of inheritance was computed using MLINK v2 [153] and Simwalk2 v2.90 [154] respectively .

Exome and Sanger sequencing

Whole exome sequencing was performed on five individuals indicated with asterisks on pedigree of family I at the Perkin Elmer facilities. Exons were captured using the Agilent SureSelect 50Mb capture kit (v4) and the sequencing was performed on an Illumina HiSeq2000. Data analysis was performed via Perkin Elmer webportal. Whole exome sequencing results were aligned to the Human reference genome (UCSC genome browser Hg19) using Burrows-Wheeler Alignment Tool (BWA v.0.6.2) [155]. Duplicates were marked using Picard tools and Genome Analysis Toolkit (GATK v.1.6) [156] was used for base-quality recalibration, local sequence realignment for indels optimization, and variant filtering to minimize base calling and mapping errors. Variant calling was performed using GATK Unified Genotyper. Finally, variants were annotated using GATK. We obtained high quality sequencing results, with an average of 98% of the reads mapping to the reference sequence and more than 60% of the nucleotides covered at

30X or more. Variants were validated by Sanger sequencing at McGill University and Genome Quebec Innovation Centre (Montreal, Quebec, Canada). The p.Leu759Pro was found in 3 unrelated participants of 1209 Care4Rare Canada Consortium WES which included trios and some larger families. None had been recruited for a muscle phenotype and information on ethnicity was not available on all individuals. The genotyping of 96 unrelated French Canadian participants without a ST from different regions of Quebec did not uncover a carrier.

Muscle biopsy

Four controls and one patient (individual I:XV, Family I) were subjected to muscle biopsies. A biopsy of the left vastus lateralis at the mid-thigh level was taken using the modified Bergstrom needle technique with suction [157]. A ~200mg sample of muscle was obtained and portioned out for the various analyses described as follows: ~50 mg of muscle was used for myoblast cell culture, two ~40 mg muscle biopsies were immediately snap frozen in liquid nitrogen for protein and RNA extraction; other ~70 mg of solid pieces of muscle were mounted with the muscle fibers in transverse and longitudinal orientation on specially engineered plastic blocs in Tragacanth gum and frozen in liquid isopentane cooled in liquid nitrogen. All samples were stored at −80◦C until analysis.

Skeletal muscle morphology analysis

Three muscle biopsies from patient I:XIX were previously analyzed in clinical pathology laboratories and no tissue was left for analysis at the launch of this study. In the clinical laboratories, the sections were reacted or stained by the following methods: H&E, modified Gomori Trichrome, cytochrome C oxidase, succinate dehydrogenase, acid phosphatase, ATPase reacted sections at pH 4.3, 4.6 and 9.4, periodic acid Schiff, and myophosphorylase. Immunostaining for desmin and actin was also performed.

Cell lines

Control and patient myoblasts were established from muscle biopsies, sorted, immortalized, propagated, and fused as described previously [158]. Myoblasts were grown in Sk MAX media (Wisent Bioproducts) complemented with Sk MAX supplement and 20% fetal bovine serum (FBS). Myoblasts differentiation was induced by exposing cells to 2% horse serum (HS) in

Dulbecco's modified Eagle's medium (DMEM) media. HEK293 Flp-In T-REx cell lines were grown in high-glucose DMEM supplemented with 10% FBS, at 37°C in an atmosphere of 5% CO^2.

DCST2 cDNA cloning, mutagenesis, and transfection

Wild-type DCST2 cDNA was amplified from pENTRY-223.1-hDCST2 plasmid (DNASU). Purified PCR products and pcDNA6V5hisB empty vector were digested with *BamH*I and *Xho*I (NEB). After gel extraction, the digested construct and vector were ligated and transformed into DH5α competent cells and plated on ampicillin lysogeny broth (LB) agar plates. Plasmid DNA extracted from bacterial clones was sequenced for the insert. BirA*-FLAG constructs were generated using Gateway cloning into the pDEST5-BirA*-FLAG-N-ter vector. Mutated DCST2-L759P construct (missense T>C at the position c.2276) was produced by site-directed mutagenesis using the QuikChange II kit (Stratagene, Agilent Technologies, Santa Clara, CA). Control myoblasts and HEK293 Flp-In T-REx cells were transfected with wildtype and mutated DCST2 plasmids with Lipofectamine 3000 (Life Technologies) as indicated by the manufacturer.

Western blotting

Total cell and tissue protein lysates were prepared in RIPA buffer followed by sonication. Protein quantification was performed using the DC colorimetric assay (Bio-Rad). Homogenates were run on a NuPAGE Bis-Tris gel (Life Technologies) and transferred onto a nitrocellulose membrane (Bio-Rad). Immunoblots were probed with the following primary antibodies: anti-DCST2 was raised against the C-terminal peptide CGQPQDEGDMENT, at position 602-614aa (MediMabs in-house rabbit), anti-STIM1 (310954, BD Biosciences), anti-SERCA1 (MA3-912, ThermoFisher), anti-FLAG (F1804, SigmaAldrich), anti-biotin (200-002-211, Jackson Immunoresearch), anti-Calumin (HPA029674, SigmaAldrich), anti-IP3R (D53A5, Cell Signaling), and anti-actin (Ab3280, Abcam).

Immunofluorescence

Cells were plated on coverslips prior to labeling. They were fixed in PBS containing 4% paraformaldehyde for 10 min at room temperature (RT) and kept in PBS at 4°C until used. Cells were permeabilized in 0.1% Triton in PBS, rinsed 3×5 min with PBS, and then blocked in horse

serum (HS, 5%) in PBS for 30 min at RT. Cells were incubated 1 hour with the primary antibody diluted in 3% HS in PBS, washed in PBS 3×5 min and then incubated for 1 hour with the appropriate secondary antibody diluted in 3% HS in PBS with donkey polyclonal anti-rabbit 488, donkey polyclonal anti-mouse 555 or donkey polyclonal anti-rat 647 (Jackson Immunoresearch). Coverslips were mounted with ProLong™ Gold antifade reagent with DAPI (ThermoFisher). Primary and secondary antibodies were mixed together during the incubation for double staining experiments. Primary antibodies used were V5 (R960-25, ThermoFisher), KDEL (ab50601, Abcam), DCST2 (MediMabs in-house antibody), p62 (sc28359, Santa Cruz), LAMP2 (ab5631, Abcam), and ubiquitin (39365, Cell Signaling). Cell cytoskeletal F-actin was labeled with Alexa Fluor™ 488 Phalloidin (ThermoFisher).

Ten micron-thick serial cross and longitudinal sections of control and patient muscle were cut in a cryostat at -22°C and mounted on lysine-coated slides (Superfrorst Fisherbrand). Human muscle sections were immunolabeled as follows: sections were fixed with 4% paraformaldehyde (PFA) for 15 minutes, blocked and permeabilized with a TBS solution containing 5% normal donkey serum (NDS), 0.25% Triton and 0.1M glycine for 1 hour, incubated overnight with primary antibodies, incubated with secondary antibodies for 1 hour and mounted. Primary MHCs antibody cocktail that was composed of a mouse IgG2b monoclonal anti-MHC type I (BA-F8, 1:25), mouse IgG1 monoclonal anti-MHC type IIa (SC-71, 1:200), mouse IgM monoclonal anti-type 2x MHC (6H1, 1:25) and a rabbit IgG polyclonal anti-laminin (L9393, Sigma), the immunolabeling was done as described previously [159]. All primary antibodies targeting MHCs were purchased from the Developmental Studies Hybridoma Bank (DSHB, University of Iowa, IA). DCST2 (MediMabs in-house antibody) was double labeled with SERCA1 (MA3-912, ThermoFisher), STIM1 (310954, BD Biosciences), RYR1 (MA3-925, ThermoFisher), DHPR (MA3-920, ThermoFisher), OPA1 (612606, BD Biosciences), and desmin (M0760, Dako).

Confocal imaging

Stained cells or tissue slides were imaged using 20x or 60x objectives on a Zeiss LSM 710 laser scanning microscope (Carl Zeiss Canada Ltd., Toronto, ON, Canada; McGill Life Sciences Imaging Facility) using Zeiss LSM acquisition software. Images were processed using Zen 2009 Image Browser software (Carl Zeiss, Jena, Germany) or Fiji software. Sister cultures were used in all experiments in which comparisons were made. Images for quantification were captured

using the same parameters to allow comparisons to be made between conditions. For the quantification of MHCs in muscle biopsies, images were acquired with Stereo Investigator software (MBF Bioscience) and quantitative and morphometric data were obtained by analyzing images with ImagePro Plus software (Media Cybernetics, Inc.). Myofiber cross-sectional area (CSA) was obtained by measuring between 200 and 300 myofibers per individual. For quantification of large puncta in differentiating myoblasts treated or not with thapsigargin (TG), only compact DCST2 puncta with an area of at least 1 μm^2 were considered. Large DCST2 puncta were counted in 200-500 cells from control and patient's myoblasts in differentiation for 2 days. Determination of the area of the large DCST2 puncta from these cells was done by creating maximum projections of stacking images to produce images containing whole cell bodies. Puncta larger than 0.8 μm^2 were measured, 20-30 puncta were analyzed per group. Quantification of DCST2 puncta number and area in control and patient's muscle sections was done counting only the puncta that were larger than 0.06 um^2. DCST2 puncta area was determined using Fiji software using its "particle analysis" tool. Analysis of DCST2 and SERCA1 or STIM1 colocalization in skeletal muscle tissue was done with the Fiji software: merged images were split, thresholded and binarized; the "Image calculator" plug-in from Fiji combined DCST2 and SERCA1 or STIM1 images through the "subtract" operation option creating a new image with just puncta that colocalized the two proteins. White pixels from the generated images were measured for quantification of DCST2 and SERCA1 or STIM1 colocalization.

BioID assay

DCST2 was N-terminally tagged with BirA*-FLAG and integrated stably in HEK293 Flp-In T-REx (Invitrogen) cells for tetracycline inducible expression. Induction of expression, in vivo biotinylation and purification of biotinylated proteins followed by their identification by mass spectrometry on a Thermo Orbitrap Elite mass spectrometer were performed in biological duplicates, essentially as described previously [160]. Data were searched using Mascot and Comet[161] against the human and adenovirus complements of the RefSeq database (v57) appended with common contaminants, and the peptides were combined into proteins using iProphet [162]. Only proteins identified with an iProphet probability ≥ 0.95 and ≥ 2 unique peptides were further considered. Data scored against a total of 37 negative controls expressing the BirA*

tag alone and non-transfected cells using SAINTexpress [163] v3.6.1 with default options and 2-fold control compression; data were sorted by decreasing fold change compared to the control.

Calcium handling assays

Cells were plated on glass bottom dishes coated with poly-D-lysine at a density of 1E5-2E5 cells/dish. Prior to recording, cells were loaded with 5 μM Fura-2 AM (Molecular Probes) + 0.1% Bovine Serum Albumin (BSA) for 40 min and then washed for 30 min with the extracellular solution containing in mM: 152 NaCl, 5 KCl, 2 CaCl2, 1 MgCl2, 10 HEPES and 10 glucose, pH 7.4, at 37°C in 5% CO_2. During recording, the cells were constantly perfused with the extracellular solution. Fluctuation of intracellular calcium levels was measured using single-cell microfluorescence. Cells were selected using an inverted TE2000-U microscope (Nikon) equipped with 40X oil-immersion objective [CFI super(S) fluor, Nikon]. Fura-2 was excited at 340 nm and 380 nm every second and emission at 510 nm was detected with a high-resolution cooled CCD camera (Cool Snap-HQ, Roper Scientific/Photometrics) interfaced to a PC. Changes in intracellular calcium levels were determined by the ratio of fluorescence at 340 nm and 380 nm (340/380 ratio) calculated using the Metafluor 7.0 software (Molecular Devices). For each cell, net increase in intracellular calcium was determined by subtracting the baseline ratio from the peak ratio of the response (ΔF=F-Fo), divided by the baseline (ΔF/Fo). All experiments were conducted at room temperature. Store-operated calcium signaling was induced in cultured HEK293 cells and differentiating myoblasts (differentiated for 2 or 5 days) by applying or not 1 μM of the SR/ER Ca^{2+} ATPase blocker thapsigargin (Tocris) for 7 min in calcium-free perfusion solution. Ca^{2+} transients were also elicited by application of 100 mM KCl for 15 seconds.

Statistical analysis

Comparisons in which just control and patient samples were analyzed were made using unpaired two-tailed Student's t-test with Welch's correction. Statistical analysis of the number of DCST2 puncta on different time points of TG treatment (Fig. 2.3H) and quantification of calcium levels on TG-evoked or KCl calcium depletion in control and patient's differentiating myoblasts (Fig. 2.3A, C, Supplementary Fig. 2.7A) were done using one-way ANOVA test for multiple comparisons with Fisher's LSD test. Significance was established at $P<0.05$. P values are specified in the figure legends.

Data availability

Raw exome sequence and BioID data are available from the corresponding author on request. Raw exome sequence data is not publicly available since they contain information that could compromise research participant privacy. The authors confirm that the data supporting the findings of this study are available within the article and in its supplementary materials.

Results

Clinical features and genetic analysis

We recruited the families of a cohort of 12 cases who consulted for muscle pain (myalgia), muscle cramps, decreased endurance and preserved large muscle bulk (despite a relatively low level of physical activity), with a family history of above normal strength in at least two members including the probands. The largest family included 20 variably symptomatic individuals out of 42 examined. We considered individuals that presented at least two of the three following signs as carrier of the Strongman trait (ST): large muscles, prolonged delayed muscle relaxation following percussion (with no electrical activity: pseudomyotonia) in multiple muscles in the cases that had EMGs, and deltoid weakness after 20 contractions (Fig. 2.1A, Family I; Table 2.1). The age of onset in the most symptomatic males in this family was adolescence, with variable severity of negative symptoms. The mean age of onset in the 12 probands was 31 (13-50) with 50% being males. In family I, the proband (I:XIX) sought medical attention at age 26 because of severe post-activity myalgia reported as muscle soreness and sustained muscular contractions that interfered with his construction work. He had a clear personal and family history of above-average strength. For example, as a young man he had successfully lifted the back of a car and turned it 270° by himself. Muscle hypertrophy in this family is illustrated by self-portraits of a cousin at age 16 and 20 (Fig. 2.1A and 2.1B, individual I:III). The proband's electromyograms were repeatedly normal, and three muscle biopsies were interpreted as normal for routine stains. Similarly, the muscle biopsies of the other 11 family probands were also considered normal with no evidence of ongoing dystrophic process or excessive glycogen storage as seen in McArdle disease [148]. The following genes associated with cramps, myalgia and muscle hypertrophy were screened by a next generation gene panel (Medical Neurogenetics, LLC) or whole exome sequencing (WES) sequencing: *CLCN1*, *SCN4A*, *ATP2A1*, *CAV3*, *RYR1*, *MSTN, ANO5, and LMNA* [38,55,111,122,137,146]. Linkage analysis using a combination of SNPs and microsatellites markers mapped the mutated gene to chromosome 1q21.3-q23.3 with a maximum LOD score of 8.6 (D1S2345-D1S2844: 11.4Mb) (Fig. 2.1C). WES was performed on five participants (Fig. 2.1A, Family I). Out of the four rare shared nucleotide variants, only *DCST2*'s (NM_144622) c.2276T>C (p.Leu759Pro, rs201399069) variant segregated appropriately and was predicted as potentially pathogenic by SIFT, PolyPhen, Mutation Taster and CADD (Fig. 2.1D). Screening of the entire *DCST2* coding sequence in 11

unrelated ST cases from the same region identified one additional ST family carrying this variant (Fig. 2.1A, family II). The leucine at position 759 is conserved from old-world monkeys to primates (Fig. 2.1E). The Genome Aggregation Database (gnomAD) reports an allele frequency of 0.06487% (1:1542), in a range compatible with a variably penetrant dominant trait. This is in accordance with our observation that carriers rarely seek medical attention, as in family I, where only the proband, and an aunt and uncle consulted for muscle symptoms (the last two consulted for spasmodic dysphagia). Though carried by 3 unrelated individuals with no known muscle condition out of 1209 in the Care4Rare WES database, it was not found in 96 unrelated FC individuals from different regions of the province of Quebec without a ST phenotype. We could obtain only a single needle quadriceps biopsy of an affected ST cousin (Fig. 2.1A, I:XV), which showed normal gross morphology using standard stains, but a decrease in type 1 myofiber cross-sectional area (CSA) and a minor increase in type 2X myofibers compared to three sex and age-matched controls (Supplementary Fig. 2.1).

DCST2 localization and protein partners in myoblasts and muscle

Very little is known about DCST2. It is the least studied of a group of four proteins that belong to a family that share six predicted transmembrane domains and a DC-STAMP-like protein domain: Dendrocyte Expressed Seven Transmembrane Protein (DCSTAMP), Osteoclast Stimulatory Transmembrane Protein (OCSTAMP), DCST1 and DCST2 (Fig. 2.1F). *DCST2*'s 16 exons code for a 773 amino acid-long, 86 kDa protein. To date, only a non-coding variant in *DCST2* (rs905938) has been associated with increased human height [164]. The Genotype-Tissue Expression (GTEx) portal shows that DCST2 is ubiquitously expressed at low levels in most tissues. In immortalized control human myoblasts transfected with wildtype V5-tagged DCST2, it partially colocalizes with the ER marker KDEL (Fig. 2.2A) while the mutated V5-tagged DCST2-L759P forms large puncta (Fig. 2.2B). To assess DCST2 endogenous localization and expression, we produced with MediMabs Inc an in-house DCST2 polyclonal rabbit antibody (Supplementary Fig. 2.2). In human differentiating myoblasts, endogenous DCST2 protein expression appears on day 1 and peaks on day 2 (Supplementary Fig. 2.3A and 3B). Larger DCST2 puncta are significantly more abundant in ST differentiating myoblasts (Fig 2.2C and 2.2D). In transverse sections of normal adult human skeletal muscle, DCST2 is found in the cytoplasm with some subsarcolemmal and perinuclear localization in all fiber types (Fig. 2.2E).

On longitudinal sections of control human muscle, DCST2 follows a striated pattern and is found in proximity, though almost never colocalizes, with: stromal interaction molecule 1 (STIM1, sarcoplasmic reticulum, SR), SERCA1 and 2 (SR), RYR1 (terminal cisternae of the SR), desmin (Z-disk) and optic atrophy protein 1 (OPA1, mitochondria) (Fig. 2.2F and 2.2G). The DCST2-rich striae are usually flanked by the T-tubules (TT) dihydropyridine receptor (DHPR)-positive striae (Fig. 2.2F and 2.2G). These results demonstrate that DCST2 localizes to the SR in the I-band in proximity to the TT. The most dramatic observation in ST muscle was the presence of larger DCST2 puncta on longitudinal sections (Fig. 2.2H-2.2J). Furthermore, the larger DCST2 puncta can contain both STIM1 and SERCA1, in particular in ST muscle, as best shown in the binary colocalization analysis (Fig. 2.3A-2.3D). A comparing of the levels of expression between two controls and the ST muscle biopsy show that DCST2 is relatively more abundant in the ST muscle while SERCA1 and the short and long isoforms of STIM1 appear less abundant in the ST muscle (Supplementary Fig. 2.3C). On the other hand, in differentiating myoblasts we did not observe any major differences in protein levels of DCST2, STIM1 and SERCA1 between ST cells and a control myoblast line (Supplementary Fig. 2.3A and 2.3B).

To identify potential DCST2's protein's interactions we took an unbiased approach, and performed an *in vitro* proximity-dependent biotinylation assay (BioID) [165]. HEK293 Flp-In T-REx cells, that do not express DCST2 endogenously, were transfected with a tetracycline-inducible DCST2-BirA vector (Supplementary Table 2.1, Supplementary Fig. 2.4). The 211 proteins detected as high-confidence proximity partners (FDR ≤1% against 37 negative controls – see Methods) and with high enrichment over the controls (Fold Change ≥ 3.15) were highly enriched in ER proteins (p=6.43e-30; Panther GO-Slim Cellular Component), involved in protein folding (p=3.32e-4; Panther GO-Slim Biological Process) and also enrich preys calcium homeostasis (p=1.40e-4; Panther GO-Slim Biological Process). Based on our hypothesis that the ST patients have stronger and longer contractions due to a prolonged increase in intracellular muscle calcium during contraction, we further studied two of the four calcium binding proteins that were in the top 10 DCST2 proximity interactors: calumin (CCDC47), STIM1, lectin mannose binding 1 (LMAN1), and inositol 1,4,5-trisphosphate receptor type 3 (ITPR3). Though little is known of calumin, it has been described as a new calcium binding protein in the ER negatively influencing calcium-release calcium-activated (CRAC) channels activity [166]. Bi-allelic

mutations in calumin cause a recessive disorder characterized by woolly hair, liver dysfunction, dysmorphic features, and global developmental delay (OMIM618268) [167], and its dysregulation is also linked to diabetic cardiomyopathy [168]. We observed a major decrease of calumin level in the ST patient skeletal muscle (Supplementary Fig. 2.3C), but no major differences in expression in ST myoblasts (Supplementary Fig. 2.3A and 2.3B). Calumin is distributed in a striated pattern in the skeletal muscle but we could not perform a colocalization with DCST2 since both available antibodies were generated in rabbits (Supplementary Fig. 2.5A and 5B). STIM1 has been extensively studied and is a sensor of low ER/SR calcium which oligomerizes and activates ORAI1 channels at the TT to allow extracellular calcium entry to replenish intracellular calcium stores [160,169-171]. We observed that STIM1 was present more often in the larger DCST2 puncta in ST muscle sections (Fig. 2.3C and 2.3D, Supplementary Table 2.1). Since STIM1 and SERCA1 are dynamic partners [172] and can be present in large DCST2 puncta (Fig. 2.3A-2.3D), we hypothesized that DCST2-L759P could influence both store-operated calcium entry (SOCE) and SR SERCA-dependent calcium reuptake.

DCST2 plays a role in calcium handling

To explore the role of DCST2 in cellular calcium handling, we performed measurements of free intracellular calcium in BioID HEK293 Flp-In T-REx lines with tetracycline-inducible DCST2 or DCST2-L759P expression and in differentiating human ST and control myoblasts. To assess SOCE activity, we measured calcium responses upon treatment with thapsigargin (TG), a SERCA inhibitor, which induces depletion of SR calcium stores, resulting in activation of STIM1 and opening of ORAI1-containing CRAC (calcium release-activated calcium) channels. This was followed by the addition of 2 mM extracellular calcium ions to evoke a rise in the levels of cytoplasmic calcium. The DCST2-L759P-expressing HEK293 cells displayed lower ER calcium release upon TG treatment and no change in CRAC response (Supplementary Fig. 2.6A). Although ST myoblasts exposed to TG also had lower SR calcium release, they showed lower CRAC activity (Fig. 2.4A and 2.4B) which likely corresponds to endogenous expression of DCST2 in these lines. To confirm that the decrease in calcium release by the SR is not due to a defective SR/ER calcium leak, we opted to trigger the calcium release using a different mechanism. We measured calcium responses following membrane depolarization using KCl, and observed lower levels of SR calcium release in ST cells (Fig. 2.4C and 2.4D). We also observed

that differentiating ST myoblasts show significantly lower basal intracellular free calcium levels than controls (Supplementary Fig. 2.6B). Together, these results suggest that DCST2-L759P leads to decreased calcium levels in the SR. To assess if low SR calcium levels in ST cells could be due to a defective calcium uptake mechanism, we repeated the same experiment to measure SOCE activity as previously, but without the SERCA inhibitor TG. We incubated differentiating myoblasts in calcium-free media followed by re-addition of extracellular calcium, and observed significantly higher intracellular calcium levels in the ST cells (Fig. 2.4E and 2.4F) suggesting that DCST2-L759P is impacting SERCA activity and causing a delay in SR calcium reuptake leading to a rise cytoplasmic calcium. Strikingly, TG treatment quickly leads to a significant increase in number and size of DCST2 puncta in ST cells, while this occurs more gradually in control cells (Fig. 2.4G-2.4I). Furthermore, SERCA1 and STIM1 are found in large DCST2 puncta in both ST and control myoblasts, including the very large puncta only observed in ST cells (Fig. 2.5). ORAI1 does not colocalize with DCST2 puncta, but can be observed close to DCST2 puncta (Fig. 2.5). The large DCST2 puncta (area > 6μm^2) do not appear to be nonfunctional aggregates, since they are observed in control and ST myoblasts and are not positive for p62 and LAMP2 (markers of autophagy) or ubiquitin (Supplementary Fig. 2.7). Together our data show that DCST2 forms larger puncta with STIM1 and SERCA1 when there is a low ER/SR calcium level. In ST cells, we observed that DCST2 forms even larger puncta, but since these were present in only ~15% of cells and that most cells display decreased calcium transients, the large DCST2 puncta may correspond to the cell's effort to increase calcium entry, which is less efficient in ST cells.

Discussion

We show that DCST2 plays a role in calcium handling in myoblasts and that the ST mutation leads to an increase in the clustering of STIM1 and SERCA1 in large DCST2-positive puncta. What is still unknown is how an apparent decrease in baseline calcium concentration in the SR of differentiating ST myoblasts can lead to muscle hypertrophy and increased strength in ST mature myofibers. The increase in DCST2 puncta size and their more frequent STIM1 and SERCA1 content in ST muscle suggests that either these larger complexes may correspond to the cell's effort to counteract the partial loss of calcium replenishing through SOCE or alternatively that mutated DCST2 interferes with dynamic puncta dissociation leading to the SOCE dysfunction and SERCA clustering. Since DCST1 has been reported to be an E3 ubiquitin-ligase [173], it is tempting to speculate that DCST2 could play such a role, and when mutated impact ubiquitination of key components of the puncta. DCST2 localization to the I-band may correspond to its participation in the newly identified calcium entry units (CEUs) [170]. These units correspond to STIM1-rich SR specialized tubular structures that surround lateral extensions of T-tubules and are thought to be a specialized site of SOCE activity to replenish intracellular calcium stores. CEUs have been shown to increase in abundance with exercise, supporting the idea that the higher requirement of calcium with repeated contractions leads to their enlargement to ensure higher calcium influx through an ORAI1-STIM1-dependent mechanism. Though more histological work is needed to confirm that DCST2 puncta are indeed localized to CEUs and that in ST muscles the CEUs are larger, the increased size and STIM1 content of ST DCST2 puncta favors this hypothesis. Furthermore, the increased SERCA content of ST DCST2 puncta could support the concept that this proximity leads to a compensatory increase of free cytosolic calcium through SOCE while compromising the rapid reuptake of calcium after every contraction by interfering with SERCA function. The relative increase in clustering of SERCA in partially functional ST puncta could lead to a relatively slower calcium reuptake after contraction that could explain the prolonged contractions due to free cytoplasmic calcium while the decremental strength observed in ST patients with each contraction could correspond to a decline in the absolute concentration of SR calcium. More work is needed to establish how mutated *DCST2* leads to a Strongman phenotype, but there is growing evidence that calcium handling dysfunctions that impact SR calcium release and reuptake could lead to larger muscles and increased strength [43,80,108].

Increased strength associated with enlarged skeletal muscles has been observed in different myopathies directly or indirectly associated with changes in muscle calcium handling. Muscle hypertrophy and increased strength has been described in certain non-dystrophic myotonias caused by mutations in the *SCN4A* and *CLCN1* genes coding respectively for sodium and chloride channels subunits [101]. Those mutations lead to prolonged depolarization ensuing prolonged increased intracellular calcium associated with prolonged contractions [101]. In Brody disease caused by recessive *SERCA1* mutations, the associated slower SR calcium reuptake and prolonged contractions clinically manifest as larger muscles, though not always increased strength [55,120]. In Brody syndrome, despite the large muscles and fatigue, patients do not carry *SERCA* mutations but some have a clear clinical overlap with ST with larger muscles, myalgia and often increased strength [55]. The most dramatic calcium handling disorder is malignant hyperthermia susceptibility caused by dominant mutations in *RYR1* where prolonged increased intracellular calcium levels are elicited upon exposure to certain anesthetics [108,174]. It can lead to death due to respiratory arrest and increased body temperature [108,174]. *RYR1* dominant mutations are increasingly observed in cases of rhabdomyolysis and myalgia in which muscle hypertrophy is a frequent finding [108]. Together, these myopathies support the concept that mutations which affect calcium handling lead to prolonged increased intracellular calcium levels and ensuing contractions are associated with increase strength and muscle hypertrophy as observed clinically in DCST2 ST cases. In contrast, SOCE dysfunction in skeletal muscle diseases has been associated with increased SOCE activity and high intracellular calcium levels leading to muscle weakness caused by dominant mutations in STIM1 and ORAI1 in certain tubular aggregate myopathies [175]. In the Strongman trait a combination of SOCE and SERCA dysfunctions may lead to the positive and negative features of the condition. Clinically the presence in patient muscles of more abundant large puncta positive for DCST2, STIM1 and SERCA1 and 2, would support this hypothesis. Sequencing of *DCST2* and other candidate genes in patients with muscle hypertrophy and myalgia should be performed by gene panel next generation sequencing. If negative, patient myoblasts can be tested electrophysiologically and analyzed histologically for puncta size after thapsigargin to further support the diagnosis. The relatively high carrier frequency of 1:1542 for the c.2276T>C (p.Leu759Pro) *DCST2* mutation in the Gnomad database suggests that it may be a frequent cause of dominant Herculean, often painful, myopathy.

Furthermore, many dominant families with overlapping phenotypes are still without a genetic diagnosis suggesting that novel mutations in other genes coding for proteins involved in muscle calcium handling remain to be uncovered.

Table 2.1: Clinical Data on sixteen ST cases with full examination

Number	I:I	I:II	I:III	I:V	I:VI	I:VII	I:VIII	I:X	I:XII	I:XIV	I:XV	I:XVI	I:XVIII	I:XIX	I:XX	II:I
Age	50	30	23	70	45	47	68	59	61	57	36	64	59	34	35	27
Sex	F	F	M	F	M	M	F	F	F	F	M	M	F	M	F	M
Above average strength	+	+	+	+	+	+	+	+	+	+	+	+	-	+	+	+
Weakness after repetitive movement	+	+	+	+	+	+	+	+	+	-	+	-	+	+	+	+
Myalgia post-activity	+	+	+	+	+	+	+	+	+	+	+	+	-	+	+	+
Large muscle bulk	+	+	+	+	+	+	+	+	+	+	+	+	+	+	+	+
Deltoid Fatigability	+	+	+	+	+	-	+	-	-	+	+	+	+	+	-	+
Superior Strength	+	+	+	+	+	+	+	-	+	+	+	+	+	+	+	+
Pseudomyotonia	+	+	+	+	+	+	+	+	-	+	+	+	+	+	+	+
Proximal Weakness	-	-	-	-	-	-	+	-	+	-	-	-	+	-	-	-

Abbreviations: F, female; M, male; +, present; -, absent.

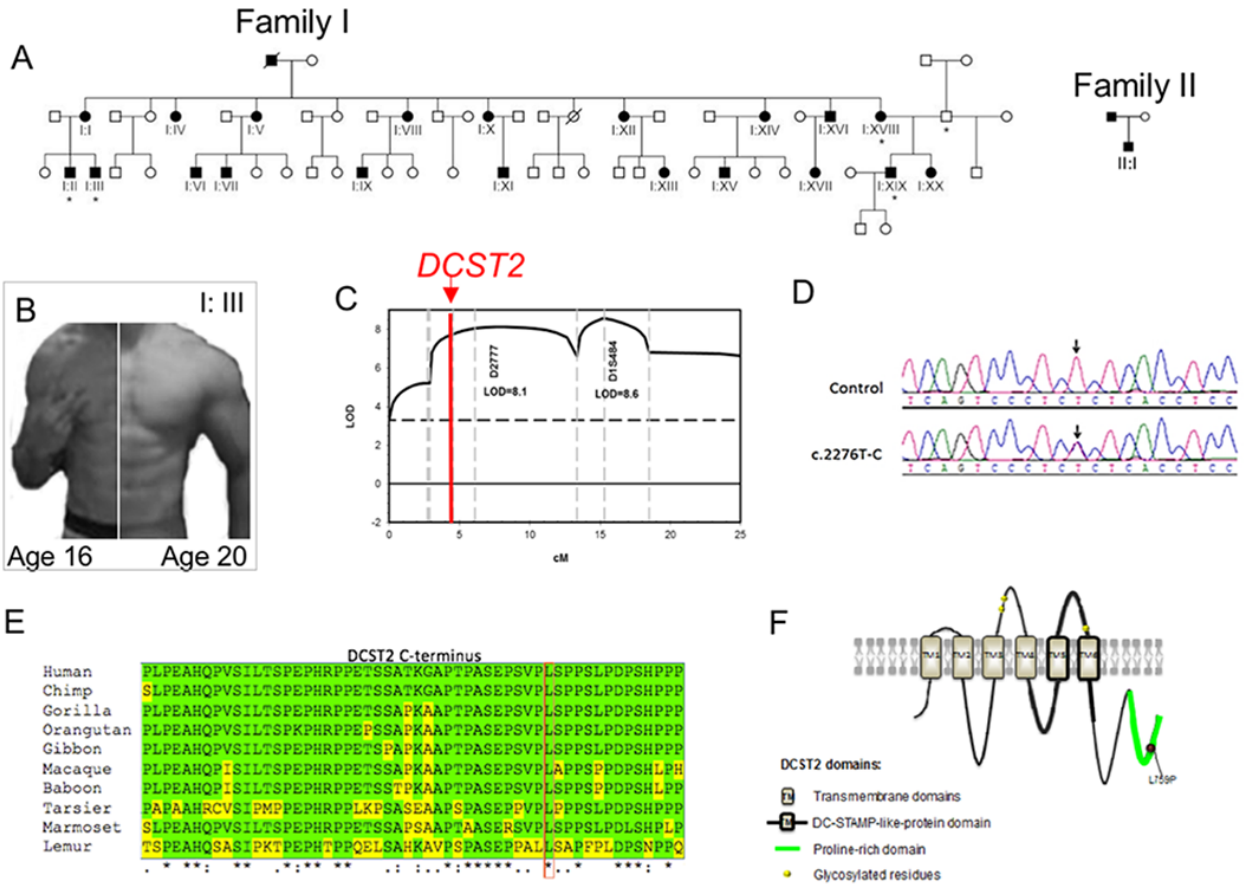

Figure 2.1. A mutation in *DCST2* gene causes Strongman Trait (ST) in two French-Canadian families. (**A**) Pedigree of families I and II with ST cases carrying mutations in *DCST2;* the DNA of individuals indicated with asterisks were submitted to whole exome sequencing (WES). (**B**) Photograph of family member I: III at age 16 (left) and 20 while bodybuilding (right). (**C**) Multipoint linkage analysis of chromosome 1 in family I; red line represents the position of *DCST2*. (**D**) Chromatogram for the c.2276T>C (p.Leu759Pro) variant. (**E**) Relative conservation of the C-terminus of DCST2 in old-world monkeys and primates; red open rectangle indicates the position of the mutation (Leu759Pro); conserved amino acids are highlighted in green. (**F**) Predicted structure and domains of DCST2.

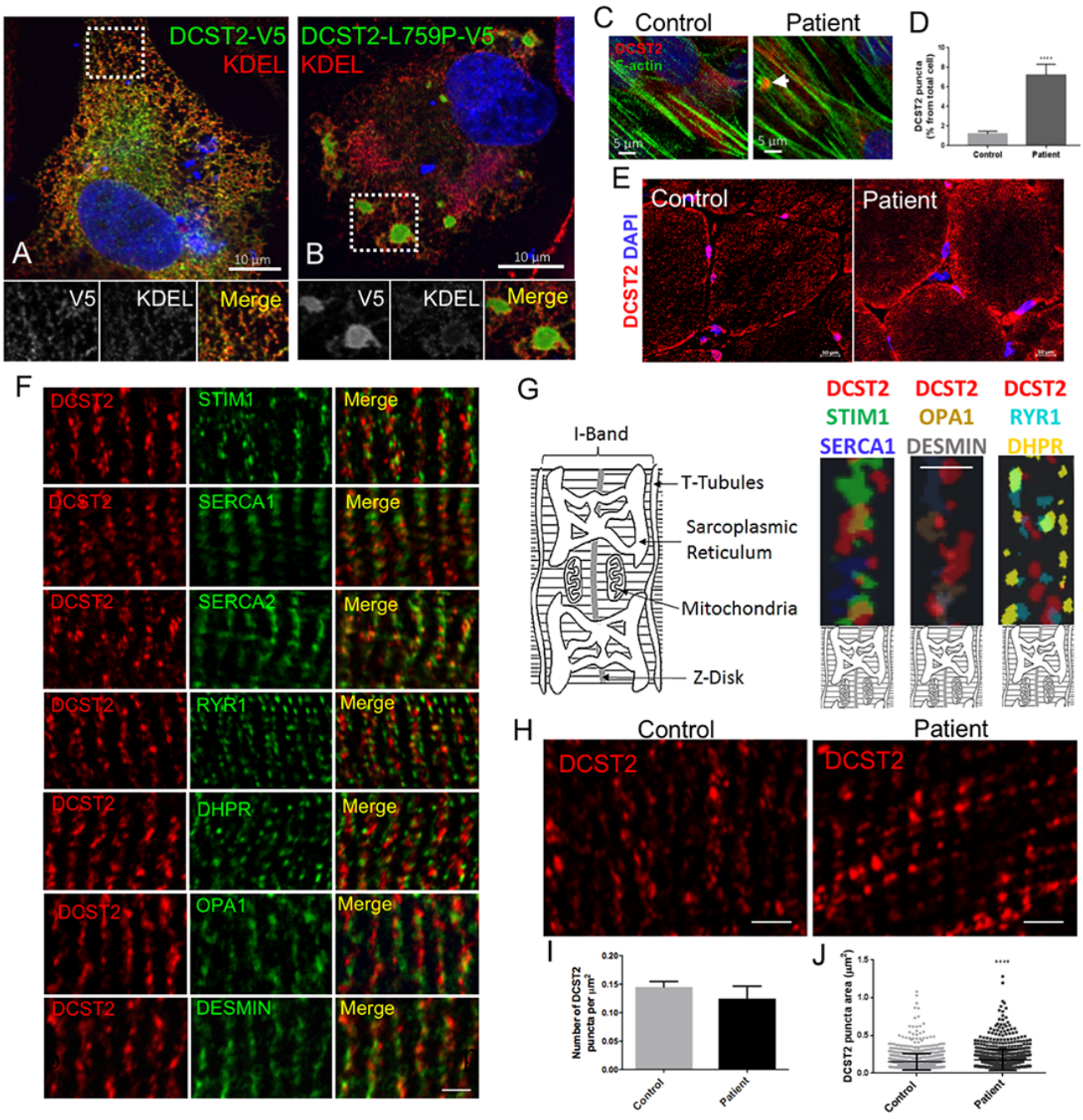

Figure 2.2 DCST2-L759P forms larger puncta in myoblasts and skeletal muscle tissue. (**A**) Confocal image of human immortalized control myoblasts transfected with DCST2-V5-His labeled with α-V5 (green) and α-KDEL (ER marker, red) antibodies; bottom panels show zoomed regions indicated by white dotted squares. (**B**) Same as in A, but transfected with DCST2-L759P-V5-His. (**C**) Confocal image of differentiating myoblasts in differentiation labeled with α-DCST2 antibody (red), phalloidin (green) and DAPI (blue) from a human control

(left) and patient (right) cell lines. (**D**) Quantification of large DCST2 puncta in control and ST myoblasts. Data are presented as mean (± SD) of ~500 cells for each group, 3 different sister cultures were used; statistical analysis (unpaired *t*-test) is indicated (****P<0.0001). (**E**) Confocal images of transverse sections of human control (left) and ST (right) skeletal muscle labeled with DCST2 in red. (**F**) Confocal images of longitudinal sections of human skeletal muscle labeled with DCST2 in red and markers of intracellular proteins in green: STIM1, SERCA1, SERCA2, RYR1, DHPR, OPA1 and desmin; Scale bar: 2 μm. (**G**) Graphic representation of the sarcotubular system around the I-band of the sarcomere on the left, and representation of DCST2 localization with respect to other markers. (**H**) Confocal images of longitudinal sections of control (left) and ST patient (right) skeletal muscle showing larger DCST2 puncta in red. (**I**) Number of DCST2 puncta in control and ST patient's muscle; Data are presented as mean (±S.D). (**J**) Average of DCST2 puncta area in control and ST muscle; Data are presented as mean (±S.D); statistical analysis by unpaired *t*-test (****P<0.0001).

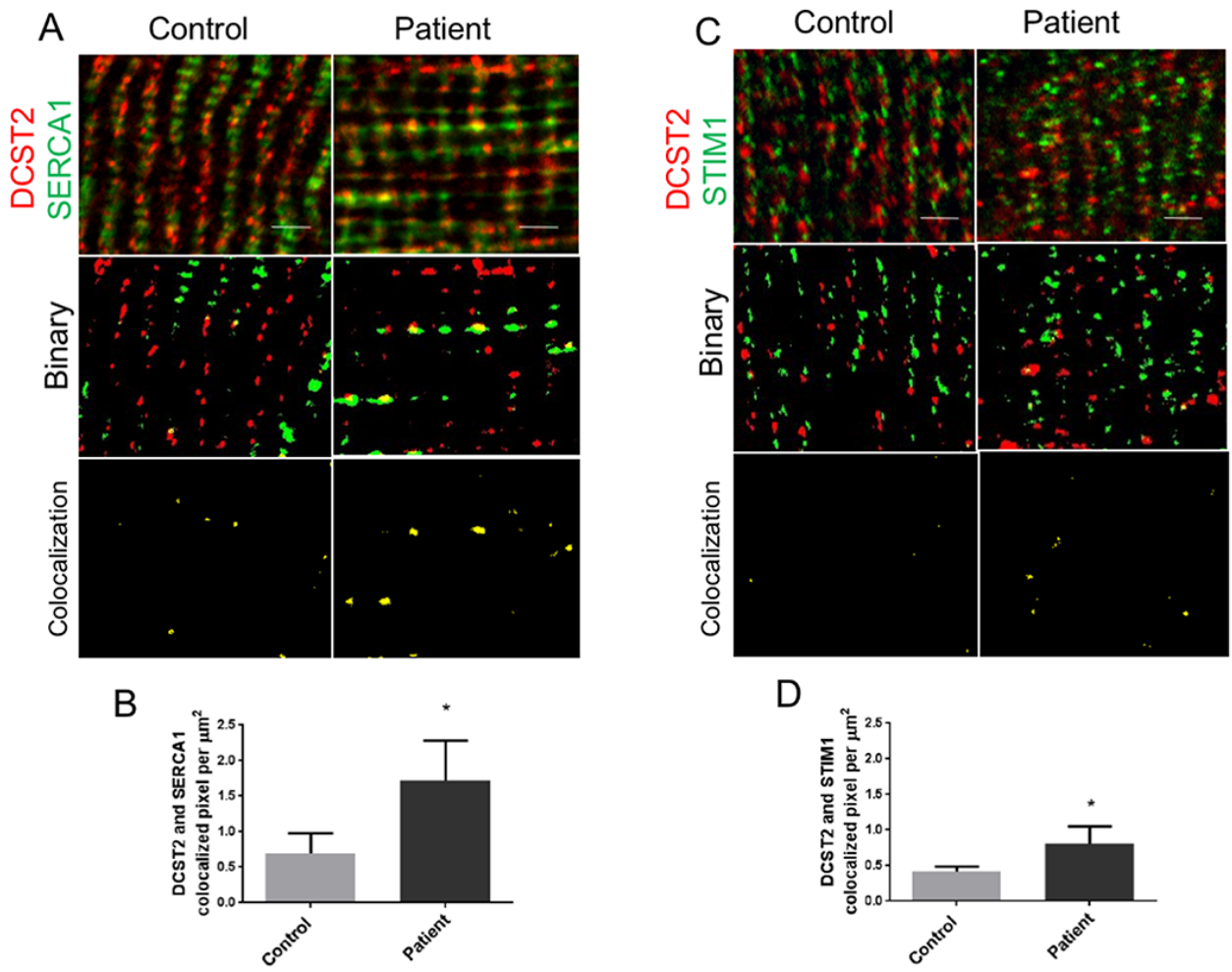

Figure 2.3 Larger DCST2 puncta colocalize with SERCA1 and STIM1 more frequently in ST muscle. (**A**) Confocal images of longitudinal sections of control and ST skeletal muscle labeled with DCST2 in red and SERCA1 in green; Binary indicates threshold binarized merged images; and Colocalization indicates binarized images of DCST2 and SERCA1 showing only area of colocalization for two the proteins labeled; Scale bar: 2 µm. (**B**) Quantification showing the mean of white pixels per μm^2 of the colocalized DCST2 and SERCA1 puncta in the control and ST patient's muscle; data are presented as mean (± SD); Statistical analysis, unpaired *t*-test (**P*=0.0477). (**C**) Same as in A, but with STIM1 colabeling. (**D**) Same as in B, but with colocalized DCST2 and STIM1 puncta. Statistical analysis by unpaired *t*-test (***P*=0.049).

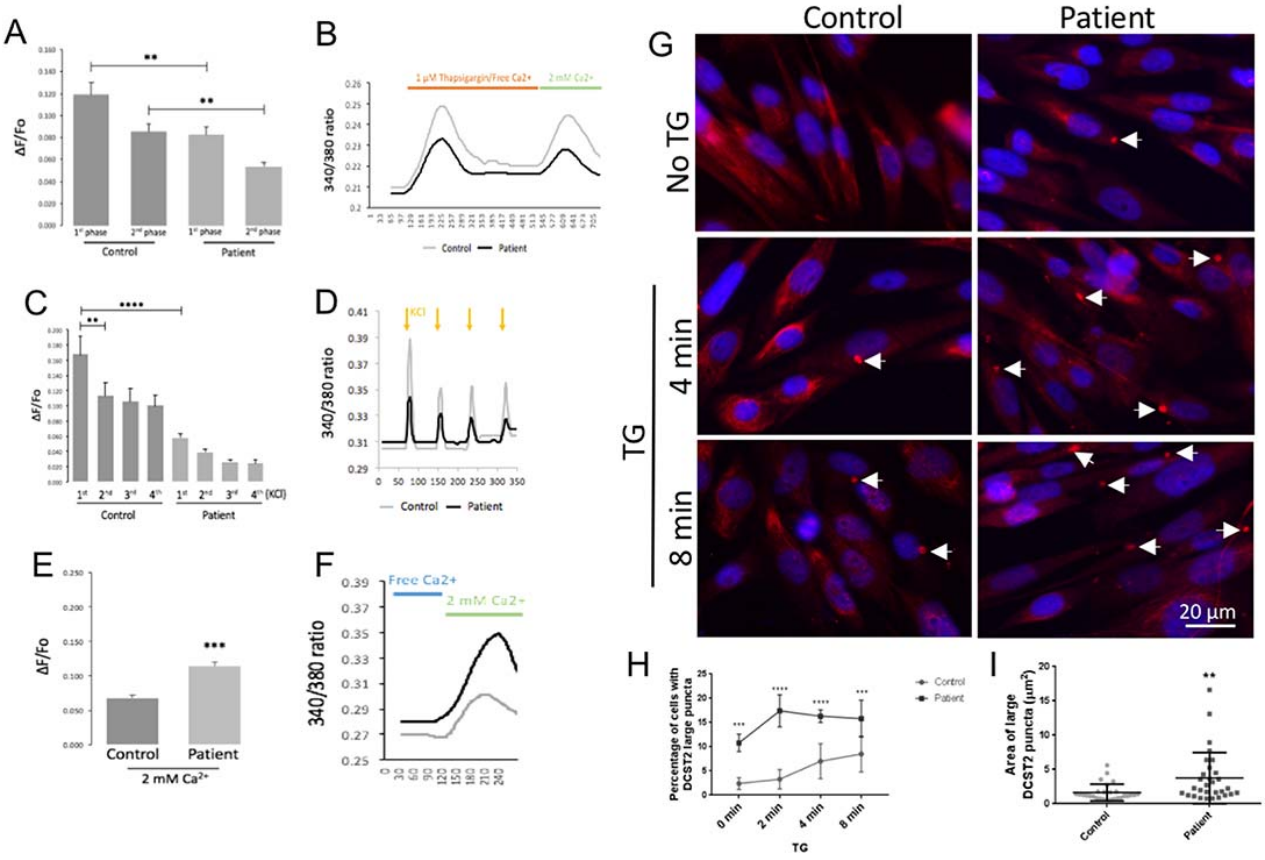

Figure 2.4 ST cells display altered calcium handling and higher abundance of large DCST2 puncta. (**A**) Summary data showing the average of calcium responses evoked by TG-evoked calcium depletion and calcium add-back in control and ST patient's differentiating myoblasts. Data are presented as mean (± SEM) of three independent assays, statistically significant differences by one-way ANOVA for multiple comparisons (***P*<0.01). (**B**) Representative traces of SOCE using TG followed by calcium add-back. (**C**) Summary data showing the average of KCl-evoked calcium responses of control and ST patient's differentiating myoblasts; Data are presented as mean (± SEM) of three independent assays, statistically significant differences assessed by one-way ANOVA for multiple comparisons (***P*=0.0031, *****P*<0.0001). (**D**) Representative traces of calcium responses evoked by KCl-induced depolarization. (**E**) Summary data showing the average of calcium responses after re-admission of extracellular calcium (2 mM) in control and ST patient's differentiating myoblasts. Data are presented as mean (± SEM) of three independent assays, statistical analysis by unpaired t-test (***P=0.0002). (**F**) Representative traces of calcium responses evoked by calcium add-back (2 mM). (**G**) Control (left) and patient's (right) fixed differentiating myoblasts labeled with DCST2 (in red) and DAPI

(in blue) before (no TG) and after treatment with TG for 4 and 8 minutes; large DCST2 puncta are indicated by white arrows. (**H**) Quantification of large DCST2 puncta in control and patients differentiating myoblasts at different time points during TG treatment; Data are presented as mean (± SD) from three different sister cultures; Statistically significant differences established by one-way ANOVA for multiple comparisons (***P<0.001, ****P<0.0001). (**I**) Greater abundance of larger DCST2 puncta in patients differentiating myoblasts compared to controls treated with TG for 4 minutes; Data are presented as mean (± SD) from three different sister cultures. Statistically significant differences established by one-way ANOVA for multiple comparisons (**P=0.0058).

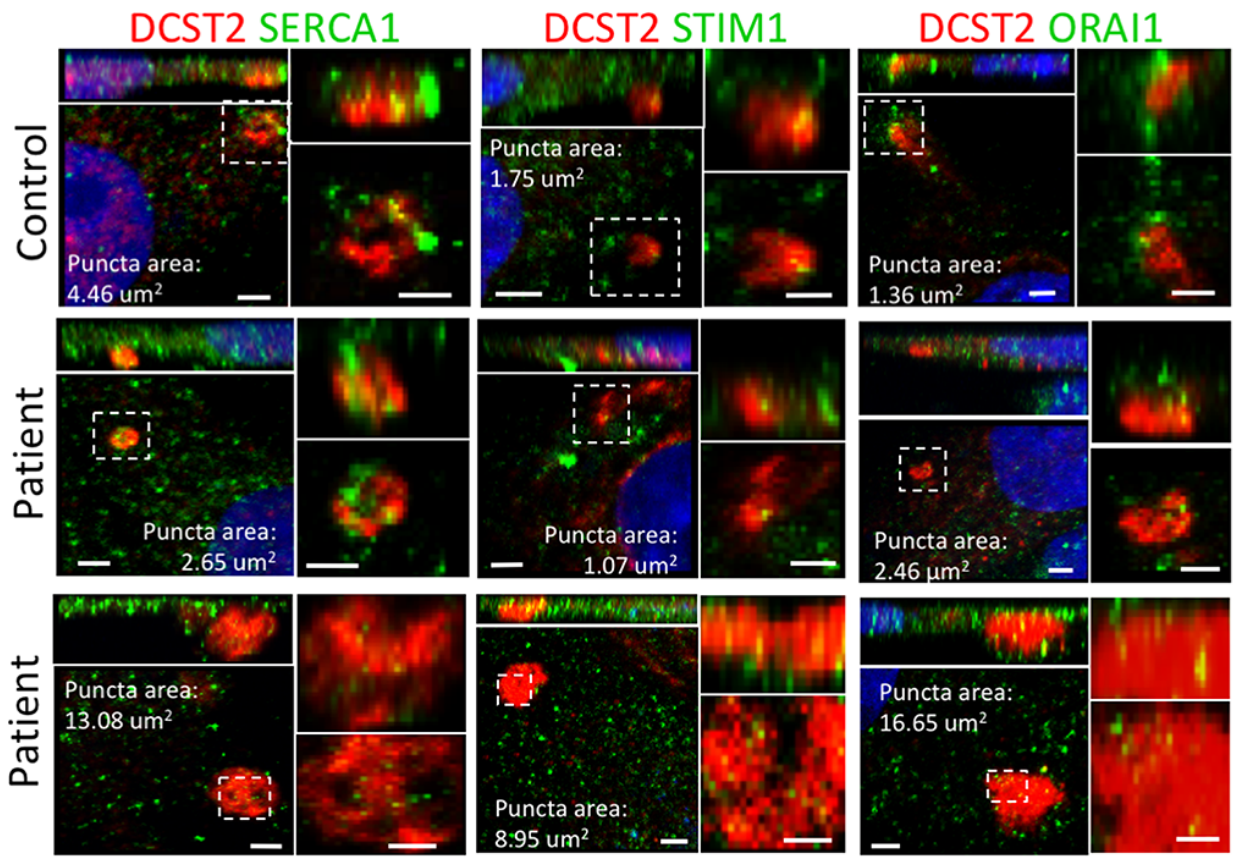

Figure 2.5 Larger DCST2 puncta contain both SERCA1 and STIM1. Maximum projection of stacking confocal images obtained from control and patient's differentiating myoblasts treated with TG and double labeled with DCST2 (in red) and SERCA1 (in green, left panel), DCST2 (in red) and STIM1 (in green, panel at the middle), DCST2 (in red) and ORAI1 (in green, right panel). Both wildtype and ST DCST2 puncta larger than 1µm^2 contain SERCA1 and STIM1, and are in proximity with ORAI1. The lower panel shows a similar sequestration of SERCA1 and STIM1 in the largest DCST2 puncta only observed in ST cells; At the top of each image, the stacking images are showed 90 degrees on Z-plan; white dotted squares indicate regions of interest (ROI) used to produce zoomed images displayed on the right side of each maximum projection image. Scale bars on original images: 2 µm

Web Resources

UCSC, https://genome.ucsc.edu/

SIFT, https://sift.bii.a-star.edu.sg/

PolyPhen-2, http://genetics.bwh.harvard.edu/pph2/

Mutation Taster, http://www.mutationtaster.org/

Gnomad, http://gnomad.broadinstitute.org/

Uniprot, https://www.uniprot.org/

GTEx, https://gtexportal.org/home/

Prohits, https://prohits-web.lunenfeld.ca/

PHYRE2 Protein Fold Recognition Server, https://www.sbg.bio.ic.ac.uk/phyre2/

Acknowledgements

We thank the patients for their cooperation and interest in this study, the Care4Rare Canada Consortium for access to allele frequency data, Sally Spendiff who offered technical assistance with the MHC staining, José A. Morais for performing a muscle biopsy in one control individual, Zhen-Yuan Lin for performing part the BioID assay and mass spectrometric analysis, Michiel Krols for assisting with the quantification analysis of the confocal images, Karine Choquet, Julien Prudent and Roxanne Larivière for revising the manuscript for intellectual content, and Claudia Kleinman for helping with the bioinformatics analysis of the proline-rich domain of DCST2.

Funding

This study was supported by the Fondation du Grand Défi Pierre Lavoie to B.Br. and by the Association Française contre les Myopathies (AFM) with a PhD fellowship to T.C.C. Work in the A.C.G. lab is supported by the Canadian Institutes of Health Research (CIHR FDN-143301). Work in the P.S. lab is supported by a CIHR grant (PJT-153098). Proteomics was performed at the Network Biology Collaborative Centre at the Lunenfeld-Tanenbaum Research Institute, a facility supported by Canada Foundation for Innovation funding, by the Ontarian Government and by Genome Canada and Ontario Genomics (OGI-097, OGI-139).

Declaration of Interests

The authors declare no competing interests.

References

Voermans, N.C. et al. Brody syndrome: a clinically heterogeneous entity distinct from Brody disease: a review of literature and a cross-sectional clinical study in 17 patients. *Neuromuscul Disord* 22, 944-54 (2012).

Brody, I.A. Muscle contracture induced by exercise. A syndrome attributable to decreased relaxing factor. *N Engl J Med* 281, 187-92 (1969).

Bolduc, V. et al. Recessive mutations in the putative calcium-activated chloride channel Anoctamin 5 cause proximal LGMD2L and distal MMD3 muscular dystrophies. *Am J Hum Genet* 86, 213-21 (2010).

Miller, T.M. Differential diagnosis of myotonic disorders. Muscle Nerve 37, 293-9 (2008).

Scalco, R.S. et al. CAV3 mutations causing exercise intolerance, myalgia and rhabdomyolysis: Expanding the phenotypic spectrum of caveolinopathies. *Neuromuscul Disord* 26, 504-10 (2016).

Walters, J. Muscle hypertrophy and pseudohypertrophy. Pract Neurol 17, 369-379 (2017).

Bayona, J.C. et al. SUMOylation pathway in Trypanosoma cruzi: functional characterization and proteomic analysis of target proteins. *Mol Cell Proteomics* 10, M110 007369 (2011).

Fermin, D., Basrur, V., Yocum, A.K. & Nesvizhskii, A.I. Abacus: a computational tool for extracting and pre-processing spectral count data for label-free quantitative proteomic analysis. *Proteomics* 11, 1340-5 (2011).

St-Denis, N. et al. Phenotypic and Interaction Profiling of the Human Phosphatases Identifies Diverse Mitotic Regulators. *Cell Rep* 17, 2488-2501 (2016).

Snoeck, M. et al. RYR1-related myopathies: a wide spectrum of phenotypes throughout life. *Eur J Neurol* 22, 1094-112 (2015).

Witting, N. et al. Phenotype and genotype of muscle ryanodine receptor rhabdomyolysis-myalgia syndrome. *Acta Neurol Scand* 137, 452-461 (2018).

Schuelke, M. et al. Myostatin mutation associated with gross muscle hypertrophy in a child. *N Engl J Med* 350, 2682-8 (2004).

Gu, H. et al. Establishment and phenotypic analysis of an Mstn knockout rat. *Biochem Biophys Res Commun* 477, 115-22 (2016).

Stantzou, A. et al. Effect of constitutive inactivation of the myostatin gene on the gain in muscle strength during postnatal growth in two murine models. *Muscle Nerve* 55, 254-261 (2017).

Cully, T.R. et al. Junctional membrane Ca(2+) dynamics in human muscle fibers are altered by malignant hyperthermia causative RyR mutation. *Proc Natl Acad Sci* U S A 115, 8215-8220 (2018).

Launikonis, B.S., Cully, T.R., Csernoch, L. & Stephenson, D.G. NHE- and diffusion-dependent proton fluxes across the tubular system membranes of fast-twitch muscle fibers of the rat. *J Gen Physiol* 150, 95-110 (2018).

Li, H. & Durbin, R. Fast and accurate short read alignment with Burrows-Wheeler transform. *Bioinformatics* 25, 1754-60 (2009).

McKenna, A. et al. The Genome Analysis Toolkit: a MapReduce framework for analyzing next-generation DNA sequencing data. *Genome Res* 20, 1297-303 (2010).

Shanely, R.A. et al. Human skeletal muscle biopsy procedures using the modified Bergstrom technique. *J Vis Exp*, 51812 (2014).

Sasarman, F., Karpati, G. & Shoubridge, E.A. Nuclear genetic control of mitochondrial translation in skeletal muscle revealed in patients with mitochondrial myopathy. *Hum Mol Genet* 11, 1669-81 (2002).

Gouspillou, G. et al. The relationship between muscle fiber type-specific PGC-1alpha content and mitochondrial content varies between rodent models and humans. *PLoS One* 9, e103044 (2014).

Koenig, X., Choi, R.H. & Launikonis, B.S. Store-operated Ca2+ entry is activated by every action potential in skeletal muscle. *Communications Biology* 1, 31 (2018).

Cottingham, R.W., Jr., Idury, R.M. & Schaffer, A.A. Faster sequential genetic linkage computations. *Am J Hum Genet* 53, 252-63 (1993).

Sobel, E. & Lange, K. Descent graphs in pedigree analysis: applications to haplotyping, location scores, and marker-sharing statistics. *Am J Hum Genet* 58, 1323-37 (1996).

Tetreault, M. et al. Adult-onset painful axonal polyneuropathy caused by a dominant NAGLU mutation. *Brain* 138, 1477-83 (2015).

van der Valk, R.J. et al. A novel common variant in DCST2 is associated with length in early life and height in adulthood. *Hum Mol Genet* 24, 1155-68 (2015).

Roux, K.J., Kim, D.I., Raida, M. & Burke, B. A promiscuous biotin ligase fusion protein identifies proximal and interacting proteins in mammalian cells. *J Cell Biol* 196, 801-10 (2012).

Konno, M. et al. Calumin, a Ca(2)(+)-binding protein on the endoplasmic reticulum, alters the ion permeability of Ca(2)(+) release-activated Ca(2)(+) (CRAC) channels. *Biochem Biophys Res Commun* 417, 784-9 (2012).

Morimoto, M. et al. Bi-allelic CCDC47 Variants Cause a Disorder Characterized by Woolly Hair, Liver Dysfunction, Dysmorphic Features, and Global Developmental Delay. *Am J Hum Genet* 103, 794-807 (2018).

Thapa, K. et al. Dysregulation of the calcium handling protein, CCDC47, is associated with diabetic cardiomyopathy. *Cell Biosci* 8, 45 (2018).

Luik, R.M., Wang, B., Prakriya, M., Wu, M.M. & Lewis, R.S. Oligomerization of STIM1 couples ER calcium depletion to CRAC channel activation. *Nature* 454, 538-42 (2008).

Boncompagni, S., Michelucci, A., Pietrangelo, L., Dirksen, R.T. & Protasi, F. Exercise-dependent formation of new junctions that promote STIM1-Orai1 assembly in skeletal muscle. *Sci Rep* 7, 14286 (2017).

Zhang, S.L. et al. STIM1 is a Ca2+ sensor that activates CRAC channels and migrates from the Ca2+ store to the plasma membrane. *Nature* 437, 902-5 (2005).

Lee, K.J. et al. Stromal interaction molecule 1 (STIM1) regulates sarcoplasmic/endoplasmic reticulum Ca(2)(+)-ATPase 1a (SERCA1a) in skeletal muscle. *Pflugers Arch* 466, 987-1001 (2014).

Nair, S., Bist, P., Dikshit, N. & Krishnan, M.N. Global functional profiling of human ubiquitome identifies E3 ubiquitin ligase DCST1 as a novel negative regulator of Type-I interferon signaling. *Sci Rep* 6, 36179 (2016).

Musaro, A., McCullagh, K.J., Naya, F.J., Olson, E.N. & Rosenthal, N. IGF-1 induces skeletal myocyte hypertrophy through calcineurin in association with GATA-2 and NF-ATc1. *Nature* 400, 581-5 (1999).

Sztretye, M. et al. SOCE Is Important for Maintaining Sarcoplasmic Calcium Content and Release in Skeletal Muscle Fibers. *Biophys* J 113, 2496-2507 (2017).

Trivedi, J.R. et al. Non-dystrophic myotonia: prospective study of objective and patient reported outcomes. *Brain* 136, 2189-200 (2013).

Odermatt, A. et al. Mutations in the gene-encoding SERCA1, the fast-twitch skeletal muscle sarcoplasmic reticulum Ca2+ ATPase, are associated with Brody disease. *Nat Genet* 14, 191-4 (1996).

Lynch, P.J. et al. Identification of heterozygous and homozygous individuals with the novel RYR1 mutation Cys35Arg in a large kindred. *Anesthesiology* 86, 620-6 (1997).

Nesin, V. et al. Activating mutations in STIM1 and ORAI1 cause overlapping syndromes of tubular myopathy and congenital miosis. *Proc Natl Acad Sci U S A* 111, 4197-202 (2014).

Supplementary material

Supplementary Table 2.1 DCST2 BioID: List of DCST2 proximity interactors with Bayesian False Discovery Rate <0.01

Prey	PreyGene	Spec	FoldChange
NP_055862.1	EMC1	119|133	1260
NP_001949.1	EEF1A2	68|68	680
NP_055422.1	UBXN4	46|53	445.5
NP_064583.2	CCDC47	90|89	402.75
NP_060917.1	EMC3	34|36	350
NP_055488.1	EMC2	31|33	320
NP_003147.2	STIM1	32|31	315
NP_064539.1	EMC7	28|27	275
NP_005561.1	LMAN1	25|29	270
NP_002215.2	ITPR3	20|28	240
NP_001123952.1	VRK2	24|23	235
NP_056417.2	TOR1AIP1	22|25	235
NP_060672.2	MACO1	21|22	215
NP_055929.1	ANKLE2	20|26	207
NP_776152.1	PDZD8	18|23	205
NP_002818.1	PTPN1	21|18	195
NP_065698.1	JPH1	19|18	185
NP_006058.1	EMC8	16|21	185
NP_940953.2	MIA3	19|17	180
NP_620409.1	VANGL1	17|23	180
NP_060244.2	CDKAL1	15|20	175
NP_001107.2	ADCY9	14|15	145
NP_000932.3	POR	10|17	135
NP_659471.1	TOR1AIP2	17|10	135
NP_006546.1	YKT6	15|14	130.5
NP_003934.1	STBD1	13|13	130
NP_065068.1	VANGL2	9|17	130
NP_004883.3	SEC22B	11|14	125
NP_060221.2	SMPD4	12|13	125
NP_689677.1	TMEM199	13|9	110
NP_001736.1	CAMLG	13|9	110
NP_057538.1	EMC4	11|11	110
NP_003625.2	NIPSNAP1	10|11	105
NP_996261.1	EMC10	11|10	105
NP_055995.4	SYNE2	12|9	105
NP_004630.3	BAG6	10|11	105

NP_849193.1	STT3B	10|10	100
NP_001123356.1	TEX264	10|10	100
NP_076424.1	DDRGK1	9|10	95
NP_005756.2	ATP6AP2	9|10	95
NP_110416.1	HM13	11|8	95
NP_004827.4	EIF2AK3	8|10	90
NP_001120676.1	HMOX2	7|11	90
NP_775741.1	MMGT1	8|10	90
NP_853553.1	AUP1	10|8	90
NP_001231595.1	STX5	10|10	90
NP_057105.2	UBE2J1	7|11	90
NP_037520.1	PREB	9|9	90
NP_001673.2	ATP2B1	10|10	90
NP_057190.2	SCFD1	10|9	85.5
NP_001174.2	ATP6AP1	8|9	85
NP_001129671.1	GRAMD1A	7|10	85
NP_060979.2	LRRC59	9|8	85
NP_001136277.1	SLC6A8	10|7	85
NP_002941.1	RPN1	31|33	82.29
NP_001132913.1	BCAP31	9|7	80
NP_001073141.1	FNDC3A	7|8	75
NP_002802.2	PSMD7	9|6	75
NP_060939.3	TEX2	7|8	75
NP_056993.2	NBAS	6|9	75
NP_003092.4	SOAT1	9|6	75
NP_940932.2	MXRA7	8|7	75
NP_001041675.1	CLCC1	29|35	72
NP_116106.2	GPAT3	5|9	70
NP_060557.3	NDC1	6|8	70
NP_001072989.1	KTN1	111|118	66.48
NP_001035938.1	ACBD5	6|7	65
NP_060069.3	VEZT	6|7	65
NP_776186.2	RABL3	8|5	65
NP_058626.1	STX18	5|8	65
NP_001026884.3	INF2	7|6	65
NP_115733.2	CCDC115	4|8	60
NP_055428.1	FAF2	6|6	60
NP_001093422.2	ITPR1	5|7	60
NP_001243390.1	SLC12A2	4|8	60
NP_001258708.1	PSMD6	7|5	60
NP_658988.2	SMCR8	5|6	55
NP_004222.2	ATP6V1F	6|5	55
NP_003038.2	SLC9A1	5|6	55

NP_001165906.1	RAB3GAP1	7|4	55
NP_036313.3	FKBP8	7|4	55
NP_001008389.1	CISD2	7|4	55
NP_006658.1	PGRMC1	5|6	55
NP_056480.1	AAAS	6|5	55
NP_073572.2	ACBD3	5|5	50
NP_001191006.1	UBE4A	7|3	50
NP_057113.1	DHRS7	5|5	50
NP_002778.1	PSMA2	5|6	49.5
NP_001036041.1	RRBP1	50|52	48.32
NP_006450.2	ERLIN1	22|28	45
NP_005834.4	STAM2	5|5	45
NP_005207.2	DDOST	4|5	45
NP_001129243.1	RPN2	6|14	45
NP_444280.2	SNAP47	4|5	45
NP_065911.3	STIM2	3|6	45
NP_848934.1	GPAT4	4|5	45
NP_005796.1	PSMD14	5|4	45
NP_056106.1	DNAJC16	4|5	45
NP_009145.1	SEC63	4|5	45
NP_055569.1	PTDSS1	6|3	45
NP_001229971.1	HLA-C	4|5	45
NP_004729.1	VAPB	18|17	45
NP_001166028.1	GOLGA3	9|14	41.4
NP_002731.4	PRKCI	4|4	40
NP_110382.3	TMX1	4|4	40
NP_434698.1	TRIM13	3|5	40
NP_079508.2	REEP4	5|3	40
NP_002789.1	PSMB6	4|4	40
NP_060142.3	TRPM7	2|6	40
NP_788276.1	CDK5RAP3	2|6	40
NP_001737.1	CANX	17|18	39.38
NP_060855.2	LSG1	21|18	39
NP_009057.1	VCP	60|54	38
NP_066565.1	NMT1	4|4	36
NP_002107.3	HLA-A	4|3	35
NP_002785.1	PSMB2	4|3	35
NP_079430.3	SUN1	11|11	33
NP_065779.1	ESYT2	6|11	30.6
NP_077306.1	SLC27A3	3|3	30
NP_001177921.1	SLC33A1	3|3	30
NP_057133.2	EMC9	3|3	30
NP_116231.2	TMEM209	3|3	30

NP_683877.1	PSMA1	3|3	30
NP_002861.1	RAB13	3|3	30
NP_002858.2	RAB3B	3|3	30
NP_004466.2	FLOT2	3|3	30
NP_068747.1	SPCS3	2|4	30
NP_068708.1	ST7	2|4	30
NP_006816.2	CKAP4	46|48	28.2
NP_056163.1	TMEM131	3|2	25
NP_065143.2	ATP13A1	3|2	25
NP_003225.2	TFRC	2|3	25
NP_002202.2	ITGB1	2|3	25
NP_071760.2	DNAJC1	3|2	25
NP_002782.1	PSMA6	2|3	25
NP_005379.3	PDCL	2|3	25
NP_085153.1	LNPK	2|3	25
NP_008910.2	SLC39A7	3|2	25
NP_694546.1	PSMC4	22|28	23.68
NP_002797.3	PSMC6	14|22	23.14
NP_003565.4	VAPA	29|17	21.79
NP_001161086.1	LEMD3	12|13	20.45
NP_113622.1	TMUB1	2|2	20
NP_001278.1	CLCN7	2|2	20
NP_689695.2	C19orf25	2|2	20
NP_219488.1	TMEM259	2|2	20
NP_003031.3	SLC4A2	2|2	20
NP_060729.2	TTC17	2|2	20
NP_115497.4	MAGT1	2|2	20
NP_002781.2	PSMA5	2|2	20
NP_001242983.1	C9orf72	2|2	20
NP_057033.2	GET4	2|2	20
NP_963920.1	USP33	2|2	20
NP_001182257.1	RAB9A	2|2	20
NP_036221.2	ABCB10	2|2	20
NP_006274.2	TACC1	45|43	17.6
NP_006311.2	PGRMC2	26|38	16.94
NP_004777.1	TXNL1	20|26	16.56
NP_004448.2	ACSL3	6|12	16.2
NP_848927.2	MTDH	40|48	15.84
NP_000373.1	ALDH3A2	22|29	15.83
NP_001124197.1	PSMB5	3|4	15.75
NP_060738.2	WDR41	5|5	15
NP_005650.2	UFD1	2|3	15
NP_076950.1	DDX50	6|12	14.73

NP_003130.2	SRPRA	27|28	14.56
NP_001198.2	BTF3	10|11	14.54
NP_065825.1	MIB1	4|4	14.4
NP_002798.2	PSMD1	31|37	13.91
NP_057227.2	NSFL1C	45|46	13.88
NP_057457.1	WWOX	66|57	12.58
NP_002793.2	PSMC1	22|25	12.09
NP_079010.2	CLMN	6|6	12
NP_006149.2	NEFL	4|4	12
NP_009106.1	ERLIN2	32|40	11.57
NP_008878.3	SRP72	12|8	11.25
NP_002806.2	PSMD11	9|7	11.08
NP_065892.1	OSBPL8	26|28	11.05
NP_001007215.1	CACYBP	7|17	10.8
NP_683704.2	OSBPL9	6|2	10.29
P05784	Krt18	5|4	10.12
NP_001189398.1	NIPSNAP2	10|10	9.47
NP_002807.1	PSMD12	6|7	9
NP_001138238.1	DNAJC7	4|6	9
NP_001531.1	HSPB1	3|3	9
NP_064555.2	NCLN	2|4	9
NP_002796.4	PSMC5	32|36	8.27
NP_060391.2	NPLOC4	6|5	8.25
NP_067026.3	SRPRB	4|7	8.25
NP_002795.2	PSMC3	17|21	7.77
NP_001934.2	DSG2	4|5	7.36
NP_005852.2	STUB1	3|5	7.2
NP_005021.2	PLK1	4|3	7
NP_065147.1	DDX24	4|7	6.6
NP_002808.3	PSMD13	8|7	6.14
NP_000108.1	EMD	39|36	6.08
NP_000692.2	ATP1A1	16|12	6
NP_036546.2	RAB3GAP2	5|8	5.85
NP_079330.2	VCPIP1	42|44	5.69
NP_002849.1	ABCD3	24|26	5.56
NP_001135770.1	SQSTM1	54|63	5.29
NP_001185946.1	LRRC49	13|16	5.22
NP_065941.2	CIP2A	21|22	5.09
NP_002287.2	LBR	86|94	4.94
NP_055205.2	SND1	11|8	4.5
NP_066390.1	HIST1H2AE	12|10	4.3
NP_002801.1	PSMD4	8|11	3.98
NP_004773.1	SNAP29	11|11	3.88

NP_002794.1	PSMC2	21|22	3.79
NP_002799.3	PSMD2	29|24	3.7
NP_005564.1	LMNB1	15|13	3.15

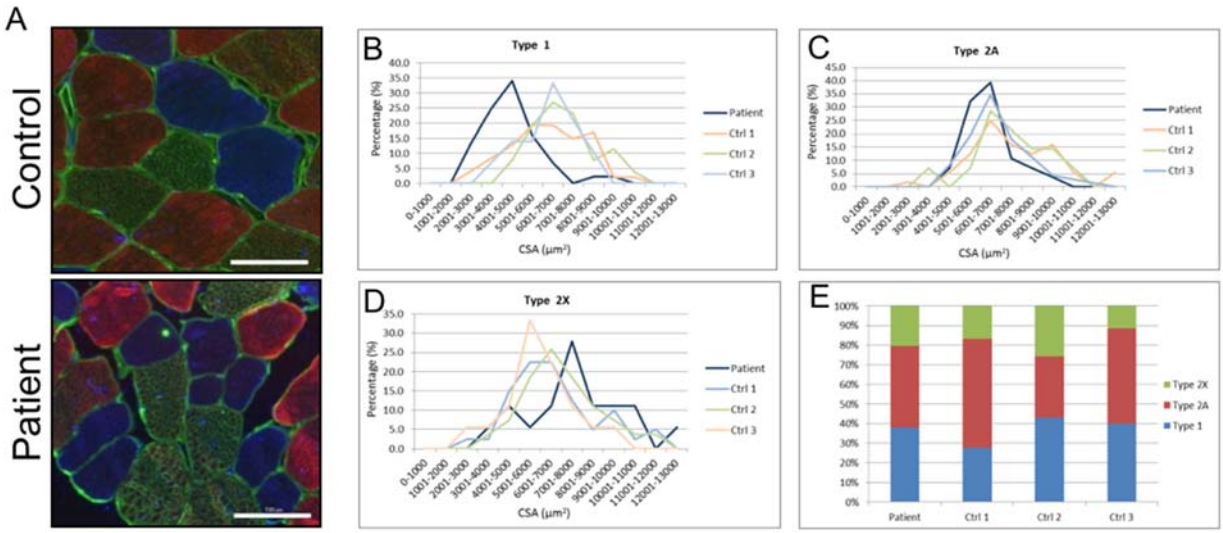

Supplemental Figure 2.1. ST patient has smaller type 1 myofibers, but slightly larger type 2X fibers. (**A**) Myosin Heavy Chains (MHC) staining of transverse sections of human control skeletal muscle (upper panel) and of ST patient (lower panel); MHC labeling: type 1 myofibers are labeled in blue, type 2B are labeled in red and type 2X in green. Scale bar: 100 µm. (**B**) Frequency distribution of type 1 myofiber cross-sectional area (CSA) with three age-match controls and one ST affected patient. (**C**) Same as in *B*, but with type 2A myofibers. (**D**) Same as in *B* and *C*, but with type 2X myofiber. (**E**). Percentage of the different fiber types found in the muscle of three controls and of one ST affected patient.

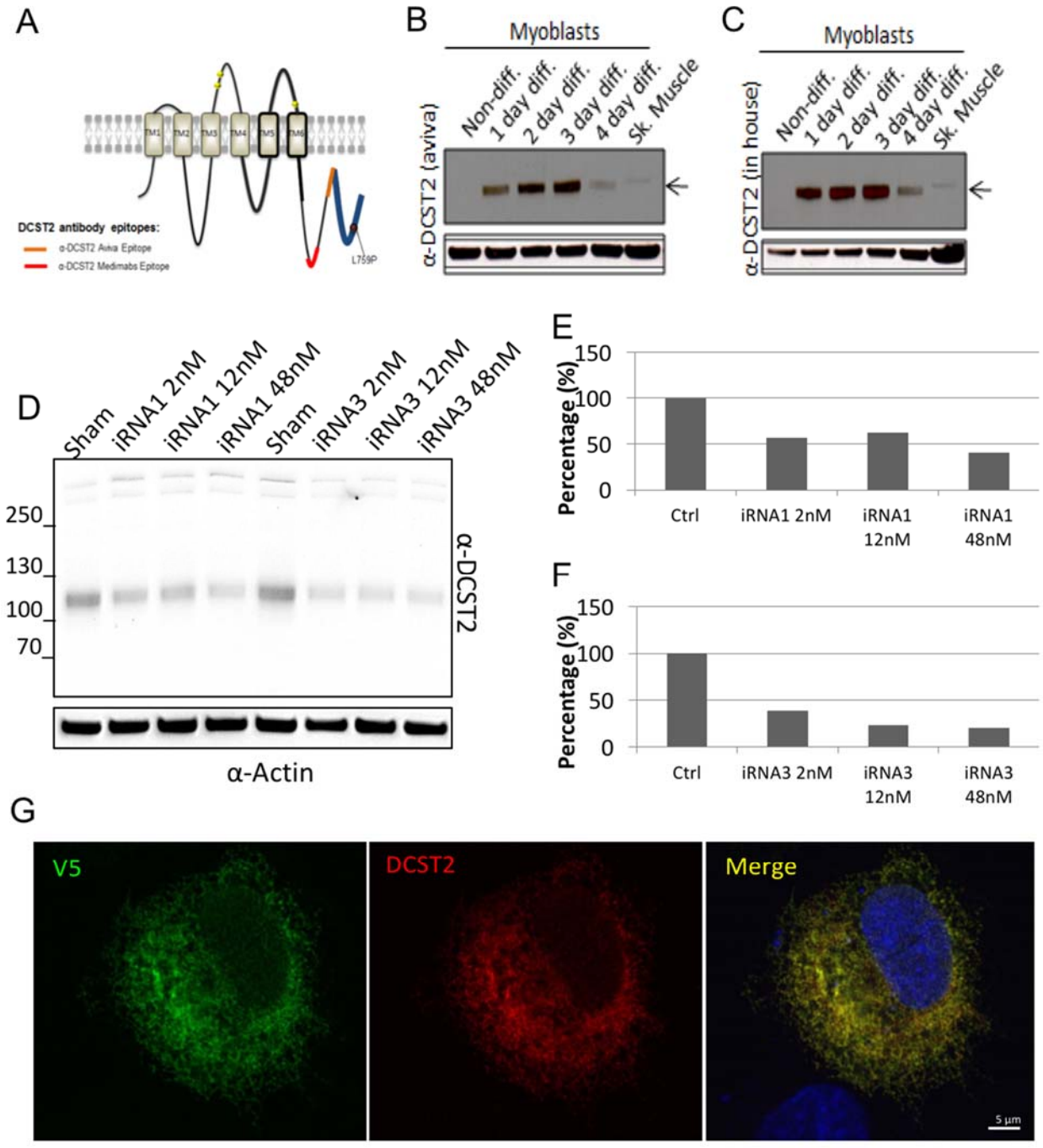

Supplemental Figure 2.2. Specificity testing of an in-house antibody produced against human DCST2. (**A**) Schematic representation of DCST2 structure and domains with the region of DCST2 antibodies epitopes represented in red (in-house antibody, by MediMabs) and orange (Aviva antibody). (**B**) Western blot of protein lysates prepared from myoblasts in differentiation at different time points and human skeletal muscle labeled with α-DCST2 Aviva antibody; Endogenous DCST2: 86 kDa. (**C**) Same western blot as in b, but labeled with in-house α-DCST2

MediMabs antibody. (**D**) Western blot of protein lysates from myoblasts submitted to DCST2 knockdown using 2 different DCST2 iRNAs. (**E and F**) Densitometry analyses of figure E showing a loss of expression in the samples submitted to DCST2 knockdown. (**G**) Co-immunolabeling of cells overexpressing DCST2-V5 protein with α-V5 antibody and in-house α-DCST2 antibody.

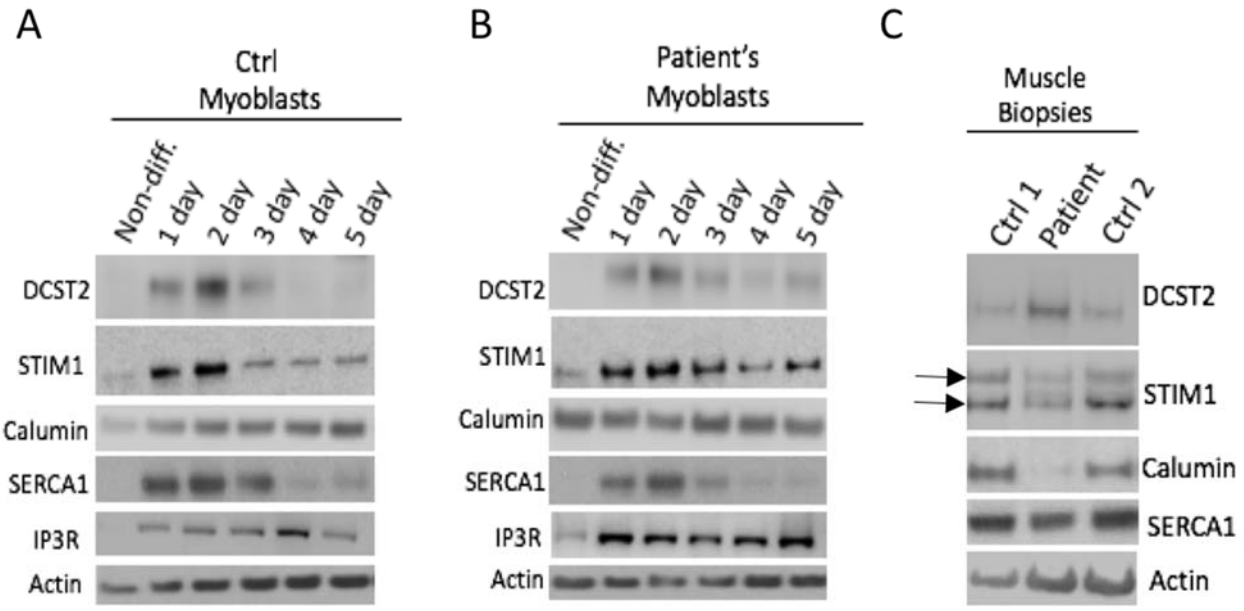

Supplemental Figure 2.3. DCST2 is expressed in differentiating myoblasts. (**A**) Western blot of protein lysates prepared from human control immortalized myoblasts line labeled with α-DCST2, α-STIM1, α-SERCA1, α-Calumin, α-IP3R and α-Actin antibodies. (**B**) Same as in *a*, but with ST myoblasts. (**C**) Western blots with protein lysates from muscle biopsies of two control individuals and one SP patient labeled for DCST2, SERCA1, Calumin, STIM1 and actin.

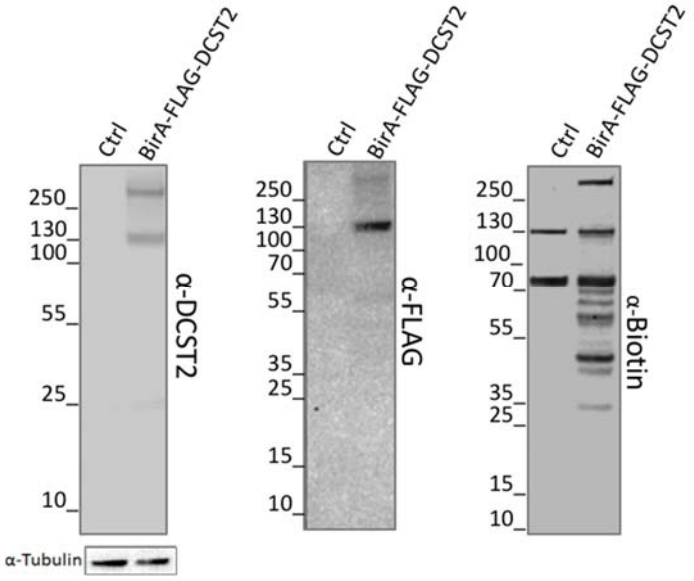

Supplemental Figure 2.4. Expression of BirA-FLAG-DCST2 for BioID assay. Western blot analysis of protein lysates of HEK293 Flp-In T-REx cells expressing BirA-FLAG-DCST2 labeled with α-DCST2 antibody (left), α-flag antibody (middle), or with α-biotin antibody (right).

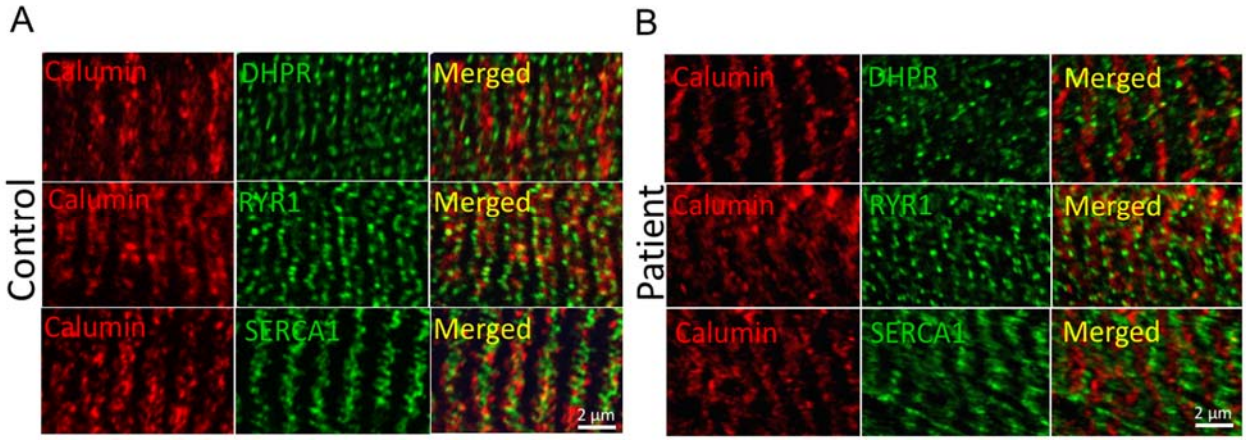

Supplemental Figure 2.5. Calumin localization in human skeletal muscle. Confocal images of longitudinal sections of human skeletal muscle labeled with Calumin in red and several markers of intracellular membranes in green as follows: DHPR (a T-tubules marker); RYR1 (a marker of terminal cisternae of the SR); and SERCA1 (a marker of longitudinal cisternae of the SR of type 2 fibers) in a control (**A**) and in a ST patient (**B**).

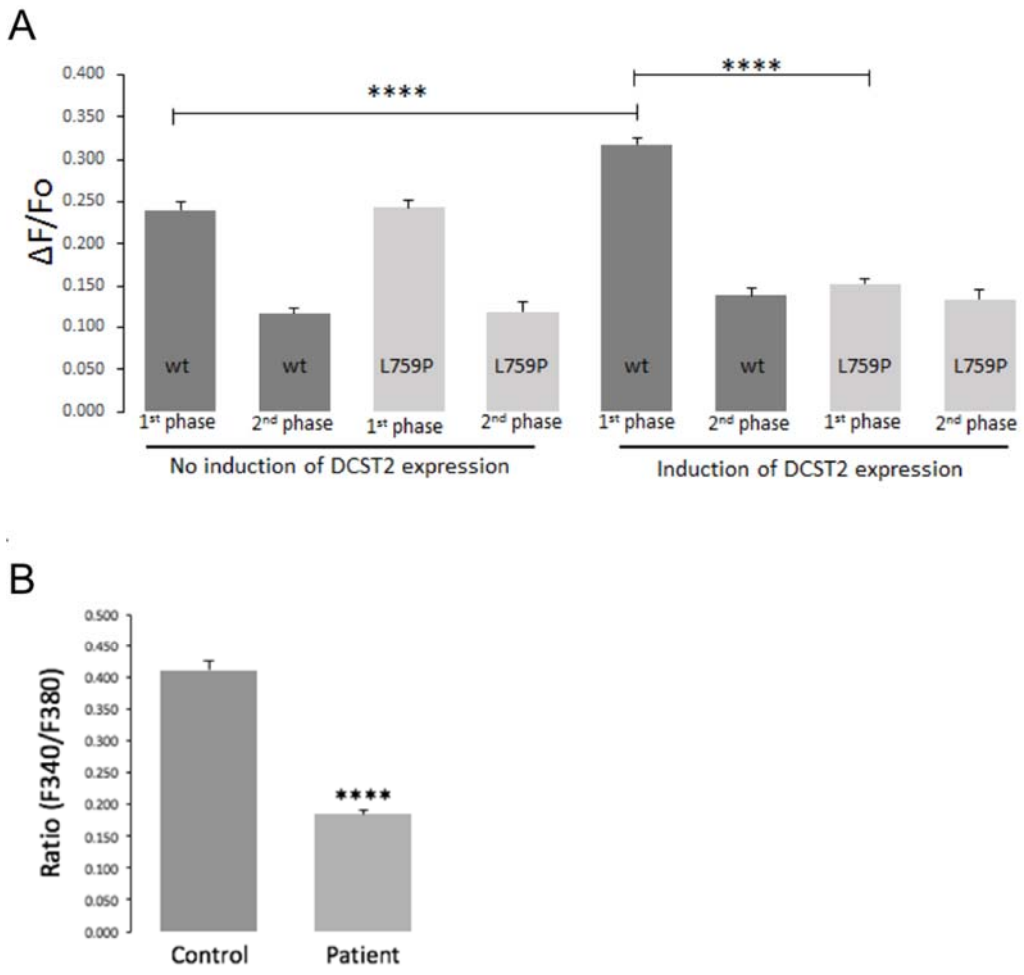

Supplemental Figure 2.6. DCST2 ST mutation influences SR calcium levels causing a major impact on calcium transients. (**A**) Summary data showing the average of TG-evoked calcium depletion and calcium add-back in HEK293 Flp-In T-REx cells induced or not to overexpress DCST2 or DCST2-L759P; Data are presented as mean (± SEM.) of three independent assays, statistically significant differences (one-way ANOVA for multiple comparisons) are indicated (****P<0.0001). (**B**) Summary data showing the average of basal intracellular calcium levels of control and patient's differentiating myoblasts; Data are presented as mean (± SEM) of three independent assays, statistical analysis, unpaired *t*-test (****P<0.0001).

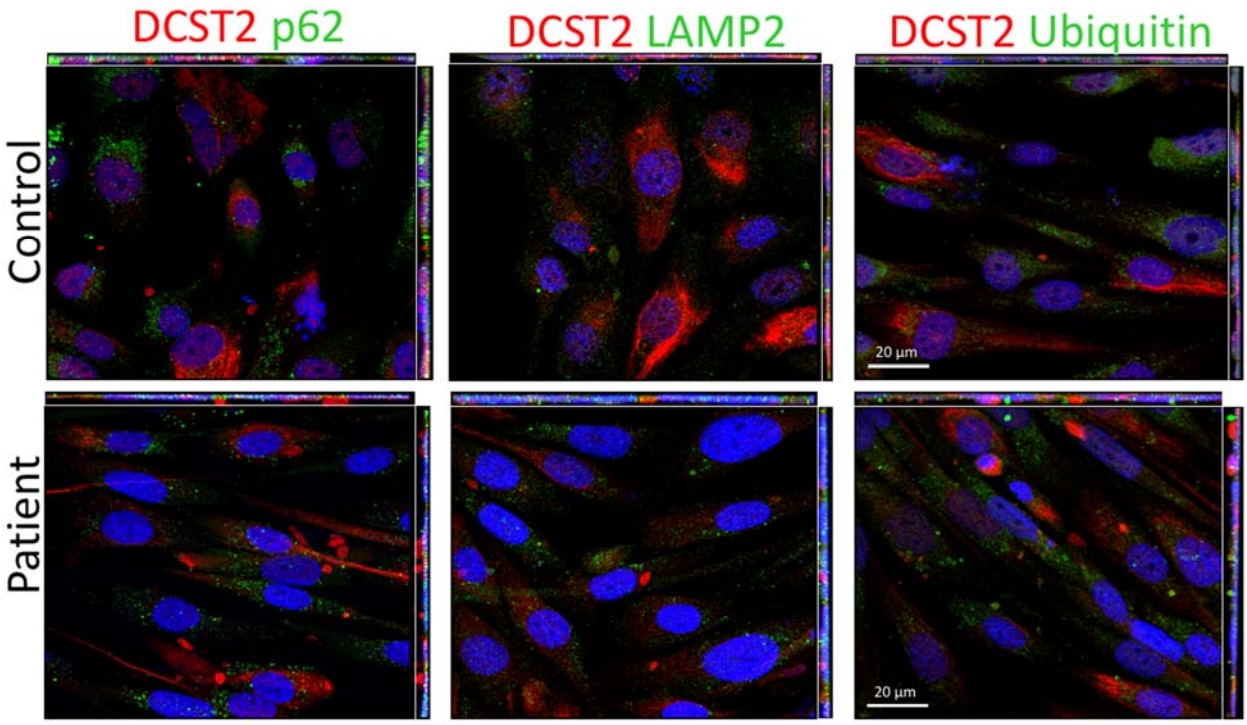

Supplemental Figure 2.7. Large DCST2 puncta are not non-functional protein aggregates. Maximum projection confocal images of control (upper panel) and ST (lower panel) myoblasts treated with TG and labeled with DCST2 in red and p62 in green (on the left), LAMP2 (at the middle) and ubiquitin (on the right).

PREFACE TO CHAPTER 3

Despite being successful in identifying the first mutated gene in two ST families, there are still several ST cases that do not carry DCST2 mutations. Considering that ST is not a rare disorder and that it is constantly misdiagnosed, it is of crucial importance to find better ways of identifying this disease. In Chapter 3, we aimed to explore the key clinical features and biomarkers of the ST.

CHAPTER 3: Enlarged skeletal muscle DCST2 positive puncta as a marker of the Strongman trait

Talita C. Conte[1,2], Xavier Allard[1,2], Rebecca Robertson[1,2], Tanja Taivassalo[3], Russell Hepple[4], Jason Karamchandani[5], Erin K. O'Ferrall[5,6], Bernard Brais[1,2]

1) Neurogenetics of Motion Laboratory, Department of Neurology and Neurosurgery, Montreal Neurological Institute, McGill University, Montreal, Quebec, Canada.
2) Department of Human Genetics, McGill University, Montréal, Québec, Canada.
3) Department of Physiology and Functional Genomics, University of Florida, Gainesville, Florida, USA.
4) Department of Physical Therapy and Muscle Biology, University of Florida, Gainesville, Florida, USA.
5) Department of Pathology, McGill University Health Centre, Montreal Neurological Institute Hospital, Montreal, QC H3A 2B4, Canada.
6) Department of Neurology and Neurosurgery, McGill University Health Centre, Montreal Neurological Institute Hospital, Montreal, QC H3A 2B4, Canada.

Manuscript in preparation

Abstract

Objective: In this study, we aimed to establish if Strongman Trait (ST) cases that do not carry *DCST2* mutations have on immunolabeling the same larger DCST2 positive puncta in their skeletal muscle biopsies as ST patients carrying *DCST2* mutations.

Methods: Three patients meeting our clinical diagnostic criteria for ST had muscle biopsies. Immunolabeling for DCST2, SERCA1 and STIM1 was completed and the size of DCST2 positive puncta was assessed in ST cases and controls.

Results: All three ST patients had a personal and family history of above normal strength. On examination, these patients presented muscle hypertrophy, prolonged muscle contraction following percussion in at least two muscles, and deltoid weakness after 20 rapid contractions. We observed a significant increase in the size of DCST2 puncta that contain SERCA1 and STIM1 in the ST muscles compared to controls.

Conclusions: We propose that the presence of larger DCST2 puncta containing SERCA1 and STIM1 can be used to support the clinical diagnosis of the ST in cases that do not carry a *DCST2* mutation.

Introduction

The diagnostic odyssey of patients consulting for muscle pain and fatigue with large muscle mass (despite a low level of physical activity) often leads to no clear diagnosis even upon extensive investigations. Muscle hypertrophy and/or increased strength can be present in a few myopathies, such as: McArdle disease caused by recessive mutations in myophosphorylase (*PYGM*) [148], non-dystrophic myotonias caused by mutations in the chloride voltage-gated channel 1 (*CLCN1*) or the sodium voltage-gated channel alpha subunit 4 (*SCN4A*) genes [149], mutations in ryanodine receptor 1 (*RYR1*) associated with malignant hyperthermia susceptibility and other RYR1 related myopathies [108,150,151], Brody disease caused by mutations in ATPase sarcoplasmic/endoplasmic reticulum Ca^{2+} transporting 1 (*SERCA1*) [55] and rippling muscle disease caused by mutations in caveolin 3 (*CAV3*) [122]. Muscle pathology combined to next generation gene panel testing will in some cases confirm a diagnosis, but in not all cases. We have recently mapped to chromosome 1 a mutation in *DCST2* causing a new type of Herculean myalgic disorder which we called the Strongman trait (ST) in two French-Canadian families (Conte et al. submitted to *Brain*). Patients with this mutation present above average strength, muscle hypertrophy, prolonged contractions, myalgia and fatigue. Since *DCST2* mutations were not uncovered in most patients of our ST cohort, we hypothesized that ST patients displaying clinical overlap may share the DCST2 pathological phenotype which consists of an increase in the size of DCST2 positive puncta that often contain SERCA1 and STIM1.

Materials and Methods

Patient recruitment

All participants underwent detailed examination by experienced neurologists. Sample collection was performed with written informed consent approved by the ethics board of the Montreal Neurological Institute. DNA was isolated from peripheral blood lymphocytes using Gentra Puregene blood kit (Qiagen) according to the manufacturer's protocol. Previous histopathological on muscle biopsies and EMG results were reviewed on three ST cases.

Mutation analysis

PCR products of DCST2 exons 1 to 15 were sent to McGill University and Genome Quebec Innovation Center for sequencing, using a 3730XL DNA Analyzer (Applied Biosystems, Foster City, CA, USA). Mutation detection analysis was performed using SeqMan v.4.03 (DNASTAR Inc., Madison, WI, USA).

Skeletal muscle morphology analysis

The three muscle biopsies were first studied in clinical pathology laboratories. The standard stains performed in the clinical laboratories included: H&E, modified Gomori Trichrome, cytochrome C oxidase, succinate dehydrogenase, acid phosphatase, ATPase reacted sections at pH 4.3, 4.6 & 9.4, periodic acid Schiff, and myophosphorylase. Immunostaining for desmin and actin was also performed.

Immunofluorescence

Ten micron thick serial cross and longitudinal sections were cut in a cryostat at -22°C and mounted on lysine coated slides (Superforst). Primary MHCs antibody cocktail composed of a mouse IgG2b monoclonal anti-MHC type I (BA-F8, 1:25), mouse IgG1 monoclonal anti-MHC type IIa (SC- 71, 1:200), mouse IgM monoclonal anti-type 2x MHC (6H1, 1:25) and a rabbit IgG

polyclonal anti-laminin (L9393, Sigma) were used for immunolabeling as described previously[159]. All primary antibodies targeting MHCs were purchased from the Developmental Studies Hybridoma Bank (DSHB, University of Iowa, IA). For DCST2, SERCA1 and STIM1 labeling, human muscle sections were immunolabeled as follows: sections were fixed with 4% paraformaldehyde (PFA) for 15 minutes, blocked and permeabilized with a TBS solution containing 5% normal donkey serum (NDS), 0.25% Triton and 0.1M glycine for 1 hour, incubated overnight with primary antibodies, incubated with secondary antibodies for 1 hour and mounted. DCST2 (in-house rabbit antibody) was double labeled with SERCA1 (MA3-912, ThermoFisher), or STIM1 (310954, BD Biosciences).

Confocal imaging

Stained tissue slides were imaged using 20x or 60x objective lenses of a Zeiss LSM 710 laser scanning microscope (Carl Zeiss Canada Ltd., Toronto, ON, Canada; McGill Life Sciences Imaging Facility) using Zeiss LSM acquisition software. Images were processed using Zen 2009 Image Browser software (Carl Zeiss, Jena, Germany). Images for quantification were captured using the same parameters to allow comparisons to be made between conditions. For the quantification of MHCs in the muscle biopsies, quantitative and morphometric data were obtained by analyzing images with ImagePro Plus software (Media Cybernetics, Inc.). Myofiber cross-sectional area (CSA) was obtained by measuring between 200 and 300 myofibers per individual. Analysis of DCST2 and SERCA1 colocalization in skeletal muscle tissue was done with the Fiji software: merged images were split, thresholded and binarized; the "Image calculator" plug-in from Fiji combined DCST2 and SERCA1 images through the "subtract" operation option creating a new image with just puncta that colocalized the two proteins. White pixels from the generated images were measured for quantification of DCST2 and SERCA1 colocalization.

Results

Clinical presentation

Three patients meeting the clinical criteria for the Strongman Trait (ST) were recruited for this study. Patients were seeking medical attention because of severe myalgia often accompanied by prolonged muscular contractions or cramps, and weakness after repeated or prolonged contractions, which together interfered with their daily living. Patients DNA were screened by a next generation gene panel (Medical Neurogenetics, LLC) and were tested negative for mutations in the following genes that can be associated with cramps and muscles hypertrophy: *CLCN1*, *SCN4A*, *ATP2A1*, *CAV3*, *RYR1*, *MSTN, ANO5, PLIN1, and LMNA*[38,55,111,122,137,146]. These patients were also negative for the missense at the position c.2276T>C in *DCST2* gene (Table 3.1).

Patient 1 is a French-Canadian male (fig. 3.1b) who had a long history of above average strength and muscle hypertrophy. He presented at age 37 with increased myalgia and fatigue that forced him to stop working as a truck driver. He described the pain as muscle burning and heaviness with some cramps. He mentioned having episodes of severe fatigue in the past, but he now had constant fatigue. CK levels were usually normal with a highest value at 97 U/L. EMG showed prominent muscle membrane irritability on needle insertion. He presented large muscle bulk and had a personal and family history of above-average strength. He reports starting to have muscle cramps at the age of 25. At age of 37, his symptoms were severe enough to lead him to permanent disability. On examination, he presents large muscle mass for his level of physical activity. He has superior strength on first contraction, but significant weakness after 20 contractions of the dominant deltoid. He also has percussion myoclonus in muscles of his four extremities. The rest of the neurological exam is normal. Gene panel sequencing did not uncover any causal mutation.

Patient 2 is a French-Canadian male who presented in clinics at age of 46 with a 4-year history of myalgia that he also described as muscle burning that increased after physical activity. He has a history of superior strength and athletic performance since youth. Since the age of 43, his increasing cramps and myalgia in his upper and lower extremities has led him to permanent disability. He has had episodic fasciculation in his upper and lower extremities. His associated

extreme fatigue has further limited his daily activities. He has superior muscle mass for his very limited level of activity. His initial contractions are extremely powerful, but his deltoid weakens after 20 contractions. Percussion myoclonus is easily elicited in all four limbs. EMG and CK were normal. Gene panel sequencing did not uncover any causal mutation.

Patient 3 is a 52-year-old French-Canadian female who first consulted at age of 50 for severe post-activity muscle pain, cramps and fatigue that made it impossible for her to return to her occupation. She presented with hypertrophied calves and spontaneous muscle fasciculation. She states that she was 36 the first time she had a significant episode of muscle pain. She reported being very active and stronger than the average when she was young. On exam, she presents large muscle bulk. Her first contractions are strong, but she significantly weakens after 20 contractions of the deltoid. She demonstrated percussion myotonia in three limbs. EMG was normal. Gene panel sequencing did not uncover any causal mutation.

Muscle biopsies

Histological analysis of the three ST patients muscle biopsies revealed no gross abnormalities and normal myofibers morphology (Fig. 3.1a). No inflammation, fibrosis, necrosis, adipocyte infiltration, centralized nuclei, or fiber splitting were observed. Analysis of the cross-sectional area (CSA) of the different fiber types showed that patient 1 presented smaller type 1 and slightly larger type 2X myofibers compared to age-match controls (fig. 3.1 c-d).

Immunofluorescent labeling of skeletal muscle cross-sections showed that DCST2 forms larger puncta in the muscle of all ST patients when compared to controls (fig. 3.2 a-b). Co-staining analysis showed that larger DCST2 puncta were frequently positive for SERCA1 or STIM1 in the ST muscles (fig. 3.2 a-b). To better analyze DCST2 large puncta, we performed quantification analysis of DCST2 staining on longitudinal sections of patient 3's biopsy. We observed that DCST2 forms significantly larger puncta that often colocalize with SERCA1 in the muscle of the ST patient than in the controls (fig. 3.2 c-d).

Discussion

The pathological comparison of muscle biopsies from three ST cases that do not carry *DCST2* mutations suggests that the presence of larger DCST2 positive puncta may be used as pathological evidence to support the ST diagnosis. Our histological findings suggest that there is a common mechanism of action causing the symptoms in the ST patients that carry or not a missense mutation in *DCST2* (Conte et al, submitted to *Brain*). As in the biopsy of a patient that carries a *DCST2* mutation, all three ST cases in this study display normal muscle morphology with only mild changes in type 1 and 2X cross-sectional area. Furthermore, these ST patients also present significantly larger DCST2 puncta that colocalize more often with STIM1 and SERCA1 than in controls. We hypothesize that the yet to be identified mutated gene in these negative *DCST2* ST patients are either direct partners of DCST2 or involved in the dynamics of the puncta formation that are clearly important for normal cellular calcium handling. Such larger puncta have been observed in other calcium handling disorders such as Tubular aggregate myopathy (TAM) caused by gain of function mutations in STIM1 or ORAI1. On cross sections of patients with TAM, these large puncta contain STIM1[108] and SERCA1[171]. Although in these publications the puncta were not measured, they seem to be larger than the ones observed in the ST muscle. We think that in TAM the much larger STIM1 and SERCA1 complexes play a role in increasing intracellular calcium transients, and thus impacting negatively the myofiber development and maintenance, which is not the case in ST. Since the majority of ST patients seen in clinic have a negative work-up (including the sequencing of *DCST2*), this study suggests that quantifying the size of DCST2 puncta and performing the colabeling of STIM1 and SERCA with DCST2 in particular on longitudinal muscle sections may help support the ST diagnosis. This is an important discovery since most of the most affected ST cases cannot continue to work because of their myalgia, cramps and severe fatigue. In this study, we explored the histological findings that may lead to a firmer diagnosis and shorten the diagnostic odyssey for ST patients until a final genetic diagnosis is arrested.

Figures and Tables

Table 3.1: Clinical features on three ST cases with full examination

Patient number	1	2	3
Age			
Sex	M	M	F
Above average strength	+	+	+
Weakness after repetitive movement	+	+	+
Myalgia post-activity	+	+	+
Large muscle bulk	+	+	+
Deltoid Fatigability	+	+	+
Superior Strength	+	+	+
Pseudomyotonia	+	+	+
Proximal Weakness	-	-	-

Abbreviations: F, female; M, male; +, present; -, absent.

.

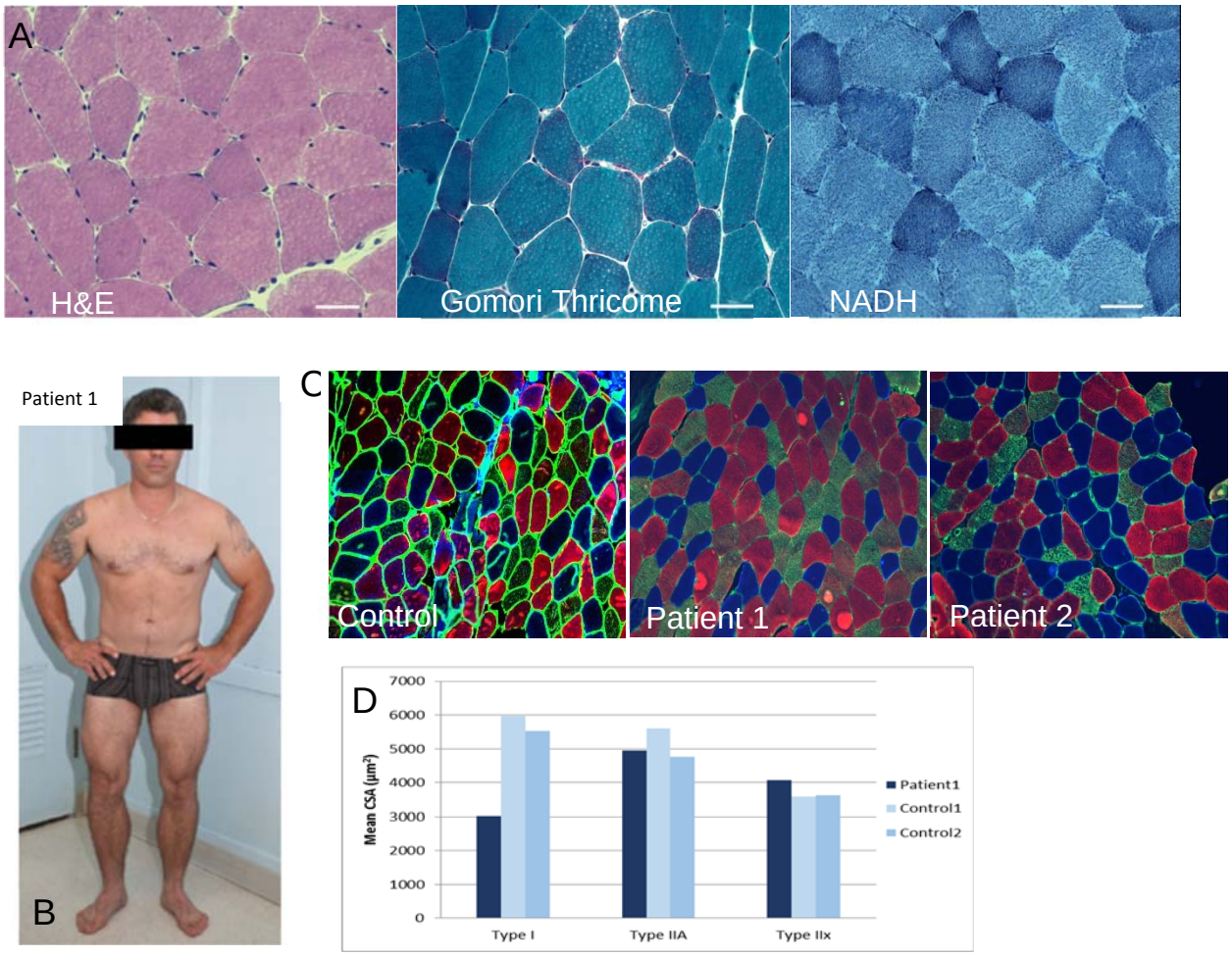

Figure 3.1| ST patients with no mutation in *DCST2* present normal muscle morphology. A. Skeletal muscle cross-sections of patient 1 stained with H&E (left), gomori thricome (middle), and NADH (right); scalebar: 50 uM. B. Photograph of patient 1. C. Skeletal muscle cross-sections stained MHCs of a control (left), patient 1 (middle) and patient 2 (right). D. Mean of myofiber CSA of different fiber types of patient 1 and 2 age-match controls.

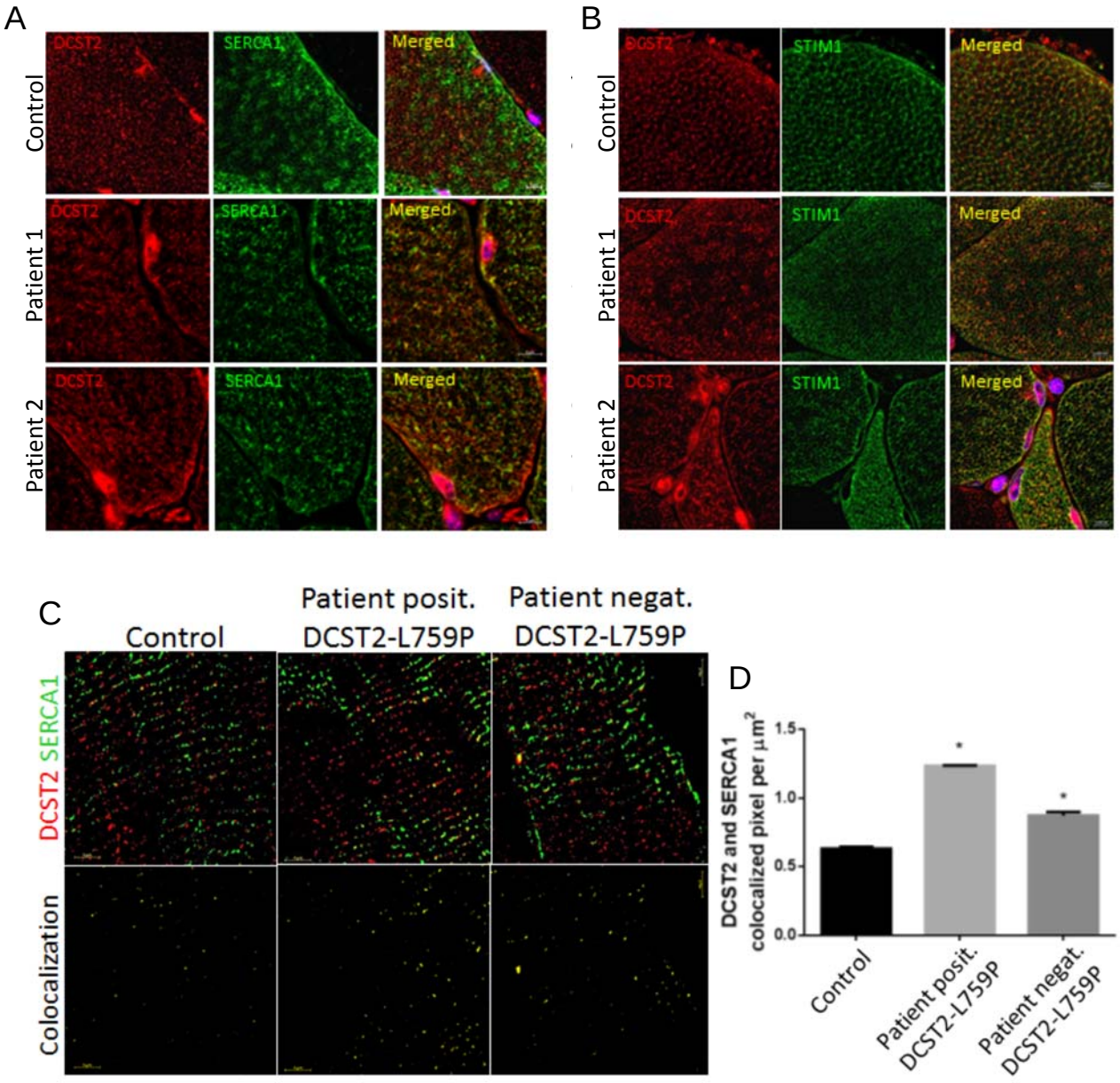

Figure 3.2. DCST2 forms large puncta that can colocalize with SERCA1 and STIM1 in the muscle of ST patients that do not carry *DCST2* mutations. A. Transverse sections of control and patients 1 and 2 muscles colabeled with DCST2 in red and SERCA1 in green. B. Same as in A, but with STIM1 in green. Scalebar: 5 µm C. Confocal binarized images of longitudinal sections of control (left panels), DCST2-L759P positive ST patient (middle panels) and DCST2-L759P negative ST patient (right panels) skeletal muscle labeled with DCST2 in red and SERCA1 in green; "DCST2 SERCA1" label indicates thresholded, binarized and merged images; and "Colocalization" indicates binarized images of DCST2 and SERCA1 showing only area of colocalization for two the proteins labeled; Scale bar: 2 µm. D. Quantification showing the mean of white pixels per μm^2 of the colocalized DCST2 and SERCA1 puncta in the control and ST patient's muscle; data are presented as mean (± SD); Statistical analysis, unpaired *t*-test (**P*<0.05).

References

Miller TM. Differential diagnosis of myotonic disorders. Muscle & nerve 2008;37:293-299.

Voermans NC, Laan AE, Oosterhof A, et al. Brody syndrome: a clinically heterogeneous entity distinct from Brody disease: a review of literature and a cross-sectional clinical study in 17 patients. Neuromuscular disorders : NMD 2012;22:944-954.

Trivedi JR, Bundy B, Statland J, et al. Non-dystrophic myotonia: prospective study of objective and patient reported outcomes. Brain : a journal of neurology 2013;136:2189-2200.

Scalco RS, Gardiner AR, Pitceathly RD, et al. CAV3 mutations causing exercise intolerance, myalgia and rhabdomyolysis: Expanding the phenotypic spectrum of caveolinopathies. Neuromuscular disorders : NMD 2016;26:504-510.

Gouspillou G, Sgarioto N, Norris B, et al. The relationship between muscle fiber type-specific PGC-1alpha content and mitochondrial content varies between rodent models and humans. PloS one 2014;9:e103044.

Brody IA. Muscle contracture induced by exercise. A syndrome attributable to decreased relaxing factor. The New England journal of medicine 1969;281:187-192.

Bolduc V, Marlow G, Boycott KM, et al. Recessive mutations in the putative calcium-activated chloride channel Anoctamin 5 cause proximal LGMD2L and distal MMD3 muscular dystrophies. American journal of human genetics 2010;86:213-221.

Schuelke M, Wagner KR, Stolz LE, et al. Myostatin mutation associated with gross muscle hypertrophy in a child. The New England journal of medicine 2004;350:2682-2688.

Bohm J, Laporte J. Gain-of-function mutations in STIM1 and ORAI1 causing tubular aggregate myopathy and Stormorken syndrome. Cell Calcium 2018;76:1-9.

Bohm J, Chevessier F, Koch C, et al. Clinical, histological and genetic characterisation of patients with tubular aggregate myopathy caused by mutations in STIM1. Journal of medical genetics 2014;51:824-833.

CHAPTER 4: General Discussion

4.1 Summary

The main goal of this thesis was to characterize clinically and molecularly a new type of Herculean myalgic muscle disorder called the Strongman trait (ST). This study contributes to the neuromuscular field by showing how a *DCST2* mutation found in two ST families affects the protein content of DCST2 puncta as well as cellular calcium handling. It also provides support that ST should be considered a new muscle trait that is clinically and genetically variable but that may share significant pathological and physiological overlap. In **Chapter 2**, we describe two ST families carrying the same dominant mutation in the *DCST2* gene that are associated with larger DCST2 puncta that decrease significantly the activity of SOCE and SERCA dependent SR calcium reuptake, important calcium handling regulators in skeletal muscle. **In Chapter 3**, we described the clinical and pathological features of muscle biopsies on three individuals with ST that do not carry a *DCST2* mutation and show that these patients share clinical and pathological features with ST patient positive for the *DCST2* mutation. These results can be used to support a ST diagnosis. We describe a new variable neuromuscular trait and its first casual gene, while defining pathological diagnostic findings that will shorten the diagnosis odyssey of patients while providing an original inroad on the molecular basis of muscle hypertrophy and Herculean strength as a familial trait.

4.2 Possible roles of DCST2 in skeletal muscle

4.2.1 Is DCST2's structure a clue to its function?

It is still not completely known what the functions of the other members of the DC-STAMP-like domain family are, making it difficult to speculate about DCST2's role. DCST2 belongs to a family of four proteins that share six predicted transmembrane domains and a DC-STAMP-like protein domain: dendrocyte expressed seven Transmembrane protein (DCSTAMP), osteoclast stimulatory transmembrane protein (OCSTAMP), DCST1 and DCST2 [173,176,177]. DCSTAMP, OCSTAMP and DCST1, and now by our work also DCST2, were shown to be ER

and/or Golgi proteins [173,176,177]. Previous studies about DCSTAMP showed its involvement in osteoclast fusion and myeloid differentiation through the nuclear factor of activated T cells 1 (NFATc1)/Ca^{2+} axis activation, but the molecular mechanism mediating this process remains unknown [176,178]. Moreover, OCSTAMP has been described to increase osteoclast and foreign body giant cells formation [177,179]. DCSTAMP and OCSTAMP proteins have been extensively used as markers of the processes mentioned above, however, their functions are still poorly understood. Prior to our work on DCST2, no other studies had shown a link between the other proteins of the DC-STAMP protein-domain family and cellular calcium transients to date.

DCST1 is a paralog of DCST2 with 19.76 % amino acid conservation (Uniprot BLAST). It does not have an N-terminal intra-luminal proline-rich domain as DCST2 (Uniprot). DCST1 lies next to DCST2 in a head to tail orientation on chromosome 1 in humans (UCSC genome browser) suggesting an ancient duplication. DCST1 was found to have an E3 ubiquitin-ligase role by interacting with and promoting ubiquitination of signal transducer and activator of transcription 2 (STAT2), leading to reduced STAT2 expression and attenuated activation of the interferon stimulated genes induction pathway [173].

Spaetzle-processing enzyme 42 (SPE-42) is an orthologue of DCST2 in *Caenorhabditis elegans* which also contains DC-STAMP-like domain and a putative really interesting new gene (RING)-finger domain [180]. A previous study showed that SPE-42 mutations affect fertilization in worms, but no molecular studies have been published so far [179]. Sequence analysis of SPE-42 predicts that the Zn^{++} ions of the predicted RING-finger domain are coordinated by eight cysteines (C4C4 pattern), unlike most E3 RING-fingers, which generally include a histidine in a C3HC4 arrangement [180]. However, the authors of this study say that they cannot rule out an E3 ligase-like function for SPE-42. The eight cysteines in the predicted RING-finger of SPE-42 are conserved in DCST2 (data not shown) raising the possibility that these proteins might have a similar function, but more studies are required to address this question. DCST2 large puncta are negative for markers of autophagosomes and ubiquitin indicating that DCST2 might not have an E3 ubiquitin-ligase activity, but further work is necessary to exclude this possibility. Analysis done with PHYRE2 Protein Fold Recognition Server (a webportal that does modeling of membrane proteins based on the protein homology) aligned with a high confidence specific residues of DCST2 predicted RING-finger with another E3-ubiquitin ligase called: ring finger

protein 25 (RNF25, confidence score of 92.1) and with RING/U-box C3HC4 domain (confidence score of 90.4).

RING-fingers are structural domains, held together by the coordination of two Zn^{++} ions by the side chains of nearby cysteine, histidine or aspartic acid side chains [181,182]. These motifs are most commonly found in E3 ubiquitin protein ligases where they facilitate ubiquitination of target proteins [183,184]. E3 RING-finger proteins simultaneously interact with a substrate and an ubiquitin-conjugated E2 enzyme, allowing transfer of ubiquitin to the substrate by the E2 [185]. Although examples of RING-fingers in proteins that are not E3s may exist, functional data support an E3 ligase activity for almost half of the 300 predicted human RING-finger proteins; the rest either have not been examined or no alternative molecular mechanism of action has been assigned [184]. Some RING-finger proteins like BRCA1 associated RING domain 1 (BARD1) do not possess intrinsic E3 ligase activity, but are instead part of a multi-protein complex that does, in this case the BRCA1 DNA repair associated (BRCA1)-BARD1 heterodimer [186,187]. Other RING-fingers like TNF receptor associated factor 6 (TRAF6) must form homodimers in order to interact with E2 ligases [185]. Multi-subunit RING domains like the cullin RING ligase superfamily includes the SCF complex, consisting of S-phase kinase-associated protein 1 (SKP1), cullin and F-box protein, and the more elaborate anaphase-promoting complex/cyclosome (APC/C) [188,189].

RING E3s mediate protein quality control by ubiquitinating an array of misfolded and unassembled proteins, as well as those whose levels must be regulated [190,191]. In the ER, the mammalian ER associated degradation (ERAD) RING E3s autocrine motility factor receptor (AMFR) and synoviolin (SYVN1) tag proteins with polyubiquitin chains and, thereby, direct them for cytosolic degradation through proteasomes [192]. Some substrates (i.e., cytochrome P450 3A4, the cystic fibrosis transmembrane conductance regulator, and others) are targeted by ERAD E3s [193,194].

SYVN1 is a protein with a very similar domain structure as DCST2 (Figure 4.1). It is formed by 617 amino acids that code for a protein with 67 kDa (Uniprot). It has an intraluminal N-terminus, six transmembrane domains, that is followed by one RING-finger domain type C3HC4, and one proline-rich domain at the intraluminal C-terminus (Uniprot). Several studies have been published regarding SYVN1 activity as a RING E3 ligase: it has been implicated in arthropathies including rheumatoid arthritis [195] and has substrates that include p53 [196] and others.

Omura and collaborators (2008) focused in the function of the other domains of SYVN1, and interestingly they found that SYVN1 lacking the proline-rich domain only ubiquitinates G protein-coupled receptor 37 (GPR37, a known substrate), while wild type SYVN1 promotes the ubiquitination and degradation of GPR37 [197]. Furthermore, they also showed that the transmembrane domain of SYVN1 is involved in the translocation of GPR37 from the ER to the cytosol[197].

Considering all of what has been discussed above, there is a high likelihood that DCST2 is a new E3-ubiquitin ligase with some specificity in skeletal muscle and that it might be implicated in the regulation of the activity of proteins involved in calcium handling. This subject will be discussed in more details in the following section.

4.2.2 DCST2: a new protein implicated in the dynamic STIM1/ORAI1 multiprotein complex?

The generation of force for movement is the main function of skeletal muscle and calcium is one of the key players regulating this process [19]. To generate contraction, the myofiber TTs are rapidly depolarized by an end-plate generated action potential [14,19]. The highly organized network of membranes composed by the TTs and the SR that form the sarcotubular system allow a rapid propagation of the membrane depolarization and ensuing activation of DHPR at the TTs followed by its binding to RYR at the terminal cisternae of the SR [14]. This coupling between DHPR and RYR are the basis of the calcium release units (CRUs) and lead to the massive release of calcium from the SR to the cytosol [198]. This rise in free cytosolic calcium levels generates muscle contraction and its removal from the cytosol back to the SR makes the muscle relax [19]. SERCAs have an important role relaxing the muscle since it is the SR ATPase calcium pump that reuptakes free cytosolic calcium back to the SR [20]. This event is known as the EC-coupling and any perturbation impacting calcium transients during this process will have a profound effect in muscle function [19]. Mutations in RYR1 and DHPR have been previously described to cause diseases like malignant hyperthermia susceptibility, central core disease and minicore myopathy; all of which cause a dysregulation of SR calcium release [19].

The SR is the main organelle in charge of calcium storage for proper muscle contraction but it relies on a machinery regulating entry of extracellular calcium for its refilling [199]. The SOCE is a crucial mechanism for extracellular calcium entry and counts on two key proteins in the muscle: STIM1 and ORAI calcium release-activated calcium modulator 1 (ORAI1). STIM1 is a calcium sensor in the ER/SR, which oligomerizes and activates ORAI1 channels once it senses low luminal calcium levels, allowing calcium to enter the cytosol from the extracellular space [200]. In skeletal muscle, this event happens at the newly described dynamic calcium entry units (CEUs) localized in ORAI1-rich TT lateral extensions that are surrounded by STIM1-rich SR cisternae that increase in abundance with repetitive muscle activity [170,200]. During contractions, calcium entering the intracellular space through these channels is pumped into the SR by SERCAs [201]. Mutations in STIM1 and ORAI1 have been previously described to cause tubular aggregate myopathy (TAM) further confirming that SOCE has an important role in skeletal muscle function [202]. SERCAs have key roles during EC-coupling for muscle relaxation and during SOCE for SR calcium refilling [20]. Not surprisingly, mutations in SERCA1 have also been described to cause Brody disease, a myopathy in which SERCA1 presents decreased calcium pump activity [120]. Taking into consideration our calcium assay results presented in chapter 2, DCST2 appears to play an important role in influencing SR calcium levels by both influencing extracellular calcium entry and SERCA dependent SR calcium reuptake. Despite the fact that DCST2 plays a role in the same pathway, mutations in SERCA, STIM1 and ORAI1 cause different clinical symptoms than the ones observed in ST patients and the reasons for this remain to be explored.

One of our preliminary results by two-dimensional polyacrylamide gel electrophoresis (2D-PAGE) with protein lysates of myoblasts overexpressing DCST2-V5 support that DCST2 can be present in three different size complexes (see appendix 2 supplemental figure 1A) suggesting that it may interact with itself and other proteins to form large functional complexes. DCST2 molecular weight is 86 kDa, but we see one complex that could correspond to a dimer at around 170 kDa, and other two larger complexes around 350 kDa and 500 kDa. When relabeling the same membrane with an antibody against STIM1, we observe that STIM1 is part of the same complexes as DCST2 in the 350 kDa and 500 kDa complexes (appendix 2 supplemental figure 1B) further supporting that STIM1 is one of DCST2's partners.

By overexpressing wildtype DCST2 in HEK293 cells, we observe an increase in SR calcium release while the overexpression of DCST2-L759P causes the opposite effect when compared to not overexpressed controls. Despite that, HEK293 cells do not display modified extracellular calcium entry (or CRAC activity) upon wildtype or mutated DCST2 overexpression, whereas we observe a decreased CRAC response in ST myoblasts. This is probably because HEK293 cells do not express DCST2 endogenously, as opposed to differentiated myoblasts, indicating that the protein expression profile of these two lines might influence cellular calcium transients. DCST2's effect on cellular calcium handling corroborates with our BioID results in which we observe that wildtype DCST2 is a proximity interactor of STIM1. Despite the fact that we have not observed SERCAs as a prey in our DCST2 BioID results, we hypothesize that DCST2 might cause an indirect impact on SERCAs activity by binding STIM1. Indeed, it was previously observed that STIM1 is SERCA1 binding partner[172]. This way DCST2 would be impacting extracellular calcium entry by dysregulating STIM1 activity and SR calcium refilling by indirectly decreasing SERCAs activity (Figure 4.2).

4.2.3 DCST2-L759P in ST muscle

I would like to propose one hypothesis to explain why the increase in DCST2 puncta size and their more frequent STIM1 and SERCA1 content could be taking place in ST muscle: DCST2-L759P interferes in the dynamics of puncta formation leading to SOCE dysfunction and SERCA clustering. I think that the larger DCST2 puncta formation is related to the cell's effort to compensate the decreased SR calcium store levels through SOCE activation (Figure 4.2).

This hypothesis is based on the potential effect of the amino acid change on DCST2's protein structure. DCST2-L759P is localized in the predicted intra-luminal C-terminus proline-rich domain of the protein, which are domains known to be implicated in protein binding [203]. The whole DCST2 proline-rich stretch is predicted to be "disordered" by several programs. "Intrinsic disorder" is a very specific term in protein structure, and refers to regions of proteins that do not have a fixed secondary or tertiary structure, such as alpha-helix or beta-sheet [204]. Disordered regions are often involved in protein-protein interactions, with the regions becoming ordered (i.e. structured) upon contact with the other protein [204]. We think that DCST2-L759P is impacting the

proline-rich domain in a way that it becomes more prone to protein-protein interactions. This would explain why in the muscle biopsy as well as in myoblasts of the ST patient we observe that DCST2 forms larger puncta. In these puncta, DCST2-L759P could be interfering in the dynamics of STIM1-ORAI1 complex formation leading to SOCE dysfunction and SERCA malfunction because of DCST2's interaction with STIM1, a known SERCA binding partner.

To explain the consequences of this effect of DCST2-L759P on STIM1 and SERCA1, we have to take a closer look to the results we obtained with the calcium measurements as well as the quantification of large DCST2 puncta in differentiating myoblasts. During the calcium assays, we observe that the majority of the ST cells respond with decreased calcium transients upon SR calcium release. However, we observe that only about 15% of the ST cells present large DCST2 puncta and this number is smaller if there is no SERCAs inhibition. Since most of the cells present defective SR calcium release and that only a fraction present large DCST2 puncta, we could speculate that the large puncta are formed to compensate the decreased SR calcium store levels.

4.3 Importance of a new diagnostic tool for mild adult onset muscle diseases

4.3.1 Strongman trait: a new skeletal muscle trait or disease?

According to Bircher (2005), the definition of health and disease should be considered as the following: "Health is a dynamic state of wellbeing characterized by a physical, mental and social potential, which satisfies the demands of a life commensurate with age, culture, and personal responsibility. If the potential is insufficient to satisfy these demands the state is disease"[205]. Following this definition, I will consider a disease as any process which will cause a negative effect in a system or tissue of an organism and that will lead to a decreased quality of life. On the other hand, I will consider a trait as an observed variation in a specific character of an organism which can be manifested by genetics and environmental factors [206].

Regulation of muscle mass and function is considered a trait since it depends on both genetics and environmental factors such as resistance training and nutrition (American College of Sports Medicine, 2009). In humans, skeletal muscle mass, fiber numbers, fiber size, and

strength vary greatly. Females on average have a lower muscle mass than males [207] which can partially be explained by low levels of the male sex hormone testosterone, which promotes muscle hypertrophy [208]. Humans have over 600 muscles and within muscles the number of fibers and their cross sectional area differs greatly [209]. An earlier study of 1,121,088 males aged 16–25 years showed that 5% of individuals could extend their leg either with a maximal force of either <333N or more than 805N [210], highlighting the large variation of strength. Muscle mass and function are additionally lost during normal aging [211] which has been termed sarcopenia [212]. In summary, muscle mass and function variables vary greatly in human populations and decline with normal aging.

Recent genetic studies have proposed that rare variants with high penetrance are a common cause of monogenic Mendelian disorders while complex traits caused by variants with higher frequency often have variable penetrance [213]. Here we report a variant in the *DCST2* gene in ST patients with a low frequency and variable penetrance. I propose that the Strongman trait is both a trait and a disease in which individuals carrying the ST mutation who have done physical work or sports throughout their lives will be the ones displaying positive symptoms (increased muscle strength and hypertrophied muscles) during their adolescence and negative symptoms (incapacitating myalgia and cramps) usually after 30 years of age. Carriers who are sedentary or that are mildly active will not present clear symptoms. Women with ST also tend to be less symptomatic than men. This clearly represents the fact the ST has a large clinical spectrum (from mild to severely affected) which can lead to decreased quality of life for more symptomatic individuals. This study reinforces the need for ST patients to have a clear diagnostic at very early stages, since any kind of physical activity will cause deleterious effects in these individuals.

4.3.2 Regulation of strength and muscle mass in ST

We were able to demonstrate that DCST2 mutation led to a modified cellular calcium handling and this would explain why ST patients present delayed muscle relaxation. However, we are still unable to demonstrate how this mutation leads to stronger contractions and muscle hypertrophy.

It has been previously speculated that the prolonged contractions of such muscles caused by delayed relaxation observed in non-dystrophic myotonias and in Brody disease would result in muscle hypertrophy because of greater energy utilization and limitation of fat deposition [55]. Previous studies also hypothesized that RYR1 mutations may lead to muscle hypertrophy and possibly improved physical performance due to increased muscle excitability [108]. I also hypothesize that the prolonged contractions of muscles in the ST patients induce similar effects that lead to muscle hypertrophy.

Our results show that the muscles of SP patients display a decrease in type 1 myofiber and a slight increase in type 2X cross-sectional area. These results are not enough to explain why ST patients develop muscle hypertrophy, but one possibility could be that ST patients present myofiber hyperplasia instead of myofiber hypertrophy, meaning that these patients probably have muscles with a greater number of myofibers. Unfortunately, we are unable to prove this hypothesis with only histological analysis since we are limited to a small region of a muscle biopsy. Only by doing a magnetic resonance imaging (MRI) could we confirm that the hypertrophied muscles are due to an increase in muscle mass due to myofiber hyperplasia. Nonetheless, finding specific controls that would match not only for age and sex, but genetic background would be challenging to generate enough results for comparison.

MTSN KO animal models show that animals have hypertrophied muscles and increased myofibers cross-sectional area, however this increase in muscle mass does not necessarily reflect an effect on muscle strength [41,42]. Together, these studies confirmed the hypothesis that muscle mass is not the only feature directly related to muscle strength indicating that other key elements are at play. A recent paper studying a rodent KO model of MSTN (*compacting, cmpt* mouse) showed that these animals present hypertrophied muscles but decreased muscle strength when compared to controls [43]. They showed that these animals have a deficiency in SOCE activity displaying lower SR calcium release as well as lower extracellular calcium entry. Probably the calcium transients elicited in these animals is not enough to reach the optimal cross-bridge activity thus leading to weaker contractions. These results suggest that if these animals had appropriate intracellular calcium transients, they could have normal or even increased strength.

Unlike cells expressing DCST2-L759P, the *cmpt* mouse muscles do not show any difference in the regulation of SERCA activity. In the ST cells, we believe that the longer

calcium transients caused by the defective SERCA reuptake would be the key reason for stronger contractions, and this could explain the difference in strength between myostatin KO models and ST.

Another mouse model of muscle hypertrophy is the transgenic overexpressed IGF1 mice [53,80]. These animals have increased myofiber cross-sectional area, a rise in the number of myofibers (hyperplasia) and increased muscle strength [53]. A study in 2014 showed that differentiating myoblasts from this mouse model also showed reduced intracellular calcium transients after stimulation with caffeine, KCl and acetylcholine, but no data has been published showing SOCE or SERCA activity in those cells to date [214]. Another earlier study showed that one of the reasons in which these mice have increased muscle mass could be due to the activation of calmodulin-calcineurin pathway [80]. In rat skeletal myocytes, IGF1 enhances charge movement by activating DHPR gene expression and thus increasing intracellular calcium transients [80]. The sustained increased levels of intracellular calcium activate the transcription factors nuclear factor of activated T-cells (NFAT), myocyte enhancer factor (MEF2) and guanine-adenosine-thymine-adenosine (GATA) that increase the transcriptional response of IGF1 related genes leading to muscle hypertrophy [80].

In summary, studies with murine models presenting muscle hypertrophy showed that these animals exhibited altered calcium transients as observed in ST cells. It is evident that skeletal muscle calcium handling plays a key role in the regulation of muscle strength and mass but more studies are necessary to address the main molecular players implicated in this process.

4.3.3 Addressing myalgia in ST patients

Myalgia is a symptom that can happen due to overuse, injury or stretch injury, but it can also be caused by diseases or medications [215]. In several muscular disorders, myalgia is caused by sarcolemmal disruption and release of myofibrillar content to the bloodstream leading to a rise of CK levels [215], however, this is not true in the ST.

Previous studies evaluating sensations of muscle fatigue and pain in humans and mice were able to narrow down which metabolites produced during contractions are linked to muscle

pain [216,217]. During contractions, there is the production of protons, lactate, and ATP in the myofiber. They found that there is no single metabolite eliciting muscle pain, all generated metabolites are necessary to achieve such effect [216,217].

In ST patients, incapacitating myalgia happens only after some level of muscle activity. We observe that in general, individuals that carry *DCST2* mutations and are not physically active display very mild symptoms. In the muscle of ST patients, the continuing contractions caused by the delayed relaxation could be responsible for causing an increase in the levels of those metabolites that could explain why these patients experience post-activity muscle pain. Nevertheless, we cannot discard that other pain mechanisms are at play. For example, glutamate plays an important role in peripherally-mediated pain signaling to the central nervous system (CNS). The glutamatergic system provides excitatory neurotransmission throughout the CNS, and dysfunction of this system seems is correlated with several disorders such as schizophrenia, depression, and pain states [218]. Alternatively, the high tensile strength generated by ST cases also appears to cause increased muscle tendon pathology that are also quite painful.

4.3.4 Overlaps and differences of Strongman symptoms

As discussed previously, symptomatic ST individuals will often show up at the neuromuscular clinics complaining of muscle pain, cramps and decreased endurance. These ST patients present prolonged delayed muscle relaxation following percussion that is silent on EMGs and with no associated pathological signs on the muscle morphology that would correspond to muscle damage. One of the subtle abnormalities observed in ST muscles is muscle membrane irritability on EMG. Furthermore, at the morphological level, nicotinamide adenine dinucleotide (NADH) staining shows more linear and less punctate staining. However these are all nonspecific signs that are often not taken into account as biomarkers. Moreover, ST symptoms can vary greatly from one patient to another making diagnostics even more challenging. Unfortunately, data on increased, rather than decreased, muscle strength has not been used as a biomarker to help physicians identify muscle disorders since only descriptions on muscle weakness or no effect on muscle strength have been explored so far. Although no effort

has been made to evaluate how certain myopathies can influence positively on muscle strength, we can find information on muscle mass.

Several overlaps and differences can be observed between muscle disorders that lead to prominent muscles and ST. Some of the main common overlaps include easy gain of muscle mass (muscle hypertrophy), exercise intolerance, and no pathological signs on muscle morphology. Some of the main differences include increased muscle strength and incapacitating post-activity myalgia. Two approaches should to be taken into consideration when evaluating individuals with this profile: 1- Consider personal and familial history of increased muscle strength, and 2- Define the level of personal physical activity. It is also important to consider that when evaluating familial history of ST individuals, relatives who are sedentary or that are only mildly active might present none or very mild symptoms meaning that a negative familial history of increased muscle strength should not be enough to discard the diagnostics. Defining the level of activity of the patient is important to confirm if the myalgia is caused by any kind of physical activity.

If we consider all myopathies in which patients present true muscle hypertrophy, we can classify them in 4 groups: Group 1- Myopathies affecting muscle membrane excitability: non-dystrophic myotonias (CLCN1 and SCN4A) and myotonic dystrophy type 2 (ZNF9); Group 2- Myopathies affecting calcium handling: RYR-related myopathies (RYR1) and Brody disease (SERCA1); Group 3- Myopathies affecting sarcolemma stability: rippling muscle disease (CAV3) and anoctaminopathies (ANO5); and Group 4- Metabolic myopathy caused by glycogen storage deficiency: McArdle disease (PYGM). The ST with mutations in *DCST2* should be added to the group 2 considering its effect in cellular calcium transients.

Molecularly speaking, all four groups share a common feature: increased cytosolic calcium transients. Increased membrane excitability caused my mutations in *CLCN1, SCN4A* and *ZNF9* lead to increased SR calcium release thus longer cytosolic calcium transients upon contraction. Mutations in *RYR1* lead to a "leaky" channel activity leading to increased cytosolic calcium transients. Loss of function mutations in *SERCA1* lead to decreased uptake of calcium to the SR leading to longer cytosolic calcium transients with contraction. Loss of function mutations in *CAV3* and *ANO5* cause decreased membrane stability leading to calcium leaking from the plasma membrane to the cytosol. Despite the fact that McArdle disease is considered a

metabolic myopathy, two previous studies showed a deficiency in SERCA1 in the muscle of patients with McArdle disease [219] and in the muscle of a mouse model of McArdle disease [220] proposing that these results explain at least in part the muscle fatigability and stiffness during exercise in this condition. And finally mutations in *DCST2* cause decreased extracellular calcium entry and decreased SERCA activity leading to longer cytosolic calcium transients upon contraction.

4.3.5 Biomarkers of ST

ST is a new myopathy and as such needs not only clinical criteria but also pathological and genetic tests to support or confirm the diagnosis. Despite being able to identify a few pathological markers, the best way to assess if a patient has the ST would be by genetic testing. With this study, we highlight the importance of adding *DCST2* to the next generation sequencing panel of genes known to cause myopathies. However, as mentioned previously, several ST patients do not carry *DCST2* mutations.

We have identified a few potential morphological biomarkers in muscle and myoblasts of suspected ST cases that carry or not a *DCST2* mutation: 1- Presence of smaller type 1 and larger type 2X myofibers; 2- Larger DCST2 puncta on muscle sections and in differentiating myoblasts; 3- Presence of SERCA1 and STIM1 in the larger DCST2 puncta; 4- Decreased SR calcium uptake and extracellular calcium entry in differentiating myoblasts. Unfortunately, the techniques used to verify biomarkers 2, 3, and 4 are not routinely done in pathological facilities today, meaning that at least a few of these techniques should be implemented as routine tests for patients presenting myalgia, cramps, reduced endurance but also increased muscle strength and mass. Minimally, DCST2 and STIM1 and/or SERCA1/2 co-staining of longitudinal slides of fibers should be performed to assess puncta size, number and colocalization. For DCST2 we have generated the best polyclonal antibody available to date to complete this type of studies.

Figures

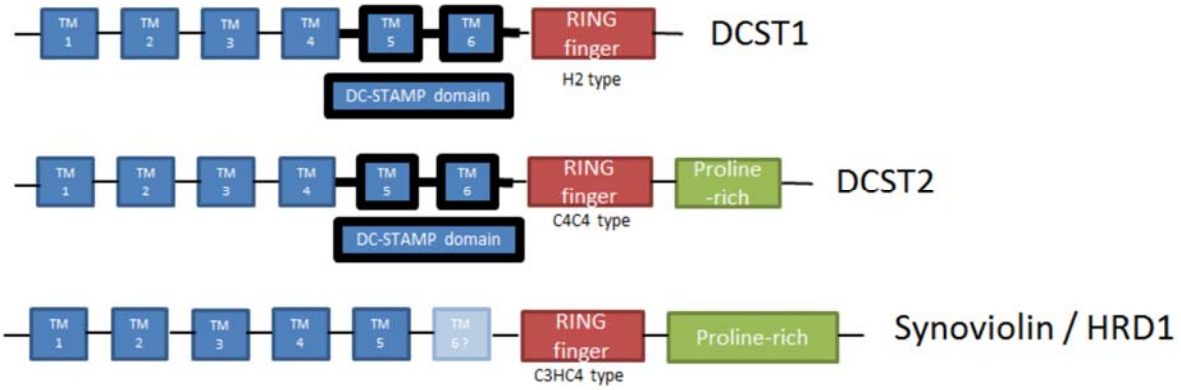

*TM = Transmembrane domain

** Light blue TM = Diverse literature, HDR1 might have 5 or 6 TMs.

Figure 4.1 Comparison of protein domain structure of DCST1, DCST2 and synoviolin proteins. All the three proteins present 5-6 transmembrane domains and a RING-finger domain indicating that these proteins could have a similar mechanism of action.

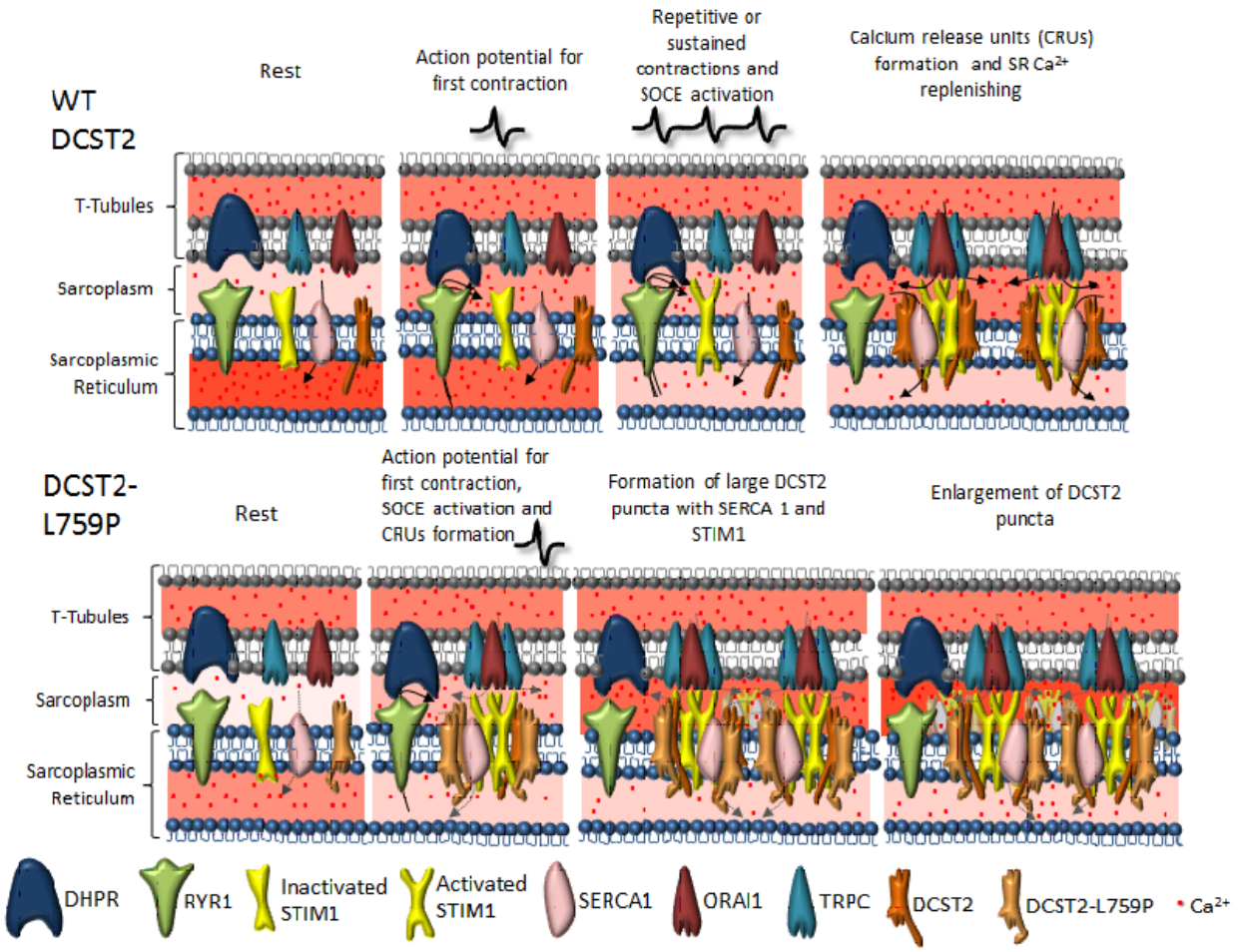

Figure 4.2 Proposed model for WT DCST2 and DCST2-L759P activity in skeletal muscle. Once there is an action potential and membrane depolarization in a myofiber, calcium is released from the SR to the cytosol to generate contraction. If the contraction is long or repetitive enough to empty SR stores, STIM1 is activated and bind to CRAC channels at the plasma membrane. CRAC channels are then activated and open, allowing calcium from the extracellular milieu enter the cell. SERCA in turn pumps this calcium to the SR replenishing the previously emptied stores. In the presence of DCST2-L759P, we observe a partial dysfunction of the CRAC channels and SERCA activity. This dysfunction is accompanied by an increase in the size of DCST2 puncta that contain STIM1 and SERCA1. We propose that DCST2 is implicated in the dynamics of STIM1-SERCA1 puncta formation and that DCST-L759P causes a negative impact in the formation of these puncta.

CHAPTER 5: Conclusion and Future Directions

5.1 Conclusion

Several studies show that muscular strength is a hereditary trait, however these studies have only explored this subject in athletes so far. A few muscle disorders have been described to cause true muscle hypertrophy, but no studies have addressed if these conditions lead to increased strength. The work described in this thesis presents the clinical and molecular characterization of a new dominant Herculean myalgic condition we have labeled the Strongman trait (ST). We showed that a mutation in *DCST2* was found in two French-Canadian families with ST presenting muscle pain, cramps and decreased endurance as negative symptoms, and increased muscle strength and mass as positive symptoms. Despite the unknown function of DCST2 when we started this work, we showed that it is localized to the SR in the skeletal muscle. Our results demonstrated that DCST2-L759P forms larger puncta in the ST muscle and myoblasts, and that these larger puncta contain SERCA1 and STIM1. This colocalization is associated with a perturbation of cellular calcium handling in patient myoblasts which we hypothesize in the adult skeletal muscle lead to hypertrophy and superior strength but also activity induced fatigue and pain. Results on muscle biopsies of ST patients that do not carry *DCST2* mutations showed that DCST2 also forms larger puncta that is positive for SERCA1 and STIM1 pointing to a common pathological mechanism in ST patients and confirming that these larger puncta can be used as pathological markers supporting the ST diagnosis. Altogether, our findings provide the characterization of a new mutation in a gene of unknown function causing a new myopathy. The data presented in this thesis opens the way to an understanding of the pathophysiological mechanisms underpinning the ST.

5.2 Future directions

To address the function of DCST2, I would propose to explore the role of DCST2 as an E3 ubiquitin ligase regulating the activity of key proteins responsible of cellular calcium handling. To do so, it would also be important to determine DCST2's binding partners in the skeletal muscle by doing immunoprecipitations with DCST2 and without the mutation followed by identification of partners through mass spectrometry. Once these partners are confirmed, *in vitro* E3 ligases assays using purified DCST2 and binding partners can confirm the E3 ligase

activity, a method previously described by Boutell et al (2002)[221]. Another approach to be considered would be by identifying proteins that have their expression altered in DCST2 KO models using an unbiased methodology, like stable isotope labeling with amino acids in cell culture (SILAC), as previously described by Zaglia et al (2014)[222] and Lang et al (2017)[223]. These proteins would also serve as clues to identify potential candidate genes to be screened in ST patients that do not carry *DCST2* mutations. In addition, ST patients should continue to be recruited for genetic studies by doing WES/WGS. Furthermore, by RNAseq analysis, new candidate genes could be identified through mRNA extracted directly from patients' skeletal muscle biopsies, and thus providing a deep overview of changes observed in specific transcripts as well as pathogenic SNPs. The fact that patients carrying or not *DCST2* mutations exhibit same clinical features and larger DCST2 puncta on muscle sections indicate that the cellular phenotype could also serve as a potential diagnostic tool for this condition. Myoblasts from ST patients negative for DCST2-L759P should be assessed for quantification of large puncta as well as for calcium handling assays to help confirming the ST diagnostic. These assays could be used to explore new pharmacological treatments that can reverse this cellular ST phenotype.

The generation of a model of ST would also be of great interest in order to explore potential therapeutic approaches to treat this disorder. The proline-rich domain of the DCST2 protein (where the DCST2 mutation lies) is conserved only in primates, and this fact adds a significant challenge to the generation of an animal model. However, with the recent advances on gene editing using CRISPR-Cas9 technology, the development of an animal model becomes more feasible as described previously by Shen B et al (2014)[224] and Dorado B et al (2019)[225].

CHAPTER 6 : References

1. Ohl, P.E. *Louis Cyr, une épopée légendaire*, 632 p., 6 f. de pl. (Libre expression, Outremont, Québec, 2005).
2. Wise, S.F. & Fisher, D. *Les grands athlètes canadiens*, 338 p. (General Pub. Co, Don Mills, 1976).
3. Laberge, A.M. *et al.* Population history and its impact on medical genetics in Quebec. *Clin Genet* **68**, 287-301 (2005).
4. Moreau, C., Vezina, H. & Labuda, D. [Founder effects and genetic variability in Quebec]. *Med Sci (Paris)* **23**, 1008-13 (2007).
5. Choquette, L. *De Français à paysans : modernité et tradition dans le peuplement du Canada français*, x, 323 p. (Septentrion ;Presses de l'Université Paris-Sorbonne, Sillery, Québec Paris, 2001).
6. Engel, A. & Franzini-Armstrong, C. *Myology : basic and clinical*, (Montreal : McGraw-Hill, New York ;, 1994).
7. Frontera, W.R. & Ochala, J. Skeletal muscle: a brief review of structure and function. *Calcif Tissue Int* **96**, 183-95 (2015).
8. Gillies, A.R. & Lieber, R.L. Structure and function of the skeletal muscle extracellular matrix. *Muscle Nerve* **44**, 318-31 (2011).
9. Schiaffino, S. & Reggiani, C. Fiber types in mammalian skeletal muscles. *Physiol Rev* **91**, 1447-531 (2011).
10. Blaauw, B., Schiaffino, S. & Reggiani, C. Mechanisms modulating skeletal muscle phenotype. *Compr Physiol* **3**, 1645-87 (2013).
11. Scott, W., Stevens, J. & Binder-Macleod, S.A. Human skeletal muscle fiber type classifications. *Phys Ther* **81**, 1810-6 (2001).
12. Purves-Smith, F.M., Sgarioto, N. & Hepple, R.T. Fiber typing in aging muscle. *Exerc Sport Sci Rev* **42**, 45-52 (2014).
13. Rios, E., Ma, J.J. & Gonzalez, A. The mechanical hypothesis of excitation-contraction (EC) coupling in skeletal muscle. *J Muscle Res Cell Motil* **12**, 127-35 (1991).
14. Bannister, R.A. Bridging the myoplasmic gap: recent developments in skeletal muscle excitation-contraction coupling. *J Muscle Res Cell Motil* **28**, 275-83 (2007).
15. Murray, B.E., Froemming, G.R., Maguire, P.B. & Ohlendieck, K. Excitation-contraction-relaxation cycle: role of Ca2+-regulatory membrane proteins in normal, stimulated and pathological skeletal muscle (review). *Int J Mol Med* **1**, 677-87 (1998).
16. Canato, M., Capitanio, P., Reggiani, C. & Cancellara, L. The disorders of the calcium release unit of skeletal muscles: what have we learned from mouse models? *J Muscle Res Cell Motil* **36**, 61-9 (2015).
17. Franzini-Armstrong, C., Protasi, F. & Ramesh, V. Shape, size, and distribution of Ca(2+) release units and couplons in skeletal and cardiac muscles. *Biophys J* **77**, 1528-39 (1999).
18. Fitts, R.H. The cross-bridge cycle and skeletal muscle fatigue. *J Appl Physiol (1985)* **104**, 551-8 (2008).
19. Berchtold, M.W., Brinkmeier, H. & Muntener, M. Calcium ion in skeletal muscle: its crucial role for muscle function, plasticity, and disease. *Physiol Rev* **80**, 1215-65 (2000).
20. Primeau, J.O., Armanious, G.P., Fisher, M.E. & Young, H.S. The SarcoEndoplasmic Reticulum Calcium ATPase. *Subcell Biochem* **87**, 229-258 (2018).
21. Kumar, S. *Muscle strength*, 538 p. (CRC Press, Boca Raton, 2004).
22. Kraemer, W.J. & Szivak, T.K. Strength training for the warfighter. *J Strength Cond Res* **26 Suppl 2**, S107-18 (2012).

23. Kraemer, W.J. & Looney, D.P. Underlying Mechanisms and Physiology of Muscular Power. *Strength and Conditioning Journal* **34**, 13-19 (2012).
24. Guellich, A., Negroni, E., Decostre, V., Demoule, A. & Coirault, C. Altered cross-bridge properties in skeletal muscle dystrophies. *Front Physiol* **5**, 393 (2014).
25. Faitg, J., Reynaud, O., Leduc-Gaudet, J.P. & Gouspillou, G. [Skeletal muscle aging and mitochondrial dysfunction: an update]. *Med Sci (Paris)* **33**, 955-962 (2017).
26. Geeves, M.A. & Holmes, K.C. The molecular mechanism of muscle contraction. *Adv Protein Chem* **71**, 161-93 (2005).
27. Mamidi, R., Li, J., Doh, C.Y., Verma, S. & Stelzer, J.E. Impact of the Myosin Modulator Mavacamten on Force Generation and Cross-Bridge Behavior in a Murine Model of Hypercontractility. *J Am Heart Assoc* **7**, e009627 (2018).
28. Schiaffino, S., Dyar, K.A., Ciciliot, S., Blaauw, B. & Sandri, M. Mechanisms regulating skeletal muscle growth and atrophy. *FEBS J* **280**, 4294-314 (2013).
29. Pion, C.H. *et al.* Muscle strength and force development in high- and low-functioning elderly men: Influence of muscular and neural factors. *Exp Gerontol* **96**, 19-28 (2017).
30. Hargreaves, M. Skeletal muscle metabolism during exercise in humans. *Clin Exp Pharmacol Physiol* **27**, 225-8 (2000).
31. Bortoluzzi, S., Scannapieco, P., Cestaro, A., Danieli, G.A. & Schiaffino, S. Computational reconstruction of the human skeletal muscle secretome. *Proteins* **62**, 776-92 (2006).
32. Pedersen, B.K. *et al.* Searching for the exercise factor: is IL-6 a candidate? *J Muscle Res Cell Motil* **24**, 113-9 (2003).
33. Pedersen, B.K. & Febbraio, M.A. Muscles, exercise and obesity: skeletal muscle as a secretory organ. *Nat Rev Endocrinol* **8**, 457-65 (2012).
34. Mosher, D.S. *et al.* A mutation in the myostatin gene increases muscle mass and enhances racing performance in heterozygote dogs. *PLoS Genet* **3**, e79 (2007).
35. Bignell, C.W., Malau-Aduli, A.E., Nichols, P.D., McCulloch, R. & Kijas, J.W. East Friesian sheep carry a Myostatin allele known to cause muscle hypertrophy in other breeds. *Anim Genet* **41**, 445-6 (2010).
36. Grobet, L. *et al.* A deletion in the bovine myostatin gene causes the double-muscled phenotype in cattle. *Nat Genet* **17**, 71-4 (1997).
37. Stinckens, A. *et al.* Characterization of the complete porcine MSTN gene and expression levels in pig breeds differing in muscularity. *Anim Genet* **39**, 586-96 (2008).
38. Schuelke, M. *et al.* Myostatin mutation associated with gross muscle hypertrophy in a child. *N Engl J Med* **350**, 2682-8 (2004).
39. Haidet, A.M. *et al.* Long-term enhancement of skeletal muscle mass and strength by single gene administration of myostatin inhibitors. *Proc Natl Acad Sci U S A* **105**, 4318-22 (2008).
40. Whittemore, L.A. *et al.* Inhibition of myostatin in adult mice increases skeletal muscle mass and strength. *Biochem Biophys Res Commun* **300**, 965-71 (2003).
41. Stantzou, A. *et al.* Effect of constitutive inactivation of the myostatin gene on the gain in muscle strength during postnatal growth in two murine models. *Muscle Nerve* **55**, 254-261 (2017).
42. Gu, H. *et al.* Establishment and phenotypic analysis of an Mstn knockout rat. *Biochem Biophys Res Commun* **477**, 115-122 (2016).
43. Sztretye, M. *et al.* SOCE Is Important for Maintaining Sarcoplasmic Calcium Content and Release in Skeletal Muscle Fibers. *Biophys J* **113**, 2496-2507 (2017).
44. Giesige, C.R. *et al.* AAV-mediated follistatin gene therapy improves functional outcomes in the TIC-DUX4 mouse model of FSHD. *JCI Insight* **3**(2018).

45. Estrellas, K.M. *et al.* Biological scaffold-mediated delivery of myostatin inhibitor promotes a regenerative immune response in an animal model of Duchenne muscular dystrophy. *J Biol Chem* **293**, 15594-15605 (2018).
46. Chen, J.L. *et al.* Specific targeting of TGF-beta family ligands demonstrates distinct roles in the regulation of muscle mass in health and disease. *Proc Natl Acad Sci U S A* **114**, E5266-E5275 (2017).
47. Walker, R.G. *et al.* Biochemistry and Biology of GDF11 and Myostatin: Similarities, Differences, and Questions for Future Investigation. *Circ Res* **118**, 1125-41; discussion 1142 (2016).
48. Lee, S.J. & McPherron, A.C. Regulation of myostatin activity and muscle growth. *Proc Natl Acad Sci U S A* **98**, 9306-11 (2001).
49. Wolfman, N.M. *et al.* Activation of latent myostatin by the BMP-1/tolloid family of metalloproteinases. *Proc Natl Acad Sci U S A* **100**, 15842-6 (2003).
50. Han, H.Q., Zhou, X., Mitch, W.E. & Goldberg, A.L. Myostatin/activin pathway antagonism: molecular basis and therapeutic potential. *Int J Biochem Cell Biol* **45**, 2333-47 (2013).
51. Schiaffino, S. & Mammucari, C. Regulation of skeletal muscle growth by the IGF1-Akt/PKB pathway: insights from genetic models. *Skelet Muscle* **1**, 4 (2011).
52. Powell-Braxton, L. *et al.* IGF-I is required for normal embryonic growth in mice. *Genes Dev* **7**, 2609-17 (1993).
53. Musaro, A. *et al.* Localized Igf-1 transgene expression sustains hypertrophy and regeneration in senescent skeletal muscle. *Nat Genet* **27**, 195-200 (2001).
54. Glass, D.J. PI3 kinase regulation of skeletal muscle hypertrophy and atrophy. *Curr Top Microbiol Immunol* **346**, 267-78 (2010).
55. Voermans, N.C. *et al.* Brody syndrome: a clinically heterogeneous entity distinct from Brody disease: a review of literature and a cross-sectional clinical study in 17 patients. *Neuromuscul Disord* **22**, 944-54 (2012).
56. Nader, G.A. Molecular determinants of skeletal muscle mass: getting the "AKT" together. *Int J Biochem Cell Biol* **37**, 1985-96 (2005).
57. Sandri, M. Protein breakdown in muscle wasting: role of autophagy-lysosome and ubiquitin-proteasome. *Int J Biochem Cell Biol* **45**, 2121-9 (2013).
58. Zhou, H. & Huang, S. The complexes of mammalian target of rapamycin. *Curr Protein Pept Sci* **11**, 409-24 (2010).
59. Crabtree, G.R. Generic signals and specific outcomes: signaling through Ca2+, calcineurin, and NF-AT. *Cell* **96**, 611-4 (1999).
60. Rusnak, F. & Mertz, P. Calcineurin: form and function. *Physiol Rev* **80**, 1483-521 (2000).
61. Sakuma, K. & Yamaguchi, A. The functional role of calcineurin in hypertrophy, regeneration, and disorders of skeletal muscle. *J Biomed Biotechnol* **2010**, 721219 (2010).
62. Friday, B.B., Horsley, V. & Pavlath, G.K. Calcineurin activity is required for the initiation of skeletal muscle differentiation. *J Cell Biol* **149**, 657-66 (2000).
63. Naya, F.J. *et al.* Stimulation of slow skeletal muscle fiber gene expression by calcineurin in vivo. *J Biol Chem* **275**, 4545-8 (2000).
64. Parsons, S.A., Wilkins, B.J., Bueno, O.F. & Molkentin, J.D. Altered skeletal muscle phenotypes in calcineurin Aalpha and Abeta gene-targeted mice. *Mol Cell Biol* **23**, 4331-43 (2003).
65. Stupka, N. *et al.* Activated calcineurin ameliorates contraction-induced injury to skeletal muscles of mdx dystrophic mice. *J Physiol* **575**, 645-56 (2006).
66. Stupka, N., Michell, B.J., Kemp, B.E. & Lynch, G.S. Differential calcineurin signalling activity and regeneration efficacy in diaphragm and limb muscles of dystrophic mdx mice. *Neuromuscul Disord* **16**, 337-46 (2006).

67. Hudson, M.B. & Price, S.R. Calcineurin: a poorly understood regulator of muscle mass. *Int J Biochem Cell Biol* **45**, 2173-8 (2013).
68. Talmadge, R.J. *et al.* Calcineurin activation influences muscle phenotype in a muscle-specific fashion. *BMC Cell Biol* **5**, 28 (2004).
69. Oh, M. *et al.* Calcineurin is necessary for the maintenance but not embryonic development of slow muscle fibers. *Mol Cell Biol* **25**, 6629-38 (2005).
70. Dunn, S.E., Chin, E.R. & Michel, R.N. Matching of calcineurin activity to upstream effectors is critical for skeletal muscle fiber growth. *J Cell Biol* **151**, 663-72 (2000).
71. Ryall, J.G., Church, J.E. & Lynch, G.S. Novel role for ss-adrenergic signalling in skeletal muscle growth, development and regeneration. *Clin Exp Pharmacol Physiol* **37**, 397-401 (2010).
72. Fink, J., Schoenfeld, B.J. & Nakazato, K. The role of hormones in muscle hypertrophy. *Phys Sportsmed* **46**, 129-134 (2018).
73. Ito, N., Ruegg, U.T., Kudo, A., Miyagoe-Suzuki, Y. & Takeda, S. Activation of calcium signaling through Trpv1 by nNOS and peroxynitrite as a key trigger of skeletal muscle hypertrophy. *Nat Med* **19**, 101-6 (2013).
74. von Maltzahn, J., Bentzinger, C.F. & Rudnicki, M.A. Wnt7a-Fzd7 signalling directly activates the Akt/mTOR anabolic growth pathway in skeletal muscle. *Nat Cell Biol* **14**, 186-91 (2011).
75. Briolay, A., Jaafar, R., Nemoz, G. & Bessueille, L. Myogenic differentiation and lipid-raft composition of L6 skeletal muscle cells are modulated by PUFAs. *Biochim Biophys Acta* **1828**, 602-13 (2013).
76. Joy, J.M. *et al.* Phosphatidic acid enhances mTOR signaling and resistance exercise induced hypertrophy. *Nutr Metab (Lond)* **11**, 29 (2014).
77. Mammucari, C. *et al.* The mitochondrial calcium uniporter controls skeletal muscle trophism in vivo. *Cell Rep* **10**, 1269-79 (2015).
78. Ruas, J.L. *et al.* A PGC-1alpha isoform induced by resistance training regulates skeletal muscle hypertrophy. *Cell* **151**, 1319-31 (2012).
79. Wen, X. *et al.* Effect of exercise intensity on isoform-specific expressions of NT-PGC-1 alpha mRNA in mouse skeletal muscle. *Biomed Res Int* **2014**, 402175 (2014).
80. Musaro, A., McCullagh, K.J., Naya, F.J., Olson, E.N. & Rosenthal, N. IGF-1 induces skeletal myocyte hypertrophy through calcineurin in association with GATA-2 and NF-ATc1. *Nature* **400**, 581-5 (1999).
81. Horsley, V. & Pavlath, G.K. Prostaglandin F2(alpha) stimulates growth of skeletal muscle cells via an NFATC2-dependent pathway. *J Cell Biol* **161**, 111-8 (2003).
82. Tu, M.K., Levin, J.B., Hamilton, A.M. & Borodinsky, L.N. Calcium signaling in skeletal muscle development, maintenance and regeneration. *Cell Calcium* **59**, 91-7 (2016).
83. Mauro, A. Satellite cell of skeletal muscle fibers. *J Biophys Biochem Cytol* **9**, 493-5 (1961).
84. Murach, K.A. *et al.* Starring or Supporting Role? Satellite Cells and Skeletal Muscle Fiber Size Regulation. *Physiology (Bethesda)* **33**, 26-38 (2018).
85. Dumont, N.A., Wang, Y.X. & Rudnicki, M.A. Intrinsic and extrinsic mechanisms regulating satellite cell function. *Development* **142**, 1572-81 (2015).
86. Pallafacchina, G., Blaauw, B. & Schiaffino, S. Role of satellite cells in muscle growth and maintenance of muscle mass. *Nutr Metab Cardiovasc Dis* **23 Suppl 1**, S12-8 (2013).
87. Bruusgaard, J.C. *et al.* No change in myonuclear number during muscle unloading and reloading. *J Appl Physiol (1985)* **113**, 290-6 (2012).
88. Blaauw, B. *et al.* Inducible activation of Akt increases skeletal muscle mass and force without satellite cell activation. *FASEB J* **23**, 3896-905 (2009).
89. Amthor, H. *et al.* Muscle hypertrophy driven by myostatin blockade does not require stem/precursor-cell activity. *Proc Natl Acad Sci U S A* **106**, 7479-84 (2009).

90. Lee, S.J. *et al.* Role of satellite cells versus myofibers in muscle hypertrophy induced by inhibition of the myostatin/activin signaling pathway. *Proc Natl Acad Sci U S A* **109**, E2353-60 (2012).
91. McCarthy, J.J. *et al.* Effective fiber hypertrophy in satellite cell-depleted skeletal muscle. *Development* **138**, 3657-66 (2011).
92. Nogales-Gadea, G. *et al.* McArdle Disease: Update of Reported Mutations and Polymorphisms in the PYGM Gene. *Hum Mutat* **36**, 669-78 (2015).
93. Nogales-Gadea, G. *et al.* Genes and exercise intolerance: insights from McArdle disease. *Physiol Genomics* **48**, 93-100 (2016).
94. Gautron, S. *et al.* Molecular mechanisms of McArdle's disease (muscle glycogen phosphorylase deficiency). RNA and DNA analysis. *J Clin Invest* **79**, 275-81 (1987).
95. Quinlivan, R. *et al.* McArdle disease: a clinical review. *J Neurol Neurosurg Psychiatry* **81**, 1182-8 (2010).
96. Martinuzzi, A. *et al.* Phenotype modulators in myophosphorylase deficiency. *Ann Neurol* **53**, 497-502 (2003).
97. Vissing, J. & Haller, R.G. A diagnostic cycle test for McArdle's disease. *Ann Neurol* **54**, 539-42 (2003).
98. Hudson, A.J., Ebers, G.C. & Bulman, D.E. The skeletal muscle sodium and chloride channel diseases. *Brain* **118 (Pt 2)**, 547-63 (1995).
99. Quinn, C. & Salajegheh, M.K. Myotonic Disorders and Channelopathies. *Semin Neurol* **35**, 360-8 (2015).
100. Burge, J.A. & Hanna, M.G. Novel insights into the pathomechanisms of skeletal muscle channelopathies. *Curr Neurol Neurosci Rep* **12**, 62-9 (2012).
101. Trivedi, J.R. *et al.* Non-dystrophic myotonia: prospective study of objective and patient reported outcomes. *Brain* **136**, 2189-200 (2013).
102. Yum, K., Wang, E.T. & Kalsotra, A. Myotonic dystrophy: disease repeat range, penetrance, age of onset, and relationship between repeat size and phenotypes. *Curr Opin Genet Dev* **44**, 30-37 (2017).
103. Sun, C., Tranebjaerg, L., Torbergsen, T., Holmgren, G. & Van Ghelue, M. Spectrum of CLCN1 mutations in patients with myotonia congenita in Northern Scandinavia. *Eur J Hum Genet* **9**, 903-9 (2001).
104. Heatwole, C.R. & Moxley, R.T., 3rd. The nondystrophic myotonias. *Neurotherapeutics* **4**, 238-51 (2007).
105. Lawal, T.A., Todd, J.J. & Meilleur, K.G. Ryanodine Receptor 1-Related Myopathies: Diagnostic and Therapeutic Approaches. *Neurotherapeutics* **15**, 885-899 (2018).
106. Hopkins, P.M., Gupta, P.K. & Bilmen, J.G. Malignant hyperthermia. *Handb Clin Neurol* **157**, 645-661 (2018).
107. Davis, M. *et al.* Malignant hyperthermia associated with exercise-induced rhabdomyolysis or congenital abnormalities and a novel RYR1 mutation in New Zealand and Australian pedigrees. *Br J Anaesth* **88**, 508-15 (2002).
108. Witting, N. *et al.* Phenotype and genotype of muscle ryanodine receptor rhabdomyolysis-myalgia syndrome. *Acta Neurol Scand* **137**, 452-461 (2018).
109. Loseth, S. *et al.* A novel late-onset axial myopathy associated with mutations in the skeletal muscle ryanodine receptor (RYR1) gene. *J Neurol* **260**, 1504-10 (2013).
110. Witherspoon, J.W. & Meilleur, K.G. Review of RyR1 pathway and associated pathomechanisms. *Acta Neuropathol Commun* **4**, 121 (2016).
111. Brody, I.A. Muscle contracture induced by exercise. A syndrome attributable to decreased relaxing factor. *N Engl J Med* **281**, 187-92 (1969).

112. Karpati, G., Charuk, J., Carpenter, S., Jablecki, C. & Holland, P. Myopathy caused by a deficiency of Ca2+-adenosine triphosphatase in sarcoplasmic reticulum (Brody's disease). *Ann Neurol* **20**, 38-49 (1986).
113. Danon, M.J., Karpati, G., Charuk, J. & Holland, P. Sarcoplasmic reticulum adenosine triphosphatase deficiency with probable autosomal dominant inheritance. *Neurology* **38**, 812-5 (1988).
114. Zhang, Y. *et al.* Characterization of cDNA and genomic DNA encoding SERCA1, the Ca(2+)-ATPase of human fast-twitch skeletal muscle sarcoplasmic reticulum, and its elimination as a candidate gene for Brody disease. *Genomics* **30**, 415-24 (1995).
115. Taylor, D.J. *et al.* Ca2+-ATPase deficiency in a patient with an exertional muscle pain syndrome. *J Neurol Neurosurg Psychiatry* **51**, 1425-33 (1988).
116. Poels, P.J. *et al.* Exertional rhabdomyolysis in a patient with calcium adenosine triphosphatase deficiency. *J Neurol Neurosurg Psychiatry* **56**, 823-6 (1993).
117. Benders, A.A. *et al.* Ca2+ homeostasis in Brody's disease. A study in skeletal muscle and cultured muscle cells and the effects of dantrolene an verapamil. *J Clin Invest* **94**, 741-8 (1994).
118. MacLennan, D.H. Ca2+ signalling and muscle disease. *Eur J Biochem* **267**, 5291-7 (2000).
119. De Ruiter, C.J., Wevers, R.A., Van Engelen, B.G., Verdijk, P.W. & De Haan, A. Muscle function in a patient with Brody's disease. *Muscle Nerve* **22**, 704-11 (1999).
120. Odermatt, A. *et al.* Mutations in the gene-encoding SERCA1, the fast-twitch skeletal muscle sarcoplasmic reticulum Ca2+ ATPase, are associated with Brody disease. *Nat Genet* **14**, 191-4 (1996).
121. Betz, R.C. *et al.* Mutations in CAV3 cause mechanical hyperirritability of skeletal muscle in rippling muscle disease. *Nat Genet* **28**, 218-9 (2001).
122. Scalco, R.S. *et al.* CAV3 mutations causing exercise intolerance, myalgia and rhabdomyolysis: Expanding the phenotypic spectrum of caveolinopathies. *Neuromuscul Disord* **26**, 504-10 (2016).
123. Kortman, H.G., Veldink, J.H. & Drost, G. Positive muscle phenomena--diagnosis, pathogenesis and associated disorders. *Nat Rev Neurol* **8**, 97-107 (2012).
124. Galbiati, F., Razani, B. & Lisanti, M.P. Caveolae and caveolin-3 in muscular dystrophy. *Trends Mol Med* **7**, 435-41 (2001).
125. Sotgia, F. *et al.* Caveolin-3 directly interacts with the C-terminal tail of beta -dystroglycan. Identification of a central WW-like domain within caveolin family members. *J Biol Chem* **275**, 38048-58 (2000).
126. Matsuda, C. *et al.* The sarcolemmal proteins dysferlin and caveolin-3 interact in skeletal muscle. *Hum Mol Genet* **10**, 1761-6 (2001).
127. Garcia-Cardena, G. *et al.* Dissecting the interaction between nitric oxide synthase (NOS) and caveolin. Functional significance of the nos caveolin binding domain in vivo. *J Biol Chem* **272**, 25437-40 (1997).
128. Smythe, G.M. & Rando, T.A. Altered caveolin-3 expression disrupts PI(3) kinase signaling leading to death of cultured muscle cells. *Exp Cell Res* **312**, 2816-25 (2006).
129. Smythe, G.M., Eby, J.C., Disatnik, M.H. & Rando, T.A. A caveolin-3 mutant that causes limb girdle muscular dystrophy type 1C disrupts Src localization and activity and induces apoptosis in skeletal myotubes. *J Cell Sci* **116**, 4739-49 (2003).
130. Scherer, P.E. & Lisanti, M.P. Association of phosphofructokinase-M with caveolin-3 in differentiated skeletal myotubes. Dynamic regulation by extracellular glucose and intracellular metabolites. *J Biol Chem* **272**, 20698-705 (1997).
131. Nixon, S.J. *et al.* Zebrafish as a model for caveolin-associated muscle disease; caveolin-3 is required for myofibril organization and muscle cell patterning. *Hum Mol Genet* **14**, 1727-43 (2005).

132. Biederer, C.H. *et al.* The basic helix-loop-helix transcription factors myogenin and Id2 mediate specific induction of caveolin-3 gene expression during embryonic development. *J Biol Chem* **275**, 26245-51 (2000).
133. Couchoux, H., Allard, B., Legrand, C., Jacquemond, V. & Berthier, C. Loss of caveolin-3 induced by the dystrophy-associated P104L mutation impairs L-type calcium channel function in mouse skeletal muscle cells. *J Physiol* **580**, 745-54 (2007).
134. Weiss, N. *et al.* Expression of the muscular dystrophy-associated caveolin-3(P104L) mutant in adult mouse skeletal muscle specifically alters the Ca(2+) channel function of the dihydropyridine receptor. *Pflugers Arch* **457**, 361-75 (2008).
135. Balijepalli, R.C., Foell, J.D., Hall, D.D., Hell, J.W. & Kamp, T.J. Localization of cardiac L-type Ca(2+) channels to a caveolar macromolecular signaling complex is required for beta(2)-adrenergic regulation. *Proc Natl Acad Sci U S A* **103**, 7500-5 (2006).
136. Vassilopoulos, S. *et al.* Caveolin 3 is associated with the calcium release complex and is modified via in vivo triadin modification. *Biochemistry* **49**, 6130-5 (2010).
137. Bolduc, V. *et al.* Recessive mutations in the putative calcium-activated chloride channel Anoctamin 5 cause proximal LGMD2L and distal MMD3 muscular dystrophies. *Am J Hum Genet* **86**, 213-21 (2010).
138. Penttila, S. *et al.* Eight new mutations and the expanding phenotype variability in muscular dystrophy caused by ANO5. *Neurology* **78**, 897-903 (2012).
139. Kadoya, M. *et al.* A Japanese male with a novel ANO5 mutation with minimal muscle weakness and muscle pain till his late fifties. *Neuromuscul Disord* **27**, 477-480 (2017).
140. Sarkozy, A. *et al.* ANO5 gene analysis in a large cohort of patients with anoctaminopathy: confirmation of male prevalence and high occurrence of the common exon 5 gene mutation. *Hum Mutat* **34**, 1111-8 (2013).
141. Oh, U. & Jung, J. Cellular functions of TMEM16/anoctamin. *Pflugers Arch* **468**, 443-53 (2016).
142. Di Zanni, E., Gradogna, A., Scholz-Starke, J. & Boccaccio, A. Gain of function of TMEM16E/ANO5 scrambling activity caused by a mutation associated with gnathodiaphyseal dysplasia. *Cell Mol Life Sci* **75**, 1657-1670 (2018).
143. Griffin, D.A. *et al.* Defective membrane fusion and repair in Anoctamin5-deficient muscular dystrophy. *Hum Mol Genet* **25**, 1900-1911 (2016).
144. Meola, G. & Cardani, R. Myotonic Dystrophy Type 2: An Update on Clinical Aspects, Genetic and Pathomolecular Mechanism. *J Neuromuscul Dis* **2**, S59-S71 (2015).
145. Thornton, C.A. Myotonic dystrophy. *Neurol Clin* **32**, 705-19, viii (2014).
146. Miller, T.M. Differential diagnosis of myotonic disorders. *Muscle Nerve* **37**, 293-9 (2008).
147. Walters, J. Muscle hypertrophy and pseudohypertrophy. *Pract Neurol* **17**, 369-379 (2017).
148. Bayona, J.C. *et al.* SUMOylation pathway in Trypanosoma cruzi: functional characterization and proteomic analysis of target proteins. *Mol Cell Proteomics* **10**, M110 007369 (2011).
149. Fermin, D., Basrur, V., Yocum, A.K. & Nesvizhskii, A.I. Abacus: a computational tool for extracting and pre-processing spectral count data for label-free quantitative proteomic analysis. *Proteomics* **11**, 1340-5 (2011).
150. St-Denis, N. *et al.* Phenotypic and Interaction Profiling of the Human Phosphatases Identifies Diverse Mitotic Regulators. *Cell Rep* **17**, 2488-2501 (2016).
151. Snoeck, M. *et al.* RYR1-related myopathies: a wide spectrum of phenotypes throughout life. *Eur J Neurol* **22**, 1094-112 (2015).
152. Gu, H. *et al.* Establishment and phenotypic analysis of an Mstn knockout rat. *Biochem Biophys Res Commun* **477**, 115-22 (2016).

153. Cully, T.R. *et al.* Junctional membrane Ca(2+) dynamics in human muscle fibers are altered by malignant hyperthermia causative RyR mutation. *Proc Natl Acad Sci U S A* **115**, 8215-8220 (2018).
154. Launikonis, B.S., Cully, T.R., Csernoch, L. & Stephenson, D.G. NHE- and diffusion-dependent proton fluxes across the tubular system membranes of fast-twitch muscle fibers of the rat. *J Gen Physiol* **150**, 95-110 (2018).
155. Li, H. & Durbin, R. Fast and accurate short read alignment with Burrows-Wheeler transform. *Bioinformatics* **25**, 1754-60 (2009).
156. McKenna, A. *et al.* The Genome Analysis Toolkit: a MapReduce framework for analyzing next-generation DNA sequencing data. *Genome Res* **20**, 1297-303 (2010).
157. Shanely, R.A. *et al.* Human skeletal muscle biopsy procedures using the modified Bergstrom technique. *J Vis Exp*, 51812 (2014).
158. Sasarman, F., Karpati, G. & Shoubridge, E.A. Nuclear genetic control of mitochondrial translation in skeletal muscle revealed in patients with mitochondrial myopathy. *Hum Mol Genet* **11**, 1669-81 (2002).
159. Gouspillou, G. *et al.* The relationship between muscle fiber type-specific PGC-1alpha content and mitochondrial content varies between rodent models and humans. *PLoS One* **9**, e103044 (2014).
160. Koenig, X., Choi, R.H. & Launikonis, B.S. Store-operated Ca2+ entry is activated by every action potential in skeletal muscle. *Communications Biology* **1**, 31 (2018).
161. Cottingham, R.W., Jr., Idury, R.M. & Schaffer, A.A. Faster sequential genetic linkage computations. *Am J Hum Genet* **53**, 252-63 (1993).
162. Sobel, E. & Lange, K. Descent graphs in pedigree analysis: applications to haplotyping, location scores, and marker-sharing statistics. *Am J Hum Genet* **58**, 1323-37 (1996).
163. Tetreault, M. *et al.* Adult-onset painful axonal polyneuropathy caused by a dominant NAGLU mutation. *Brain* **138**, 1477-83 (2015).
164. van der Valk, R.J. *et al.* A novel common variant in DCST2 is associated with length in early life and height in adulthood. *Hum Mol Genet* **24**, 1155-68 (2015).
165. Roux, K.J., Kim, D.I., Raida, M. & Burke, B. A promiscuous biotin ligase fusion protein identifies proximal and interacting proteins in mammalian cells. *J Cell Biol* **196**, 801-10 (2012).
166. Konno, M. *et al.* Calumin, a Ca(2)(+)-binding protein on the endoplasmic reticulum, alters the ion permeability of Ca(2)(+) release-activated Ca(2)(+) (CRAC) channels. *Biochem Biophys Res Commun* **417**, 784-9 (2012).
167. Morimoto, M. *et al.* Bi-allelic CCDC47 Variants Cause a Disorder Characterized by Woolly Hair, Liver Dysfunction, Dysmorphic Features, and Global Developmental Delay. *Am J Hum Genet* **103**, 794-807 (2018).
168. Thapa, K. *et al.* Dysregulation of the calcium handling protein, CCDC47, is associated with diabetic cardiomyopathy. *Cell Biosci* **8**, 45 (2018).
169. Luik, R.M., Wang, B., Prakriya, M., Wu, M.M. & Lewis, R.S. Oligomerization of STIM1 couples ER calcium depletion to CRAC channel activation. *Nature* **454**, 538-42 (2008).
170. Boncompagni, S., Michelucci, A., Pietrangelo, L., Dirksen, R.T. & Protasi, F. Exercise-dependent formation of new junctions that promote STIM1-Orai1 assembly in skeletal muscle. *Sci Rep* **7**, 14286 (2017).
171. Zhang, S.L. *et al.* STIM1 is a Ca2+ sensor that activates CRAC channels and migrates from the Ca2+ store to the plasma membrane. *Nature* **437**, 902-5 (2005).
172. Lee, K.J. *et al.* Stromal interaction molecule 1 (STIM1) regulates sarcoplasmic/endoplasmic reticulum Ca(2)(+)-ATPase 1a (SERCA1a) in skeletal muscle. *Pflugers Arch* **466**, 987-1001 (2014).

173. Nair, S., Bist, P., Dikshit, N. & Krishnan, M.N. Global functional profiling of human ubiquitome identifies E3 ubiquitin ligase DCST1 as a novel negative regulator of Type-I interferon signaling. *Sci Rep* **6**, 36179 (2016).
174. Lynch, P.J. *et al.* Identification of heterozygous and homozygous individuals with the novel RYR1 mutation Cys35Arg in a large kindred. *Anesthesiology* **86**, 620-6 (1997).
175. Nesin, V. *et al.* Activating mutations in STIM1 and ORAI1 cause overlapping syndromes of tubular myopathy and congenital miosis. *Proc Natl Acad Sci U S A* **111**, 4197-202 (2014).
176. Eleveld-Trancikova, D. *et al.* The DC-derived protein DC-STAMP influences differentiation of myeloid cells. *Leukemia* **22**, 455-9 (2008).
177. Khan, U.A., Hashimi, S.M., Bakr, M.M., Forwood, M.R. & Morrison, N.A. Foreign body giant cells and osteoclasts are TRAP positive, have podosome-belts and both require OC-STAMP for cell fusion. *J Cell Biochem* **114**, 1772-8 (2013).
178. Chiu, Y.H. *et al.* Dendritic Cell-Specific Transmembrane Protein (DC-STAMP) Regulates Osteoclast Differentiation via the Ca(2+) /NFATc1 Axis. *J Cell Physiol* **232**, 2538-2549 (2017).
179. Witwicka, H. *et al.* Studies of OC-STAMP in Osteoclast Fusion: A New Knockout Mouse Model, Rescue of Cell Fusion, and Transmembrane Topology. *PLoS One* **10**, e0128275 (2015).
180. Wilson, L.D. *et al.* Fertilization in C. elegans requires an intact C-terminal RING finger in sperm protein SPE-42. *BMC Dev Biol* **11**, 10 (2011).
181. Borden, K.L. & Freemont, P.S. The RING finger domain: a recent example of a sequence-structure family. *Curr Opin Struct Biol* **6**, 395-401 (1996).
182. Borden, K.L. RING domains: master builders of molecular scaffolds? *J Mol Biol* **295**, 1103-12 (2000).
183. Chasapis, C.T. & Spyroulias, G.A. RING finger E(3) ubiquitin ligases: structure and drug discovery. *Curr Pharm Des* **15**, 3716-31 (2009).
184. Deshaies, R.J. & Joazeiro, C.A. RING domain E3 ubiquitin ligases. *Annu Rev Biochem* **78**, 399-434 (2009).
185. Yin, Q., Lamothe, B., Darnay, B.G. & Wu, H. Structural basis for the lack of E2 interaction in the RING domain of TRAF2. *Biochemistry* **48**, 10558-67 (2009).
186. Woodsmith, J., Jenn, R.C. & Sanderson, C.M. Systematic analysis of dimeric E3-RING interactions reveals increased combinatorial complexity in human ubiquitination networks. *Mol Cell Proteomics* **11**, M111 016162 (2012).
187. Hashizume, R. *et al.* The RING heterodimer BRCA1-BARD1 is a ubiquitin ligase inactivated by a breast cancer-derived mutation. *J Biol Chem* **276**, 14537-40 (2001).
188. Hua, Z. & Vierstra, R.D. The cullin-RING ubiquitin-protein ligases. *Annu Rev Plant Biol* **62**, 299-334 (2011).
189. Petroski, M.D. & Deshaies, R.J. In vitro reconstitution of SCF substrate ubiquitination with purified proteins. *Methods Enzymol* **398**, 143-58 (2005).
190. Hershko, A. & Ciechanover, A. The ubiquitin system. *Annu Rev Biochem* **67**, 425-79 (1998).
191. Zheng, N., Wang, P., Jeffrey, P.D. & Pavletich, N.P. Structure of a c-Cbl-UbcH7 complex: RING domain function in ubiquitin-protein ligases. *Cell* **102**, 533-9 (2000).
192. Bernasconi, R. & Molinari, M. ERAD and ERAD tuning: disposal of cargo and of ERAD regulators from the mammalian ER. *Curr Opin Cell Biol* **23**, 176-83 (2011).
193. Pabarcus, M.K. *et al.* CYP3A4 ubiquitination by gp78 (the tumor autocrine motility factor receptor, AMFR) and CHIP E3 ligases. *Arch Biochem Biophys* **483**, 66-74 (2009).
194. Younger, J.M. *et al.* Sequential quality-control checkpoints triage misfolded cystic fibrosis transmembrane conductance regulator. *Cell* **126**, 571-82 (2006).
195. Amano, T. *et al.* Synoviolin/Hrd1, an E3 ubiquitin ligase, as a novel pathogenic factor for arthropathy. *Genes Dev* **17**, 2436-49 (2003).

196. Yamasaki, S., Yagishita, N., Nishioka, K. & Nakajima, T. The roles of synoviolin in crosstalk between endoplasmic reticulum stress-induced apoptosis and p53 pathway. *Cell Cycle* **6**, 1319-23 (2007).
197. Omura, T. *et al.* Novel functions of ubiquitin ligase HRD1 with transmembrane and proline-rich domains. *J Pharmacol Sci* **106**, 512-9 (2008).
198. Protasi, F. Structural interaction between RYRs and DHPRs in calcium release units of cardiac and skeletal muscle cells. *Front Biosci* **7**, d650-8 (2002).
199. Michelucci, A., Garcia-Castaneda, M., Boncompagni, S. & Dirksen, R.T. Role of STIM1/ORAI1-mediated store-operated Ca(2+) entry in skeletal muscle physiology and disease. *Cell Calcium* **76**, 101-115 (2018).
200. Cho, C.H., Lee, K.J. & Lee, E.H. With the greatest care, stromal interaction molecule (STIM) proteins verify what skeletal muscle is doing. *BMB Rep* **51**, 378-387 (2018).
201. Koenig, X., Choi, R.H. & Launikonis, B.S. Store-operated Ca(2+) entry is activated by every action potential in skeletal muscle. *Commun Biol* **1**, 31 (2018).
202. Bohm, J. & Laporte, J. Gain-of-function mutations in STIM1 and ORAI1 causing tubular aggregate myopathy and Stormorken syndrome. *Cell Calcium* **76**, 1-9 (2018).
203. Morgan, A.A. & Rubenstein, E. Proline: the distribution, frequency, positioning, and common functional roles of proline and polyproline sequences in the human proteome. *PLoS One* **8**, e53785 (2013).
204. Kjaergaard, M. & Kragelund, B.B. Functions of intrinsic disorder in transmembrane proteins. *Cell Mol Life Sci* **74**, 3205-3224 (2017).
205. Bircher, J. Towards a dynamic definition of health and disease. *Med Health Care Philos* **8**, 335-41 (2005).
206. Strachan, T., Read, A.P. & Strachan, T. *Human molecular genetics*, xxv, 781 p. (Garland Science, New York, 2011).
207. Janssen, I., Heymsfield, S.B., Wang, Z.M. & Ross, R. Skeletal muscle mass and distribution in 468 men and women aged 18-88 yr. *J Appl Physiol (1985)* **89**, 81-8 (2000).
208. Sinha-Hikim, I. *et al.* Testosterone-induced increase in muscle size in healthy young men is associated with muscle fiber hypertrophy. *Am J Physiol Endocrinol Metab* **283**, E154-64 (2002).
209. Lexell, J., Taylor, C.C. & Sjostrom, M. What is the cause of the ageing atrophy? Total number, size and proportion of different fiber types studied in whole vastus lateralis muscle from 15- to 83-year-old men. *J Neurol Sci* **84**, 275-94 (1988).
210. Silventoinen, K., Magnusson, P.K., Tynelius, P., Kaprio, J. & Rasmussen, F. Heritability of body size and muscle strength in young adulthood: a study of one million Swedish men. *Genet Epidemiol* **32**, 341-9 (2008).
211. Mitchell, W.K. *et al.* Sarcopenia, dynapenia, and the impact of advancing age on human skeletal muscle size and strength; a quantitative review. *Front Physiol* **3**, 260 (2012).
212. Rosenberg, I.H. Sarcopenia: origins and clinical relevance. *J Nutr* **127**, 990S-991S (1997).
213. McCarthy, M.I. *et al.* Genome-wide association studies for complex traits: consensus, uncertainty and challenges. *Nat Rev Genet* **9**, 356-69 (2008).
214. Guarnieri, S. *et al.* New insights into the relationship between mIGF-1-induced hypertrophy and Ca2+ handling in differentiated satellite cells. *PLoS One* **9**, e107753 (2014).
215. Karpati, G., Griggs, R.C. & Hilton-Jones, D. *Disorders of voluntary muscle*, xiv, 775 p. (Cambridge University Press, Cambridge, 2001).
216. Pollak, K.A. *et al.* Exogenously applied muscle metabolites synergistically evoke sensations of muscle fatigue and pain in human subjects. *Exp Physiol* **99**, 368-80 (2014).
217. Gregory, N.S., Whitley, P.E. & Sluka, K.A. Effect of Intramuscular Protons, Lactate, and ATP on Muscle Hyperalgesia in Rats. *PLoS One* **10**, e0138576 (2015).

218. Miladinovic, T., Nashed, M.G. & Singh, G. Overview of Glutamatergic Dysregulation in Central Pathologies. *Biomolecules* **5**, 3112-41 (2015).
219. Nogales-Gadea, G. *et al.* A transcriptomic approach to search for novel phenotypic regulators in McArdle disease. *PLoS One* **7**, e31718 (2012).
220. Fiuza-Luces, C. *et al.* Muscle Signaling in Exercise Intolerance: Insights from the McArdle Mouse Model. *Med Sci Sports Exerc* **48**, 1448-58 (2016).
221. Boutell, C., Sadis, S. & Everett, R.D. Herpes simplex virus type 1 immediate-early protein ICP0 and is isolated RING finger domain act as ubiquitin E3 ligases in vitro. *J Virol* **76**, 841-50 (2002).
222. Zaglia, T. *et al.* Atrogin-1 deficiency promotes cardiomyopathy and premature death via impaired autophagy. *J Clin Invest* **124**, 2410-24 (2014).
223. Lang, F. *et al.* Dynamic changes in the mouse skeletal muscle proteome during denervation-induced atrophy. *Dis Model Mech* **10**, 881-896 (2017).
224. Shen, B. *et al.* Efficient genome modification by CRISPR-Cas9 nickase with minimal off-target effects. *Nat Methods* **11**, 399-402 (2014).
225. Dorado, B. *et al.* Generation and characterization of a novel knockin minipig model of Hutchinson-Gilford progeria syndrome. *Cell Discov* **5**, 16 (2019).

APPENDIX

Appendix 1: Significant contributions to other projects

a) Peer-reviewed articles:

Vihola A, Luque H, Savarese M, Penttilä S, Lindfors M, Leturcq F, Eymard B, Tasca G, Brais B, Conte TC, Charton K, Richard I, Udd B. Diagnostic anoctamin-5 protein defect in patients with ANO5-mutated muscular dystrophy. *Neuropathol Appl Neurobiol.* **5,** 441-448 (2018)
T.C.C. assisted in the production of one of the ANO5 monoclonal antibodies presented in this study.

Larivière R, Gaudet R, Gentil BJ, Girard M, Conte TC, Minotti S, Leclerc-Desaulniers K, Gehring K, McKinney RA, Shoubridge EA, McPherson PS, Durham HD, Brais B. Sacs knockout mice present pathophysiological defects underlying autosomal recessive spastic ataxia of Charlevoix-Saguenay. *Hum Mol Genet* **3**, 727-39 (2015)
T.C.C. generated the results of the analysis of the skeletal muscles.

b) Articles under review or in preparation:

Robertson R, Conte TC, M Dicaire MJ, Rymar VV, Sadikot AF, Bryson-Richardson R, Lavoie JN, O'Ferrall E, Young JC, Brais B. $BAG3^{P215L/KO}$ mice as a model of $BAG3^{P209L}$ myofibrillar myopathy. *Manuscript in preparation.*
T.C.C. established mouse colony and generated preliminary data on skeletal muscle histology and immunolabeling.

Appendix 2: Two-dimensional PAGE (2D-PAGE) of myoblasts overexpressing DCST2-V5

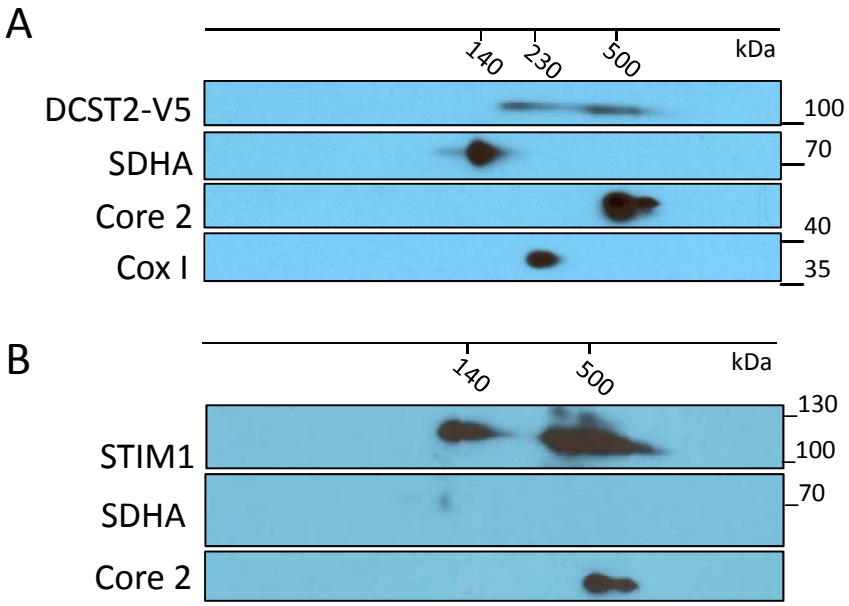

Appendix Supplemental Figure 1. DCST2 forms 3 different complexes in differentiating myoblasts. A. Two-dimensional BN-PAGE/SDS-PAGE electrophoresis analysis of differentiating myoblasts overexpressing DCST2-V5 and labeled with anti-V5, anti-SDHA, anti-Core 2 and anti-Cox I. DCST2 molecular weight is 86 kDa. B. Same membrane as in A, but labeled with anti-STIM1 antibody.

MUHC REB – NEUPSY / CÉR CUSM – NEUPSY
3801, rue University, # 686
Montréal (Québec) H3A 2B4
Tel. 514.398.1046
reb.neuro@mcgill.ca
www.leneuro.ca

STATUTS POUR LE PROJET STRONGMAN SYNDROME

Information générale

Identifiant Nagano (acronyme)	Strongman Syndrome
Numéros	MP-37-2015-99, NEU-14-013, MP-CUSM-NEU-14-013
Type de projet	Essai clinique, recherche clinique
Processus accéléré	Non
Si sous-étude, étude principale	Aucune étude principale
Champ d'application	
Bureau CÉR	Comité d'éthique de la recherche du CUSM (Panel NEUPSY)
Lieu d'évaluation éthique	Évaluation multicentrique locale
Statut	Autorisé pour la recherche
Utilisateur principal	Brais, Bernard
Date d'approbation du CÉR évaluateur	2014-10-02
Date de renouvellement	2019-10-26

Statuts du projet CÉR

Statut	Date de création	Utilisateur
Approbation	2016-02-18 15:57	Nagano, Semiweb
À l'étude	2016-02-18 15:57	Nagano, Semiweb
Dossier complet	2016-02-18 15:57	Nagano, Semiweb
Déposé	2016-02-18 15:57	Nagano, Semiweb
En préparation	2016-02-18 15:57	Nagano, Semiweb

Statuts des formulaires

9 - Demande de renouvellement annuel de l'approbation d'un projet de recherche

Formulaire	Créé le	Déposé le	Approuvé / traité	Déposé par
F9 - 23021	2018-02-14 11:18	2018-03-27 14:23	2018-05-28 12:22	Brais, Bernard
F9 - 35768	2018-09-05 10:30	2018-10-17 13:52	2018-11-09 15:09	Brais, Bernard

7 - Mise à jour d'un projet de recherche

Formulaire	Créé le	Déposé le	Approuvé / traité	Déposé par
F7 - 12855	2017-12-18 09:55	2017-12-19 15:13	2018-02-12 11:07	Brais, Bernard

9 - Demande de renouvellement annuel de l'approbation d'un projet de recherche

Formulaire	Créé le	Déposé le	Approuvé / traité	Déposé par
F9 - 7248	2017-03-25 23:15	2017-04-03 14:17	2017-04-19 23:01	Brais, Bernard

1MP - Demande de conversion ou d'ajout de site

Formulaire	Créé le	Déposé le	Approuvé / traité	Déposé par
F1MP - 465	2016-03-11 14:04	2016-03-15 10:55	2016-03-15 10:58	Boyer, Catherine

11 - Formulaire de dépôt d'un projet de recherche

Formulaire	Créé le	Déposé le	Approuvé / traité	Déposé par
F11 - 122	2016-02-18 15:57	2016-02-18 15:57	2016-02-18 15:57	Nagano, Semiweb